QEX

$7

January/February 2017

www.arrl.org

A Forum for Communications Experimenters

Issue No. 300

300th Issue!

KC7CJ re-purposes an enclosure from obsolete equipment for a new project.
The 1981 premiere issue of *QEX* is reprinted inside.

ARRL The national association for AMATEUR RADIO®
225 Main Street
Newington, CT USA 06111-1494 USA

New APRS® / D-STAR®

TH-D74A 144/220/430 MHz Tribander

Introducing the TH-D74A for the ultimate in APRS and D-STAR performance. KENWOOD has already garnered an enviable reputation with the TH-D72A handheld APRS amateur radio transceiver. And now it has raised the bar even further with the new TH-D74A, adding support for D-STAR, the digital voice & data protocol developed by the JARL, and enabling simultaneous APRS and D-STAR operation – an industry first.

- APRS compliance using packet communication to exchange real-time GPS position information and messages
- Compliant with digital/voice mode D-STAR digital amateur radio networks
- Built-in high performance GPS unit with Auto Clock Setting
- Wide-band and multi-mode reception
- 1.74” (240 x 180 pixel) Transflective color TFT display
- IF Filtering for improved SSB/CW/AM reception
- High performance DSP-based audio processing & voice recording
- Compliant with Bluetooth, microSD & Micro-USB standards
- External Decode function (PC Decode 12kHz IF Output, BW:15 kHz)
- Free software for Memory and Frequency Control Program
- Data Import / Export (Digital Repeater List, Call sign, Memory Channel)
- Four TX Power selections (5/2/0.5/0.05 W)
- Dust and Water resistant IP54/55 standards

APRS (The Automatic Packet Reporting System) is a registered American trademark of WB4APR (Mr. Bob Bruninga).
D-Star is a digital radio protocol developed by JARL (Japan Amateur Radio League).

KENWOOD

Customer Support/Distribution Customer Support:
(310) 639-4200 Fax: (310) 537-8235

www.kenwood.com/usa

ADS#29016

QEX (ISSN: 0886-8093) is published bimonthly in January, March, May, July, September, and November by the American Radio Relay League, 225 Main Street, Newington, CT 06111-1494. Periodicals postage paid at Hartford, CT and at additional mailing offices.

POSTMASTER: Send address changes to: QEX, 225 Main St, Newington, CT 06111-1494
Issue No 299

Publisher
American Radio Relay League

Kazimierz "Kai" Siwiak, KE4PT
Editor

Lori Weinberg, KB1EIB
Assistant Editor

Zack Lau, W1VT
Ray Mack, W5IFS
Contributing Editors

Production Department

Steve Ford, WB8IMY
Publications Manager

Michelle Bloom, WB1ENT
Production Supervisor

Sue Fagan, KB1OKW
Graphic Design Supervisor

David Pingree, N1NAS
Senior Technical Illustrator

Brian Washing
Technical Illustrator

Advertising Information Contact:

Janet L. Rocco, W1JLR
Business Services
860-594-0203 – Direct
800-243-7768 – ARRL
860-594-4285 – Fax

Circulation Department

Cathy Stepina, *QEX Circulation*

Offices

225 Main St, Newington, CT 06111-1494 USA
Telephone: 860-594-0200
Fax: 860-594-0259 (24 hour direct line)
e-mail: **qex@arrl.org**

Subscription rate for 6 issues:

In the US: $29;

US by First Class Mail: $40;

International and Canada by Airmail: $35

Members are asked to include their membership control number or a label from their QST when applying.

In order to ensure prompt delivery, we ask that you periodically check the address information on your mailing label. If you find any inaccuracies, please contact the Circulation Department immediately. Thank you for your assistance.

About the Cover

Scott Roleson, KC7CJ, found that non-functioning and obsolete equipment can be relatively inexpensive, and can be easily re-purposed as rugged and attractive enclosures for new projects.

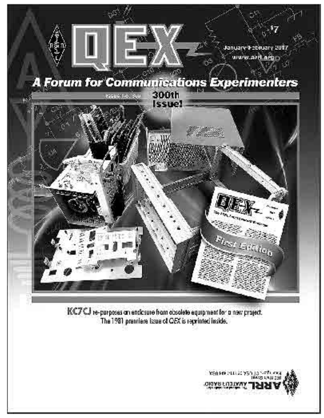

In This Issue

Features

Index of Advertisers

The American Radio Relay League

The American Radio Relay League, Inc, is a noncommercial association of radio amateurs, organized for the promotion of interest in Amateur Radio communication and experimentation, for the establishment of networks to provide communications in the event of disasters or other emergencies, for the advancement of the radio art and of the public welfare, for the representation of the radio amateur in legislative matters, and for the maintenance of fraternalism and a high standard of conduct.

ARRL is an incorporated association without capital stock chartered under the laws of the state of Connecticut, and is an exempt organization under Section 501(c)(3) of the Internal Revenue Code of 1986. Its affairs are governed by a Board of Directors, whose voting members are elected every three years by the general membership. The officers are elected or appointed by the Directors. The League is noncommercial, and no one who could gain financially from the shaping of its affairs is eligible for membership on its Board.

"Of, by, and for the radio amateur," ARRL numbers within its ranks the vast majority of active amateurs in the nation and has a proud history of achievement as the standard-bearer in amateur affairs.

A *bona fide* interest in Amateur Radio is the only essential qualification of membership; an Amateur Radio license is not a prerequisite, although full voting membership is granted only to licensed amateurs in the US.

Membership inquiries and general correspondence should be addressed to the administrative headquarters:

ARRL
225 Main Street
Newington, CT 06111 USA
Telephone: 860-594-0200
FAX: 860-594-0259 (24-hour direct line)

Officers

President: Rick Roderick, K5UR
PO Box 1463, Little Rock, AR 72203

Chief Executive Officer: Tom Gallagher, NY2RF

The purpose of *QEX* is to:

1) provide a medium for the exchange of ideas and information among Amateur Radio experimenters,

2) document advanced technical work in the Amateur Radio field, and

3) support efforts to advance the state of the Amateur Radio art.

All correspondence concerning *QEX* should be addressed to the American Radio Relay League, 225 Main Street, Newington, CT 06111 USA. Envelopes containing manuscripts and letters for publication in *QEX* should be marked Editor, *QEX*.

Both theoretical and practical technical articles are welcomed. Manuscripts should be submitted in word-processor format, if possible. We can redraw any figures as long as their content is clear. Photos should be glossy, color or black-and-white prints of at least the size they are to appear in *QEX* or high-resolution digital images (300 dots per inch or higher at the printed size). Further information for authors can be found on the Web at **www.arrl.org/qex/** or by e-mail to **qex@arrl.org**.

Any opinions expressed in *QEX* are those of the authors, not necessarily those of the Editor or the League. While we strive to ensure all material is technically correct, authors are expected to defend their own assertions. Products mentioned are included for your information only; no endorsement is implied. Readers are cautioned to verify the availability of products before sending money to vendors.

Kazimierz "Kai" Siwiak, KE4PT

Perspectives

300 *QEX* Issues and Going Strong

QEX was first published in December 1981 as the "ARRL Experimenter's Exchange," with Founding Editor Paul Rinaldo, W4RI. We celebrate *QEX* issue #300 by reprinting the entire contents of *QEX* issue #1. Over the years, *QEX* has partnered with the *AMSAT Satellite Journal*, and later hosted *Gateway*, the ARRL packet radio newsletter. The conductors of these two publications, as well as several Contributing Editors, have sustained the quality of the magazine.

Jon Bloom, KE3Z, became Editor in 1992. His considerable expertise built *QEX* into one of the most respected technical publications in its field. This was a time when Amateur Radio, and radio technology in general, were undergoing rapid changes.

Zack Lau, W1VT, the award-winning ARRL Senior Laboratory Engineer, came aboard with his "RF" column, detailing advanced work across the RF spectrum. The "RF" column ran from August 1992 through January 2005.

Rudy Severns, N6LF, took over the editorial reins in 1997. On his watch, the magazine went from monthly to bimonthly publication. The number and depth of articles increased dramatically. *QEX* took on a new look as well, with full-color covers and enhanced content. Rudy's talent for soliciting top-quality articles from the leading technical authors in Amateur Radio took the magazine to a higher plateau.

Bob Schetgen, KU7G, known for his editorship of *The ARRL Handbook* and for his columns in *QST*, also began work on *QEX* in 1997. Bob served as Managing Editor until his sudden passing in December 2005.

In January 2000, ARRL purchased the Amateur Radio technical journal *Communications Quarterly* from CQ Communications and merged it with *QEX*, creating the combined *QEX/Communications Quarterly*. Published for the preceding nine years under the editorship of Terry Littlefield, KA1STC, *Communications Quarterly* billed itself as the philosophical successor to *ham radio* magazine, which was founded by "Skip" Tenney, W1NLB, and Jim Fisk, W1HR. Littlefield was Editor of *Ham Radio* when CQ Communications purchased it in 1990.

Ray Mack, W5IFS, joined as Contributing Editor with the January/February 2002 issue. Ray conducts his column "Out of the Box," about new product availability and also serves as our proofreader. With the January/February 2009 issue, Ray also began a new column, "SDR: Simplified," presenting hands-on experiments and investigations into the world of software defined radio (SDR) and digital signal processing (DSP).

L.B. Cebik, W4RNL, came aboard as Contributing Editor as of July/August 2004. His column "Antenna Options" covered antenna design, performance and construction until his passing in April 2008. The final "Antenna Options" column appeared in the July/August 2008 issue.

Doug Smith, KF6DX, became *QEX* Editor with the September/October 1998 issue. His enthusiasm and technical expertise continued to improve the magazine's technical content.

Larry Wolfgang, WR1B, began work on *QEX* in late 2005 and became Managing Editor for the March/April 2006 issue. Larry became the *QEX* Editor with the September/October 2007.

Kazimierz "Kai" Siwiak, KE4PT, stepped in as *QEX* Editor with the March/April 2016 issue. Kai also edits *QST* technical articles (since the July 2013 issue of *QST*), and serves on the ARRL RF Safety Committee.

In this Issue

We've increased the cover thickness to 50# stock to help it better survive the postal mail. Our *QEX* authors describe propagation measurements and modes, filter characteristics, and tuning an L-network. Help determine the content of future *QEX* issues by putting your favorite topic or innovative measurement on paper. Share it on these pages with fellow readers. Just follow the details on the **www.arrl.org/qex-author-guide** web page, and contact us at **qex@arrl.org**. We value your feedback, comments and opinions about these pages.

In this issue, we've recreated the entire first issue of *QEX*. Flavio Egano, IK3XTV, followed long term observations that suggest long path echoes might propagate with low attenuation by ionospheric ducts; Bill Kaune, W7IEQ, details the inductor losses in Pi-network; Tom C. McDermott, N5EG, describes hardware and software for ionospheric sounding; Scott Roleson, KC7CJ, repurposes an enclosure from obsolete equipment; and Robert J. Zavrel, W7SX, presents a different approach to a multi-band Yagi-Uda design.

Please continue to support *QEX*, and help it remain a strong technical publication. Submit articles via e-mail to **qex@arrl.org** or via US Mail to *QEX*, ARRL HQ, 225 Main St, Newington, CT 06111.

73,

Kazimierz "Kai" Siwiak, KE4PT
Editor

Maty Weinberg, KB1EIB
Assistant Editor

QEX

December

1981

Number 1

The ARRL Experimenters' Exchange

This is the premiere issue of *QEX: The ARRL Experimenters' Exchange*. Beginning with this issue, *QEX* is a special League publication by and for Amateur Radio experimenters. It is available to both ARRL members and nonmembers at subscription rates shown on the last page of this issue.

Initially, *QEX* will be published every other month. As soon as we are assured that we can get the quality and quantity of material that we need and get the logistical handling well greased, monthly publication can begin.

It is our intent to achieve a balance in the editorial content. In one respect, we want to feature about as much original research and development as we do practical construction articles. In another, we want to keep some sort of a balance between digital electronics (computers, etc.) and the analog world of receivers and transmitters. Within the digital domain, it makes sense to include some software as well as hardware. But that doesn't mean that *each issue* will reflect that balance. Also, we may concentrate more than a fair share of space on a topic when it's hot and rolling. It seems reasonable to push the newer technology as much as possible, even at the expense of overlooking some more mature topics.

Computer program listings present a special problem. We would like to include computer programs relating to Amateur Radio and have one in this issue by Dave Meier, N4MW. Fortunately, Dave's program listing and sample run were relatively short. Longer ones could completely fill an issue of *QEX*. So, we are happy to print the shorter ones, but suggest that authors of longer ones make the programs available either on diskettes or on hard copies. Of course, we'd like to have the narrative description of the program in article form for *QEX*. In case you do have a short computer listing for printing in *QEX*, please set up your printer to produce a column no more that 43 spaces wide. Use a new ribbon and print on clean, white paper.

Because *QEX* is an exchange, the names, mailing addresses and (where furnished) telephone numbers of the authors will be included with all articles and correspondence. If you are interested in an article, we're sure that the author would like to hear from you. The whole idea is to get dialog going between experimenters who are geographically separated. If you think that other *QEX* readers might benefit in some way from the dialog, please consider dropping a copy to the Editor, *QEX*. In some cases, we can print parts of the correspondence, space permitting. But, we would hope that the exchange will generate one or more good articles for *QEX* and *QST*.

You will note that we have several columns in this first issue. There is one more column that we need as soon as possible -- one called "Components" or "Devices." The column should include the latest semiconductor devices as well as passive components of interest to Amateur Radio experimenters. We have some feelers out but are open to suggestions on this and other possible columns.

What about new technology? The "Data Communications" column by Dave Borden, K8MMO will be a regular feature on packet-radio technology. We expect to carry material on amateur spread spectrum experimentation from time to time. Radio amateurs are experimenting with speech I/O, medium-scan TV, computer control of everything in the shack, error detection and error correction codes, etc., and we need to spread the word on these efforts. The trade journals are full of new developments and new products such as ICs that handle many complex functions. If you want to boggle your mind a bit, find a copy of *EDN* magazine, October 14, 1981 issue and read the series entitled, "Electronic Technology-The Next 25 Years." Perhaps you know a hermit experimenter who is doing neat things in the basement. Team up and try to get the work of the hermit experimenter into print so that the rest of us can benefit. *QEX* is particularly interested in liberating these experimental results. - W4RI

THE AMERICAN RADIO RELAY LEAGUE, INC.

HEADQUARTERS SOCIETY OF THE INTERNATIONAL AMATEUR RADIO UNION

ADMINISTRATIVE HEADQUARTERS NEWINGTON, CONNECTICUT, U.S.A. 06111

November 10, 1981

Mr. Paul L. Rinaldo, W4RI
1524 Springvale Avenue
McLean, VA 22101

Dear Paul:

For years, many of us within the ARRL organization have felt that the League ought to be doing more to promote advanced technical experimentation by radio amateurs. With the appearance of QEX, those feelings have been turned into action. You're uniquely qualified to serve as the editor of the League's technical newsletter, and with the help of enthusiastic and active members like yourself I know QEX will be a source of pride for the officers, directors, staff and the entire membership.

Best of luck with the innaugural issue.

73,

Sincerely,

Harry J. Dannals, W2HD
President

HJD:dlf

FEDERAL COMMUNICATIONS COMMISSION

WASHINGTON, D.C. 20554
September 22, 1981

IN REPLY REFER TO:

Paul L. Rinaldo, W4RI
Editor, QEX
1524 Springvale Avenue
McLean, Virginia 22101

Dear Paul:

This is to wish you and the American Radio Relay League well as you launch QEX.

As you know, the Office of Science and Technology is looking to amateur radio experimenters to play a more active role in new communications techniques. Amateurs are a unique resource possessing not only the talent but the time and energy to devote to projects which may have no immediate commercial payoff. Hams are now experimenting with spread spectrum, packet radio and error-correction codes under recent rules changes or waivers by the F.C.C. We encourage further innovation, particularly those which may contribute to better spectrum management.

Sincerely yours,

S. J. Lukasik

SINCE 1914 — OF, BY AND FOR THE RADIO AMATEUR

THE AMERICAN RADIO RELAY LEAGUE, INC.

HEADQUARTERS SOCIETY OF THE INTERNATIONAL AMATEUR RADIO UNION

ADMINISTRATIVE HEADQUARTERS NEWINGTON, CONNECTICUT, U.S.A. 06111

HARRY J. DANNALS
W2HD, PRESIDENT
CARL L. SMITH
FIRST VICE PRES
LARRY E. PRICE
VICE PRES
MAX ARNOLD
VICE PRES
NOEL B. EATON
VICE PRES
INTERNATIONAL AFFAIRS
JAMES E. McCOBB
TREASURER
RICHARD L. BALDWIN
W1RU, SEC & GEN MGR
203-666-1541
QST—
OFFICIAL JOURNAL

30 June 1981

Mr. Paul L. Rinaldo W4RI
1524 Springvale Avenue
McLean, Va. 22101

Dear Paul;

Congratulations on taking over the new experiementer's newsletter. QEX. I cannot think of a more competent person for the job!

I will be anxiously awaiting the first publication and I believe so will many other amateurs throughout the nation, and the world.

If there is anything I can do to help you please feel free to let me know. Meanwhile the very best of luck in the new endeavor for the League.

73

Sincerely

Gay W4UG
Director Roanoke Div.

THE AMERICAN RADIO RELAY LEAGUE, INC.

HEADQUARTERS SOCIETY OF THE INTERNATIONAL AMATEUR RADIO UNION

ADMINISTRATIVE HEADQUARTERS NEWINGTON, CONNECTICUT, U.S.A. 06111

HARRY J. DANNALS
W2HD, PRESIDENT
CARL L. SMITH
FIRST VICE PRES
LARRY E. PRICE
VICE PRES
MAX ARNOLD
VICE PRES
NOEL B. EATON
VICE PRES
INTERNATIONAL AFFAIRS
JAMES E. McCOBB
TREASURER
RICHARD L. BALDWIN
W1RU, SEC & GEN MGR
203-666-1541
QST—
OFFICIAL JOURNAL

October 1, 1981

Mr. Paul Rinaldo, W4RI
1524 Springvale Avenue
McLean, VA 22101

Dear Paul:

I wish us well in the QEX project. "Us" because you as editor have an important role in whether this is a successful venture and because for "us" the membership this may signal a new facet of the League's services to the membership. If QEX is successful, and I am confident that it will be, I foresee additional specialized newsletters by the League covering other specialized technical and operating areas.

So, you and QEX are blazing a new trail. Good luck!

73,

Sincerely yours,

Richard L. Baldwin, W1RU
General Manager

RLB:dlf

VHF and UHF Low Noise Preamplifiers

By G. H. Krauss,* WA2GFP

For the past 4 years, I have been systematically designing, building and testing low-noise-figure preamplifiers (LNAs) for 30, 50, 144, 220, 432 and 1296 MHz. A very early set of results, along with historical background and basic theory, was reported earlier.[1] A full report, covering some 200 LNAs, is presented here, in "cookbook" style. The measurements were done in an engineering lab, using quality equipment; noise figure was measured using the Y technique, a solid-state noise source and calibration/measurement against a hot/cold noise source of known accuracy. Even though I believe I have removed all sources of error, the reader is cautioned to interpret all noise-figure listings as relative, with an absolute accuracy range of -0.1/0.3 dB.

The layout for the vhf GaAsFET LNAs is given in Fig.1, and for the 1296 MHz Π LNAs in Fig. 2. The remaining LNAs were all built on a single-sided pc board (see Fig. 8 of ref),[1] soldered into a fully shielded box; these LNAs differ only in (a) device used and (b) input and output circuits necessary to match the chosen device for best noise figure. I have found that only four different types of matching circuits, with values adjusted for each different band, are required for use with the full range of devices. Several possible bias circuits are also shown.

The result tables list devices, for each band, in order of increasing noise figure. The Ga and Gr figures are forward and reverse gain, respectively, when the LNA is adjusted for minimum noise figure. Generally, greater forward gain can be achieved, but the noise figure will always be worse. The difference between Ga and Gr is the gain margin Gm = -(Ga-Gr). The greater the value of Gm, the more stable the LNA, especially with a reactive bandpass filter (cavity, helical resonator and the like) in front of, or after, the preamp. LNAs with a Gm value of less than about 8 dB may be marginally stable, and one with a value less than about 3 dB will often oscillate when the T/R relay presents an open circuit at the LNA input. The noise measure M is an indication of the input noise figure of a long chain of cascaded LNAs having the same NF and Ga; it is mainly given to show the effect of LNA gain, which should be about 10 dB greater than the noise figure of the following stage. Too high a stage gain will lead to front-end overload, although it is rarely the 1st LNA that is overloaded. However, the GaAsFET devices not only have the lowest noise figures, but have relatively high (and therefore desirable) third-order output IMD intercepts (I_3); the I_3 points of some LNAs were measured and listed in the tables. Another LNA characteristic having a bearing on IMD is bandwidth (BW); most bipolar devices require extremely broad-band (BB) input circuits and substantially resistive output circuits. This leads to higher susceptibility of overload from out-of-band signals (especially near fm and TV stations!). The GaAsFETs, having a much higher input impedance for optimum noise figure, allow a higher Q input circuit to be used, although the Q cannot be too high or input loss (and noise figure) will rise.

TO BREW AN LNA:

(1) Choose a device, based on the table data; you make the most important choices based on availability, cost and performance. A key to the manufacturers, or their agents if they do not sell direct in the U.S., is provided.

(2) For the chosen device, obtain the input and output circuits. If GaAsFET or 1296 Π, see Figs. 1 and 2. Use the best components you can obtain; remember that you want to keep input loss as low as possible.

(3) Choose a bias circuit (the "active" circuit - on the right - is recommended). The GaAsFETs have their own bias circuit in Fig. 1; at 1296 MHz, a separate and well-regulated $-V_1$ supply is necessary.

(4) Use the "Universal" layout of Ref. 1, Fig. 8; the vhf GaAsFET layout of Fig. 1 or the 1296 layout of Fig. 2, to build.

(5) Tune: monitor the current into, and voltage at, the collector/drain feedthru capacitor and do not exceed manufacturer's ratings. Tune all L&Cs for maximum gain. Now, set input circuit and bias for minimum noise figure - do not touch output circuit adjustments, if any.

*16 Riviera Dr., Latham, NY 12110

I would be happy to correspond with anyone concerning these, or any other, LNAs if an SASE is provided. Any leads on a reasonably accurate noise source for 2304 MHz would be appreciated.

[1]Krauss, "VHF Preamplifiers," *Ham Radio*, Dec. 1979.

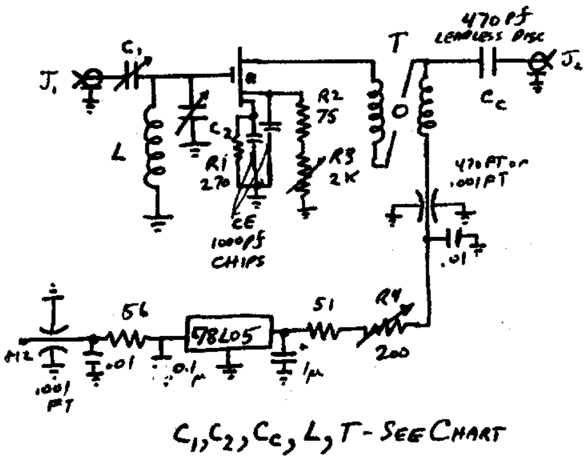

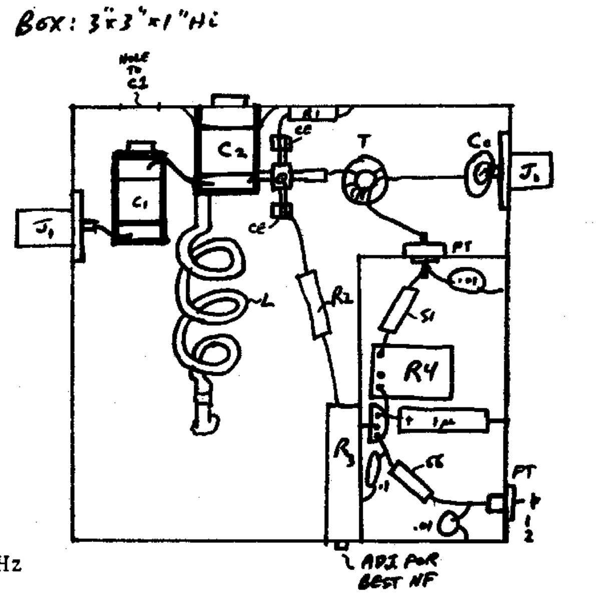

Fig. 1 - GaAsFET Preamp - 144, 220,and 432 MHz

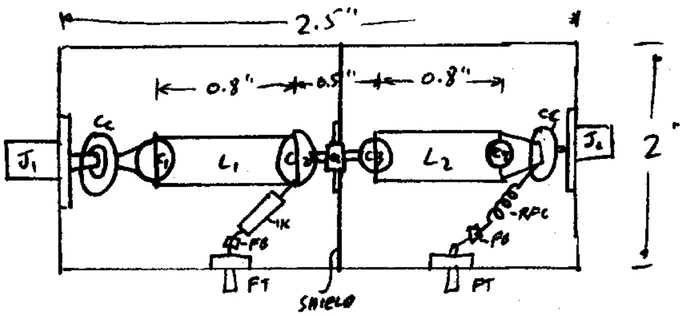

Fig. 2 - 1296 MHz π-input/output Preamp.

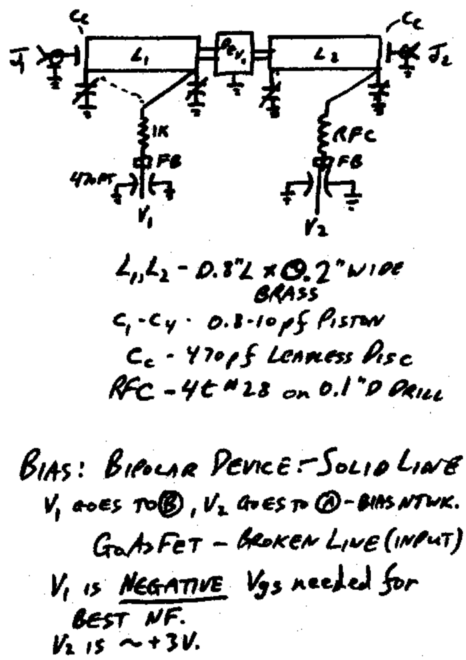

30 MHz PREAMPLIFIERS

DEVICE	COST $	MFGR	NF (dB.)	Ga (dB.)	Gr (dB.)	Gm (dB.)	M (dB.)	BW (MHz.)	INPUT CKT.	OUTPUT CKT.	REMARKS
MS300H	~10.00	TI	0.82	18.1	-49	30.9	0.83	BB	I	I	
NE41632E-2	3.30	NEC	0.94	25.5	-38	12.5	0.94	BB	IV	III	Rs=200Ω
			1.03	23.5	-34	10.5	1.03	BB	I	I	TUNED
			1.07	21.0	-39	18.0	1.08	BB	III	III	Rs=50Ω
MA42001-509	11.50	MA	1.05	18.0	-33	15.0	1.06	10	II	I	
3N204	2.00	-	1.21	16.6	-38	21.4	1.23	3.4	I	I	DGFET
MA42014-509	~ 9.00	MA	1.32	14.0	-48	34.0	1.37	30	II	I	
2N5109	1.25	-	1.44	14.4	-39	24.6	1.49	BB	I	III	LOW IMD
MRF901	1.55	M	1.47	26.2	-34	7.8	1.47	BB	II	IV	
MPF102	0.35	M	1.60	16.0	-16	*0.0	1.63	1	I	I	FET
2N4416	0.50	-	1.62	13.1	-22	8.9	1.69	1	I	III	FET
MRF904	1.25	M	1.65	23.0	-34	11.0	1.66	BB	IV	IV	
40673	1.75	RCA	2.1	22.0	-23	*1.0	2.1	1	I	I	DGFET
A485	1.75	AMP	2.1	26.7	-49	22.3	2.1	BB	I	III	LOW IMD
NE02135/37	~ 4.00	NEC	2.2	16.7	-47	30.3	2.2	BB	I	IV	
TIS189	0.90	TI	2.6	14.0	-64	50.0	2.7	17	I	I	DGFET
A430	1.90	AMP	4.5	22.9	-51	28.1	4.5	BB	I	III	LOW IMD
A210	2.25	AMP	6.1	18.3	-46	27.7	6.2	BB	I	III	LOW IMD

NOTES:

Rs = source resistance
FET = field-effect transistor
DGFET = dual-gate FET
IMD = intermodulation distortion
SE = single emitter/source lead
DOE - dual, opposed emitter/source leads
BB = Broadband
A = Aertech
AMP = Amperex
AND = AND Transistors
DXL = Dexcel
HP = Hewlett Packard
M = Motorola
MA = Microwave Associates
MIT = Mitsubishi (Applied Invention, Hillsdale, N.Y.)
NEC - Nippon Electric (California Electronic Labs.)
PAN = Panasonic
RCA - RCA
SIL = Siliconix
TI = Texas Instruments

50 MHz PREAMPLIFIERS

DEVICE	COST $	MFGR	NF (dB.)	Ga (dB.)	Gr (dB.)	Gm (dB.)	M (dB.)	BW (MHz.)	INPUT CKT.	OUTPUT CKT.	REMARKS
MA42001-509	11.50	MA	0.95	15.3	-34	18.7	0.97	2	II	I	
NE41632E-2	3.30	NEC	0.98	24.0	-32	8.0	0.98	BB	IV	III	Rs=200 Ω
			1.07	22.0	-33	11.0	1.08	6	I	I	TUNED
			1.13	22.0	-35	13.0	1.14	BB	III	III	Rs=50 Ω
MS300H	~ 10.00	TI	1.11	15.5	-43	27.5	1.12	BB	I	I	
MA42014-509	~ 9.00	MA	1.15	18.3	-37	18.7	1.17	BB	II	I	
2N4416	0.50	-	1.37	13.0	-15	*2.0	1.43	2	I	I	FET
MA42003-509	~ 5.00	MA	1.50	13.7	-28	14.3	1.57	BB	II	I	
3N204	2.00	-	1.51	17.4	-24.5	7.1	1.53	5	I	I	DGFET
NE02135/7	4.00	NEC	1.55	15.0	-27	12.0	1.59	BB	I	IV	
MRF901	1.55	M	1.67	25.0	-32	7.0	1.67	BB	II	IV	
2N5109	1.00	-	1.72	18.0	-29	11.0	1.74	BB	I	III	LOW IMD
MRF904	1.25	M	2.0	28.0	-36	8.0	2.0	BB	IV	IV	
MPF102	0.35	M	2.0	13.0	-27	14.0	2.1	2	I	I	FET
TIS-189	0.90	TI	2.1	20.0	-40	20.0	2.1	2.2	I	I	DGFET
A485	1.75	AMP	2.1	25.8	-46	20.2	2.1	BB	I	III	LOW IMD
U310	4.00	SIL	2.5	10.3	-26	15.7	2.7	2	I	I	FET
40673	1.75	RCA	2.6	18.2	-27	8.8	2.6	7	I	I	DGFET
MP1006	11.00	AND	3.7	27.0	-29	*2.0	3.7	BB	I	I	
A430	1.90	AMP	4.3	23.0	-50	27.0	4.3	BB	I	III	LOW IMD
A210	2.25	AMP	6.3	17.1	-44	26.9	6.4	BB	I	III	LOW IMD

144 MHz PREAMPLIFIERS

DEVICE	COST $	MFGR	NF (dB.)	Ga (dB.)	Gr (dB.)	Gm (dB.)	M (dB.)	BW (MHz.)	INPUT CKT.	OUTPUT CKT.	REMARKS
MGF-1400	23.00	MIT	0.47	20.0	-33	13.0	0.47	11	I	III	GaAsFET I3= ① +23dBm
D432	25.00	DXL	0.49	19.6	-29	9.4	0.50	18	I	III	GaAsFET I3= ① +15dBm
MGF-1200	13.00	MIT	0.51	18.9	-29	10.1	0.52	20	I	III	GaAsFET I3= ① +17dBm
3SK48	4.00	PAN	0.62	27.2	-29	*1.8	0.62	BB	I	I	DGFET I3= +40dBm
NE21937	3.50	NEC	0.89	21.0	-33	12.0	0.90	BB	II	IV	
NE64535	7.50	NEC	1.00	22.0	-36	14.0	1.00	BB	I	IV	
NE73437	1.75	NEC	1.03	22.0	-40	18.0	1.04	BB	I	I	
MS300H	~10.00	TI	1.10	17.0	-36	19.0	1.12	36	I	I	
MA42001-509	11.50	MA	1.10	14.0	-42	28.0	1.14	BB	I	I	
MA42014-509	~ 9.00	MA	1.12	20.5	-28	7.5	1.13	BB	I	I	
3SK97	~ 2.00	PAN	1.17	18.9	-23	*4.1	1.18	21	I	I	DGFET
MA42002-509	~ 7.00	MA	1.22	18.8	-26	7.2	1.23	BB	I	I	
MP-1006	11.00	AND	1.37	16.6	-28	11.4	1.40	BB	I	IV	
MS2110JE	~15.00	TI	1.40	15.0	-35	20.0	1.44	28	I	I	
MRF901	1.55	M	1.40	23.0	-28	*5.0	1.41	BB	II	IV	
MRF904	1.25	M	1.41	17.0	-32	15.0	1.43	BB	IV	IV	
NE41632E-2	3.30	NEC	1.54	13.7	-32	18.3	1.63	BB	I	I	
U310	4.00	SIL	1.60	12.0	-27	15.0	1.69	2	I	I	FET COMMON GATE
3N204	2.00	-	1.64	15.6	-29	13.4	1.68	2	I	I	DGFET
MA42003-509	~ 5.00	MA	1.67	21.5	-25	*3.5	1.68	BB	I	I	
NE02135/7	4.00	NEC	1.81	23.5	-31	7.5	1.82	BB	I	IV	
2N4416	0.50	-	1.90	17.5	-20	*2.5	1.93	2	I	I	FET
2N5109	1.00	-	2.5	12.5	-23	10.5	2.6	BB	I	III	LOW IMD
TIS-189	0.90	TI	2.6	14.3	-39	24.7	2.6	3.1	I	I	DGFET
A485	1.75	AMP	2.6	24.1	-42	17.9	2.6	BB	I	III	LOW IMD
NE22235	4.00	NEC	2.8	17.0	-38	21.0	2.8	BB	I	IV	
40673	1.75	RCA	3.1	13.9	-31	17.1	3.2	14	I	I	DGFET
MPF102	0.35	M	3.7	11.0	-24	13.0	3.9	4	I	I	FET
A430	1.90	AMP	4.1	22.0	-47	25.0	4.1	BB	I	III	LOW IMD
A210	2.25	AMP	5.7	17.3	-43	25.7	5.7	BB	I	III	LOW IMD
J308	1.00	SIL	6.2	13.0	-18	*5.0	6.4	4	I	II	FET COMMON GATE

REF: ① See Figure 1

220 MHz PREAMPLIFIERS

DEVICE	COST $	MFGR	NF (dB.)	Ga (dB.)	Gr (dB.)	Gm (dB.)	M (dB.)	BW (MHz.)	INPUT CKT.	OUTPUT CKT.	REMARKS
MGF-1400	23.00	MIT	0.47	19.9	-28.4	8.5	0.47	16	I	III	GaAsFET I3= ① +23dBm
D-432	25.00	DXL	0.48	18.4	-27.0	8.6	0.49	28	I	III	GaAsFET I3= ① +20dBm
MGF-1200	13.00	MIT	0.54	18.7	-30	11.3	0.55	50	I	III	GaAsFET I3= ① +18dBm
MS2110JE	~15.00	TI	0.86	14.0	-30	16.0	0.89	24	I	I	
NE64535	7.50	NEC	0.96	19.0	-34	15.0	0.97	BB	I	IV	
MS300H	~10.00	TI	1.05	14.5	-26	11.5	1.08	40	I	I	
NE73437	1.75	NEC	1.10	18.5	-29	10.5	1.11	2	I	I	
MA42001-509	11.50	MA	1.13	12.3	-26	13.7	1.20	BB	I	I	
3SK97	~ 2.00	PAN	1.23	16.3	-19.5	3.2	1.26	32	I	I	DGFET
MRF904	1.25	M	1.35	14.5	-28	13.5	1.39	BB	IV	IV	
MA42014-509	~ 9.00	MA	1.35	15.1	-26	10.9	1.39	BB	I	I	
NE21937	3.50	NEC	1.36	13.5	-27	13.5	1.41	BB	II	IV	
MRF901	1.55	M	1.40	18.1	-24	5.9	1.42	BB	II	IV	
MA42002-509	~ 7.00	MA	1.44	14.3	-26	11.7	1.48	BB	I	I	
MP1006	11.00	AND	1.66	15.1	-28	12.9	1.70	BB	I	I	
NE41632E2	3.30	NEC	1.68	13.0	-24	11.0	1.75	BB	I	I	
3N204	2.00	-	1.82	13.5	-26	12.5	1.89	2	I	I	DGFET
NE02135/7	4.00	NEC	1.87	20.8	-30	9.2	1.88	BB	I	IV	
MA42003-509	~ 5.00	MA	1.95	16.5	-23	6.5	1.97	BB	I	I	
2N4416	0.50	-	2.0	10.0	-20	10.0	2.2	4	I	I	FET
U310	4.00	SIL	2.0	9.1	-28	18.9	2.2	4	I	I	FET COMMON GAT
NE22235	4.00	NEC	2.1	29.3	-26	-3.3	2.1	BB	I	I	
TIS-189	0.90	TI	2.5	18.0	-23	5.0	2.6	5.2	I	I	DGFET
A485	1.75	AMP	3.1	23.0	-41	18.0	3.1	BB	I	III	LOW IMD
40673	1.75	RCA	4.3	15.1	-21	5.9	4.4	6	I	I	DGFET
2N5109	1.00	-	4.6	7.9	-21	13.1	5.1	BB	I	III	LOW IMD
A430	1.90	AMP	4.9	20.1	-43	23.0	5.0	BB	I	III	LOW IMD
A210	2.25	AMP	5.9	16.0	-59	23.0	6.1	BB	I	III	LOW IMD

432 MHz PREAMPLIFIERS

DEVICE	COST $	MFGR	NF (dB.)	Ga (dB.)	Gr (dB.)	Gm (dB.)	M (dB.)	BW (MHz.)	INPUT CKT.	OUTPUT CKT.	REMARKS
MGF1400A	28.30	MIT	0.39	18.2	-27	8.8	0.40	20	I	III	GaAsFET I3-1 +20dBm
D432	25.00	DXL	0.49	18.1	-29	6.9	0.51	50	I	III	GaAsFET I3-1 +21dBm
MGF1400	23.00	MIT	0.52	21.6	-33	11.4	0.52	50	I	II	GaAsFET I3-1 +24dBm
MGF1200	13.00	MIT	0.58	20.4	-28	7.6	0.59	25	I	III	GaAsFET I3-1 +21dBm
NE24483	35.00	NEC	0.75	15.3	-25	9.7	0.76	60	I	II	GaAsFET
NE64535	7.50	NEC	0.86	16.0	-24	8.0	0.88	BB	I	IV	
MS2110JE	~15.00	TI	1.07	20.0	-28	8.0	1.08	BB	I	I	
NE73437	1.75	NEC	1.25	17.1	-25	7.9	1.27	BB	I	I	
NE02135	4.00	NEC	1.27	11.2	-27	15.8	1.36	BB	I	IV	
MRF904	1.25	M	1.38	11.0	-25	14.0	1.48	BB	IV	IV	
3SK97	2.00	PAN	1.39	11.5	-12.8	*1.3	1.48	60	I	I	DG GaAsFET
MRF901	1.55	M	1.40	16.1	-22	*5.9	1.43	BB	II	IV	
MA42111-509	~15.00	MA	1.40	11.3	-19	7.7	1.49	BB	I	I	
MA42141-510	~17.00	MA	1.52	14.0	-25	11.0	1.57	BB	I	I	
MA42161-511	~25.00	MA	1.57	16.3	-26	9.7	1.61	BB	I	I	
MS300H	~10.00	TI	1.59	13.2	-25	11.8	1.66	40	I	I	
NE22235	4.00	NEC	1.60	11.0	-26	15.0	1.71	BB	I	IV	
MA42001-509	11.50	MA	1.73	11.3	-25	13.7	1.89	BB	I	I	
NE21937	3.50	NEC	1.76	20.5	-32	11.5	1.77	BB	II	IV	
BFR91	3.00	AMP	1.78	15.1	-27	11.9	1.83	BB	II	IV	
MP-1006	11.00	AND	1.90	17.7	-28	10.3	1.93	BB	I	I	
TIS-189	0.90	TI	1.98	14.5	-43	28.5	2.04	17	I	I	DGFET
MP-1004	~14.00	AND	2.0	12.2	-34	21.8	2.1	BB	II	I	
MA42142-509	14.00	MA	2.2	13.8	-35	21.2	2.3	BB	I	I	
BFQ-23	3.75	AMP	2.2	16.1	-27	10.9	2.3	BB	II	IV	
BFR-90	2.70	AMP	2.2	16.4	-26	9.6	2.3	BB	II	IV	
ON536	3.35	AMP	2.3	14.0	-25	11.0	2.4	BB	II	IV	
MP-1001	8.00	AND	2.4	16.5	-23	*6.5	2.5	BB	II	IV	
BFR-96	4.30	AMP	3.0	14.6	-23	8.4	3.1	BB	II	IV	
NE4162E-2	3.30	NEC	3.7	10.3	-18.5	8.2	3.9	BB	I	I	
MA42003-509	~ 5.00	MA	4.3	7.7	-23	15.3	4.8	BB	I	I	
U-310	4.00	SIL	4.7	5.0	-30	25.0	5.6	10	I	I	FET COMMON GATE

1296 MHz PREAMPLIFIERS

DEVICE	COST $	MFGR	NF (dB.)	Ga (dB.)	Gr (dB.)	Gm (dB.)	M (dB.)	BW (MHz.)	CKT π	CKT μ	PKG	REMARKS
NE21889	75.00	NEC	0.62	18.7	-27	8.3	0.63	40	X		DOE	GaAsFET
MGF1400	23.00	MIT	0.82	16.2	-23	6.8	0.84	45	X		DOE	GaAsFET
NE24483	35.00	NEC	0.83	17.4	-27	9.6	0.84	50	X		DOE	GaAsFET
D432	25.00	DXL	0.97	14.9	-22	7.1	1.00	90	X		DOE	GaAsFET
MGF1200	13.00	MIT	1.03	13.6	-21	7.4	1.07	60	X		DOE	GaAsFET
NE64535	7.50	NEC	1.40	12.0	-16	*4.0	1.48	60	X		DOE	
MS2110JE	~15.00	TI	1.49	12.0	-18	6.0	1.57	140	X		DOE	
NE645+ MRF901	14.55	-	1.61	19.9	-37	11.1	1.62	160		X	DOE	WA2AAU DESIGN
ABT7701	25.00	A	1.63	13.8	-27	13.2	1.69	120	X		DOE	
NE21935	~ 4.50	NEC	1.74	9.9	-19.2	9.3	1.90	180	X		DOE	
NE21937	~ 4.00	NEC	1.79	9.8	-13	*3.2	1.96	100	X		DOE	PLASTIC
HXTR-6105	28.00	HP	1.81	12.2	-24	11.8	1.90	50		X	DOE	μS – BPF
NE73437	3.30	NEC	1.92	6.0	-12	6.0	2.41	200	X		DOE	PLASTIC
HXTR-2101	22.00	HP	2.1	12.0	-21	9.0	2.4	50		X	DOE	μS – BPF
MRF901	1.55	M	2.3	10.1	-16.5	6.5	2.6	120	X		DOE	PLASTIC Avg. of 8 units
			2.3	10.5	-16.6	6.1	2.6	>200		X	DOE	PLASTIC Avg. of 2 units
NE22235	4.00	NEC	2.3	14.0	-26	12.0	2.4	115	X		DOE	
BFR-91	3.00	AMP	2.5	7.6	-14.0	6.4	2.9	100	X		SE	PLASTIC
NE02135	3.50	NEC	2.6	12.5	-22	9.5	2.7	115	X		DOE	Avg. of 5 units
			2.6	9.8	-21	11.2	2.9	>200		X	DOE	Avg. of 2 units
MRF911	2.00	M	2.7	7.8	-17.4	9.6	3.1	150	X		DOE	PLASTIC
BFR-90	2.70	AMP	2.8	7.3	-17.3	10.0	3.2	100	X		SE	PLASTIC
MRF901+ MRF901	3.10	M	3.1	18.3	-36	17.7	3.2	>200		X	DOE	PLASTIC Avg. of 7 units
NE02137	3.00	NEC	2.8	8.3	-12.7	*4.4	3.2	100	X		DOE	PLASTIC Avg. of 2 units
NE02135(TWO)	7.00	NEC	3.0	16.6	-40	23.4	3.0	>200		X	DOE	
BFR-96	4.30	AMP	3.0	6.0	-16.5	10.5	3.6	120	X		SE	PLASTIC
MA42162-511	~18.00	MA	3.5	14.7	-18	*3.3	3.6	140	X		DOE	
MA42141-510	~15.00	MA	4.2	7.3	-14	6.7	4.8	140	X		DOE	

π = CKT. of Fig. 2

μ = Microstrip layout

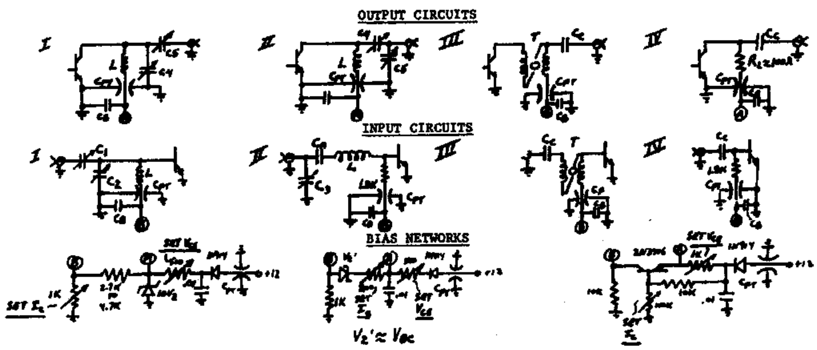

F(MHz.)	C1	C2	C3	CA	CB	Cc	Cft	C4	C5	L	L'	T
30	6-60 pf	6-80 pf	6-80 pf	470 pf	0.05 μf	0.01 μf	0.0015 μf	6-80 pf	6-80 pf	15t #28 on T25-6 core	8-10t #20 formed on 1/4-20 bolt	10t #28 Bifilar on T37-10 core
50	5-25 pf	5-25 pf	5-25 pf	270 pf	0.01 μf	0.005 μf	0.001 μf	5-25 pf	5-25 pf	8t #28 on T25-10 core	5-6t #20 1/8"D, 1/4"L	8t #28 Bifilar on T37-10 core
144	2-20 pf	2-20 pf	1-14 pf	180 pf	0.005 μf	330 pf	680 pf	2-20 pf	2-20 pf	4t #18 1/4"D, 1/4"L	4-5t #18 1/4"D, 3/8"L	6t #28 Bifilar on T25-12 core
220	2-20 pf	2-20 pf	2-14 pf	150 pf	0.005 μf	220 pf	470 pf	2-20 pf	2-20 pf	3t #18 1/4"D, 1/4"L	3-4t #12 1/4"D, 1/4"L	4t #28 Bifilar T25-12 core
432	1-10 pf	1-18 pf	1-10 pf	100 pf	0.001 μf	100 pf	470 pf	1-10 pf	1-10 pf	1t #16 1/4"D or 2" of 1/8"D tube	3-4t of lead of C_A, 1/8"D	4t #28 Bifilar on T25-0 core

EME System Survey

By David G. Meier, N4MW*

This is a computer program entitled "EME System Survey," written in Microsoft BASIC. The purposes of the program are to: (1) help determine what sort of station must be assembled to work earth-moon-earth (EME) or moonbounce paths, (2) compare on-the-air observations with theoretical calculations, and (3) evaluate alternatives for system improvement.

A signal-to-noise ratio of 0 dB represents signal power equal to system noise power. All antenna gains are isotropic. Average lunar distance is assumed; add or subtract one dB for perigee or apogee, respectively. Lunar reflectivity of 6.5% is assumed.

Operation consists of the following steps:

1. Load and run program.

2. Select unknown.

3. Enter variable parameters as prompted.

4. Observe calculated value of unknown.

5. Select new case, new parameter or new unknown.

The program will solve for any of nine parameters. It is not guaranteed to be accurate -- it seems to be conservative. If you can achieve 0 dB, get on the air! I would appreciate your comments.

```
1000 REM EME SYSTEM SURVEY
1010 REM BY DAVID MEIER N4MW
1040 T$(1)="FREQUENCY (MHz)"
1041 T$(2)="TRANSMIT POWER (watts)"
1042 T$(3)="TRANSMIT FEEDLINE LOSS (dB)"
1043 T$(4)="TRANSMIT ANTENNA GAIN (dBi)"
1044 T$(5)="RECEIVE ANTENNA GAIN (dBi)"
1045 T$(6)="RECEIVE FEEDLINE LOSS (dB)"
1046 T$(7)="RECEIVE NOISE FIGURE (dB)"
1047 T$(8)="RECEIVE BANDWIDTH (Hz)"
1048 T$(9)="SIGNAL TO NOISE RATIO (dB)"
1050 CC=1
1200 REM LIST CHOICES
1210 PRINT:PRINT,"*  EME SYSTEM SURVEY  *"
1220 FORI=1TO9:PRINT:PRINT,I"> "T$(I):NEXT
1230 PRINT:INPUT"WHICH IS YOUR CHOICE";CP
1240 IFCC=2ANDCX=CPGOTO1230
1250 IFCC<>2THENCX=CP:IFCC=3GOTO1600
1260 T(CX)=0
1300 REM INPUT PARAMETERS
1310 FORI=1TO9
1320 IF(CC=1ANDCP<>I)OR(CC=2ANDCP=I)THENPRINT:PRI
NTT$(I),:INPUTT(I)
1330 NEXTI
1400 REM CALCULATE AND FORMAT UNKNOWN
1410 X=174-T(3)+T(4)+T(5)-T(6)-T(7)-T(9)
1420 IFT(1)<>0THENX=X-222-20*LOG(T(1))/LOG(10)
1430 IFT(2)<>0THENX=X+30+10*LOG(T(2))/LOG(10)
1440 IFT(8)<>0THENX=X-10*LOG(T(8))/LOG(10)
1450 T(CX)=X:IFCX=4ORCX=5THENT(CX)=-X
1460 IFCX=1THENT(1)=10^((X-222)/20)
1470 IFCX=2THENT(2)=10^(-(X+30)/10)
1480 IFCX=8THENT(8)=10^(X/10)
1600 REM OUTPUT AND CONTINUE
1610 PRINT:PRINT:PRINT
1615 PRINT"*  EME SYSTEM SURVEY  *"
1620 FORI=1TO9:PRINT
1625 PRINTT$(I),INT(10*T(I)+.5)/10,
1630 IFCX=ITHENPRINT"(UNKNOWN)";
1640 PRINT:NEXTI
1650 PRINT:PRINT"1> NEW CASE  2> NEW PARAMETER  3
> NEW UNKNOWN"
1660 PRINT:INPUT"WHICH IS YOUR CHOICE";CC
1670 GOTO1200
```

*3205 Covington Pike, Memphis, TN 38128, 901-377-0834.

See next page for sample run

```
        *  EME SYSTEM SURVEY  *
         1 > FREQUENCY (MHz)
         2 > TRANSMIT POWER (watts)
         3 > TRANSMIT FEEDLINE LOSS (dB)
         4 > TRANSMIT ANTENNA GAIN (dBi)
         5 > RECEIVE ANTENNA GAIN (dBi)
         6 > RECEIVE FEEDLINE LOSS (dB)
         7 > RECEIVE NOISE FIGURE (dB)
         8 > RECEIVE BANDWIDTH (Hz)
         9 > SIGNAL TO NOISE RATIO (dB)
WHICH IS YOUR CHOICE? 9
FREQUENCY (MHz)              ? 144.1
TRANSMIT POWER (watts)       ? 600
TRANSMIT FEEDLINE LOSS (dB)  ? .75
TRANSMIT ANTENNA GAIN (dBi)  ? 27.1
RECEIVE ANTENNA GAIN (dBi)   ? 27.1
RECEIVE FEEDLINE LOSS (dB)   ? .75
RECEIVE NOISE FIGURE (dB)    ? .5
RECEIVE BANDWIDTH (Hz)       ? 100

*  EME SYSTEM SURVEY  *
FREQUENCY (MHz)               144.1
TRANSMIT POWER (watts)        600
TRANSMIT FEEDLINE LOSS (dB)   .8
TRANSMIT ANTENNA GAIN (dBi)   27.1
RECEIVE ANTENNA GAIN (dBi)    27.1
RECEIVE FEEDLINE LOSS (dB)    .8
RECEIVE NOISE FIGURE (dB)     .5
RECEIVE BANDWIDTH (Hz)        100
SIGNAL TO NOISE RATIO (dB)   -1.2          (UNKNOWN)

1> NEW CASE  2> NEW PARAMETER  3> NEW UNKNOWN
WHICH IS YOUR CHOICE? 2
        *  EME SYSTEM SURVEY  *
         1 > FREQUENCY (MHz)
         2 > TRANSMIT POWER (watts)
         3 > TRANSMIT FEEDLINE LOSS (dB)
         4 > TRANSMIT ANTENNA GAIN (dBi)
         5 > RECEIVE ANTENNA GAIN (dBi)
         6 > RECEIVE FEEDLINE LOSS (dB)
         7 > RECEIVE NOISE FIGURE (dB)
         8 > RECEIVE BANDWIDTH (Hz)
         9 > SIGNAL TO NOISE RATIO (dB)
WHICH IS YOUR CHOICE? 2
TRANSMIT POWER (watts)       ? 700

*  EME SYSTEM SURVEY  *
FREQUENCY (MHz)               144.1
TRANSMIT POWER (watts)        700
TRANSMIT FEEDLINE LOSS (dB)   .8
TRANSMIT ANTENNA GAIN (dBi)   27.1
RECEIVE ANTENNA GAIN (dBi)    27.1
RECEIVE FEEDLINE LOSS (dB)    .8
RECEIVE NOISE FIGURE (dB)     .5
RECEIVE BANDWIDTH (Hz)        100
SIGNAL TO NOISE RATIO (dB)   -.5           (UNKNOWN)
1> NEW CASE  2> NEW PARAMETER  3> NEW UNKNOWN
WHICH IS YOUR CHOICE? 3
        *  EME SYSTEM SURVEY  *

 etc.
```

Data Communications

Conducted by
David W. Borden, K8MMO*

Let me introduce myself. I am an experimenter located in the Washington, DC metro area and a member of the Amateur Radio Research and Development Corporation (AMRAD). I have been a radio amateur for 22 years and have owned some form of home computer for six years. Hooking my computer to my ham radio equipment has always been a desired activity. Networking, that is hooking my computer to a large network of microcomputers has also been a long-standing desire of mine. AMRAD has been doing this sort of experimentation for a number of years, but packet radio has really made the idea of a continent-wide network a possibility. The Canadian radio amateurs have a two-year head start on this sort of activity and thus when ASCII was authorized by the FCC in March, 1980, AMRAD looked to the Canadian technology to begin packet radio experimentation.

The Vancouver Amateur Digital Communications Group (VADCG) Terminal Node Controller (TNC) board has since become the *defacto* standard in use by United States radio amateurs engaged in packet radio communications. It is possible that in the construction of a continent-wide packet-radio network, only a very few gateway stations (interfaces to other types of protocols) will be required. Actually, this is not surprising. The TNC board makes entry into packet-radio experimenting painless. The software running on the board can be varied to cause the board to act as a beacon, terminal-to-terminal communications board, repeater or host node for another computer.

Let us begin to examine closely the terminal node controller and the software contained in the PROMs on the board. We will learn what makes it work and discuss possible enhancements if anyone is interested in making any.

The TNC is a packet-radio controller and is not a totally new idea (except to the Amateur Radio community). Dedication of a microcomputer to communications is an old idea to private industry. The idea has lots of merit. A great number of experimenters own microcomputers. If packet radio is the idea of the moment, why not just build a packet-radio board and plug in the already existing computer owned by the experimenter? That idea has some merit also, and will be examined in future columns. But, the microcomputer owned by the experimenter would have to work almost full time making packets if it were to take on that task. No (or very few) cycles would be left over for computing in that mode. It makes more sense to devote a single-board microcomputer to the communications task and save the "big machine" for normal computing. A few words about applications may be in order here.

In a fully connected network, each end user employs a TNC board. It acts as a "black box" communications controller. One of the RS-232-C ports on the TNC board is connected to a Bell 202 modem and radio (typically two-meter fm). The other port may be connected to any number of devices such as:

- a data communications terminal (teletypewriter or TV typewriter)
- a serial printer
- a serial facsimile machine
- a computer (called "host node")
- a speech interface
- a remote telemetry site serial interface.

Thus it should become clear that the "black box" TNC takes care of all communications, and the experimenter concentrates on using the computer to maximum benefit for network users of like thinking. In fact, greatest benefit to all accrues when a fully connected network is "out there." Building an experimenters network, similar to the commercial GTE Telenet or the government ARPANET is what this effort is all about. Shared data bases, almost instant communication between experimenters of like interests is the desired end result. Puting this newsletter out of business, or at least making it totally electronic, is a possibility. The beginning (and ultimate bottom line) is that all users will own TNC boards and enter data into the network and remove data from the networking using it.

Wait a minute, you say! You mean I have to buy this TNC to just get in on the action? Yes, that is the intent. But stop and think about it a minute. You did not complain when you had to buy a transceiver to join in on fm activity in your area. You did not complain when you had to buy a TV set to receive entertainment from the ether. The TNC board is just another appliance required to gain benefit from the experimenter network. Wait again, you say. I am not an appliance operator or I would not be reading this publication. The truth slips out at last. The true experimentation and developmental work to be done does not lie on the TNC board and will not change much in the next year. It has reached a state of →

*Route 2, Box 233B, Sterling, VA 22170, 703-450-5284.

acceptability. The great work to be done lies in the station nodes that enter local area data onto the backbone network. These computers will not be TNC boards. They will require more memory and much more program. But it all begins on Doug Lockhart's TNC board. So, let us begin our study of it as an introduction to packet radio communications.

The hardware of the TNC packet radio communications controller board uses an 8085 microprocessor. This chip is almost identical to the familiar 8080 microprocessor except for the superior interrupt structure it enjoys and a few extra instructions to control the interrupts. 4k of 2708 EPROM memory contains the resident programs (2). 4k of 2114 RAM memory is used to buffer data and maintain needed variables (pointers, etc.). An 8273 high-level data-link controller performs all the actual work of generating a bit-oriented (HDLC) protocol. This bit-oriented approach (as opposed to the start-stop byte-oriented protocol) puts the radio amateur near the state of the art in data communication. Bit-oriented protocols are very efficient. The user connects his/her serial device to an 8250 USART device or an 8255 parallel device as desired (greatest use is made of serial devices currently).

Some features of the serial interface are: asynchronous with 5-, 6-, 7- or 8-bit characters; even, odd or no-parity bit generation and detection; 1 and 1.5 stop bit generation and detection; full double buffering; prioritized interrupts under software control; and, all modem signals (RTS, CTS, DSR, DTR, RI and CD).

The study of the software running on this board will occupy several future columns. The bare board and documentation may be purchased from VADCG, and details on ordering were published on page 30 of *QST* for October 1981.[1] Software is in the public domain and available on CP/M floppy disk from VADCG or on line (300-baud Bell 103 modem) from the AMRAD Computerized Bulletin Board System (CBBS), 703-734-1387.

It is not intended to print the software here, so copies should be obtained for study with the explanations provided in this column.

In the next issue, we will begin study of the Line Interface Program (LIP) which controls the 8273 HDLC chip.

[1]Borden and Rinaldo, "The Making of an Amateur Packet-Radio Network," *QST*, October 1981, p. 28.

Learning

Ed. Note: This column is to let the experimenter know about short courses, technical talks, books and other ways of keeping up with the continuing education process. It is unfortunate that the university short courses and commercial video tape productions cost as much as they do. We will include some of the more interesting ones on the chance that your employer might pick up the tab. What we'd really like to see is some courses and video tapes done by and for amateur experimenters and available at cost. Please let QEX know of any of these about 2 months ahead of time so we can get the word out.

New Book on Packet Switching

This new book entitled, "Packet Switching: Tomorrow's Communications Today," by Roy D. Rosner, K4YV covers techniques, equipment, standards, commercial services and other related topics. It is available at $34 from Lifetime Learning Publications, 10 Davis Dr, Belmont, CA 94002, 415-595-2350 or 606-525-2230.

Long Island 2-Meter Technical Talks

W2KPQ will transmit technical talks for the LI chapter of the IEEE and LIARC on 147.375 MHz at 8:30 P.M. certain evenings. Dec 9 topic will be secure communications, while spread-spectrum communications will be taken up on Jan 13, 1982. For more info contact Ed Piller at 516-349-2484 (work) or 516-938-5661 (home).

Data Communications Chip Workshop

Intel is sponsoring courses in Chicago Dec 14-17 and Feb 15-18 on the following communications chips: 8251A, 8253, 8256, 8273, 8274 and 8051. The 4-day course also covers protocols, modems, X.25 and Ethernet. Fee $795. Contact 312-981-7250.

Protocols for Packet Switching Course

On Jan 7-8, George Washington University, Washington, DC 20052, 202-676-6106, is offering this course in Washington, DC. The course fee is $530.

IEEE Course via Satellite TV Broadcast

The IEEE will begin a course on project management on Jan 12 from TV station WRLK in Columbia, SC. It will be telecast via Satcom I and Westar from 10 A.M. to noon and 2 to 4 P.M. EST for reception by TVRO antennas at universities, cable services and public TV stations. The course fee is $125 members, $150 nonmembers. Call 212-644-7871.

Circuits

Conducted by Bob Heil, K9EID*

Amateur Radio - The Greatest Hobby

Amateur Radio has been one of the most fascinating hobbies since the early 1900s, when Marconi began experimenting with "wireless." Amateurs have a craving to work with equipment, to achieve things that haven't been done, or to do things that others say can't be done.

It will be the purpose of this column to present some practical solutions. Let us hear from you, and let's make this a useful tool for the fraternity.

Multi-Purpose Preamplifier

This utility amplifier is a valuable tool for the experimenter, for tracing signals, testing for audio changes or listening to weak af signals. Be sure to use a high quality shielded cable for the input test lead. You can also use it for a crystal or dynamic microphone. Mount the microphone in a parabolic reflector such as a large hub cap or saucer sled to listen to things far away. A telephone pick-up coil on the input will allow you to detect electromagnetic signals from motors, power lines and some electronic watches.

You can spend countless hours experimenting with other transducers and detectors. Adding a tuned circuit and a diode will allow you to hear a-m broadcast stations. A suitable diode (1N21 or 34) and a uhf loop antenna will hear signals up to several GHz.

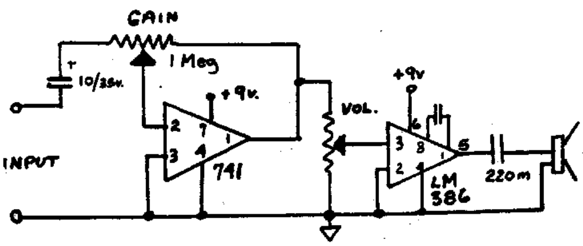

Solid-State Switching

Solid-state technology is making it much easier to switch voltages and currents with transistor switches instead of old mechanical relays. Reliability is much better, transients are reduced, and the keying is much faster. You can also get rid of those horrible "clunking and clicking" sounds of the mechanical devices.

Some circuits do not lend themselves to solid-state switching, but devices are available for switching just about any frequency and current that we could imagine. High-speed diodes will switch uhf antenna systems, SCRs can be used to switch ac power lines, while LDRs (light dependent resistors) mounted with photo cells make terrific devices to hang across signal lines without disrupting the circuit.

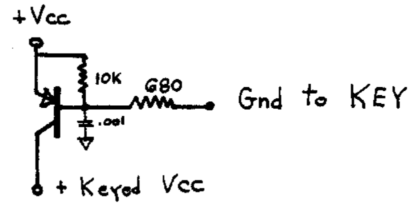

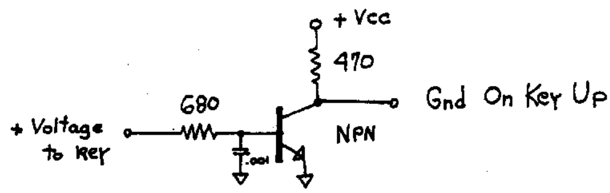

In the two circuits shown, the npn device is used to bring a control line to ground, while the pnp circuit is used to produce a positive voltage control. By combining the two, you can have various combinations of switching from zero to + voltages of around 24 volts.

Be cautious not to exceed the current capacity of the device. Should you need more current-handling capability, you can use one small device to drive a larger device such as a 2N3055, to give you 10 to 12 amps of current capacity. Several of the 3055s can even be paralleled to give you lots more.

It is advisable to bypass the inputs and outputs of the devices so that spurs up in the rf spectrum are not created as they can cause all kinds of havoc around radio receivers! Use the good building practice of short leads and proper harnessing to keep things away from rf and magnetic fields.

Have fun and keep those soldering irons hot!

*P.O. Box 68, Marissa, IL 62257, 618-295-3000 work, 618-295-2383 home.

Products

Ed. Note: This column is for calling your attention to new products and perhaps some that have been around for a while and not noticed by the amateur experimenter. This information is based largely on manufacturers' releases and has not been independently verified. New product information is published without ARRL endorsement and without any implication that the products have been examined in the ARRL laboratory. Readers are invited to send new product information on items of particular interest to the experimenter to the Editor, QEX.

Switched-Capacitor Audio Filters

EG&G Reticon, Sunnyvale, CA 94086, 408-738-4266, has announced nine models of general-purpose monolithic audio filters using the switched-capacitor technique. They can be used for low-pass, high-pass, band-pass and notch filter requirements at audio frequencies. The 5609 is a low-pass filter. The 5610 is a programmable array of four state-variable filters, each filter section having a low-pass and high-pass output. The 5611 is a high-pass filter. 300-baud modem filter requirements can be handled by the 5630 which has double band-pass filters for each frequency band. Unit prices (if they exist) are unknown. Large quantity prices are around $7.

Dot-Matrix LCD for Pocket Terminals

The PCIM 200 liquid crystal display (LCD) can display up to 54 ASCII characters. Overall dimensions are 69 by 10 by 38 mm. It operates from a single 5-V power supply and draws 7.5 mA. Price (in 100s) is $48. Contact James Pfieffer, Printed Circuits International, Sunnyvale, CA 94086, 408-733-4603.

RS-232-C Connector Cutouts

MISCO, a computer supply and accessory mail order house, has in their latest catalog some standard 19-inch panels with 16 and 32 cutouts for DB-25 data connectors at $65 and $95 respectively. Write: MISCO Inc., Box 399, Holmdel, NJ 07733. Other computer supply dealers may have them, so you may find a better price by looking around.

The above panels would be difficult for the average experimenter to homebrew using the time-honored drill-and-file technique. Does any reader know of the availability of (Greenlee or other) DB-25 punches?

Computer-Controlled Drill Press

Black & Decker's new 9413 drill press sports a built-in microcomputer which: a) maintains constant speed under varying loads, b) digitally displays depth to 0.02 inch, c) gradually shifts speed when changing drilling speeds, d) remembers last speed used, and e) blinks display and shuts down when incorrect speed and drilling pressure are used. The price is around $200. It is available from Black & Decker consumer products stores.

Clock-Controlled Active Filter

National Semiconductor has announced a type MF10 CMOS monolithic active filter IC in 20-pin DIPs. They can be used to implement classical filter configurations such as Chebyshev, Cauer, Bessel or Butterworth. The MF10 includes separate bandpass, low-pass and high-pass outputs. Contact Art Coon, 408-737-6527. Price is $3.70 each (100s).

Packet Radio Terminal Node Controllers

Dave Borden, K8MMO, Rt 2, Box 233B, Sterling, VA 22170 has Vancouver Amateur Digital Communications Group Terminal Node Controller pc boards for $30 and the basic 8273/8250 chip set for $46.50. Please add $2 for postage. They are also available on the West Coast from Hank Magnuski, KA6M, 311 Stanford Ave, Menlo Park, CA 94025. A complete TNC board (with the other parts added) will cost around $250.

Power Line Noise Detector

Caywood Electronics, Inc., 67 Maplewood St, P.O. Drawer U, Malden, MA 02148, 617-322-4455, is offering Millen type 71001 power line noise interference detectors for $220. It is used with an oscilloscope or panel-meter-equipped receiver.

Monolithic Filter for RS-232-C Ports

ITT Cannon is one of several companies manufacturing one-piece RFI/EMI filters with male and female DB-25 data connectors. The filter is designed to help computer equipment meet FCC Docket 20780. Price is not known. For more info contact Jack Engbrecht, Cannon Electric Division, 2801 Air Ln, Phoenix, AZ 85034, 602-275-4792. The filter is mounted between the normal male and female DB-25 connectors such as I/O ports on a personal computer back panel.

Correspondence

Data on New Products

I hope that your new publication will include some information that is not generally available to those hams not directly active in the electronic design field. Now that I am retired I do not have access to the free publications that announce new products & piece parts. To continue experimentally with electronics I need data on such items as low noise vhf & uhf transistors and rf (power) amplifier transistors. - *Eugene Sternke, K6AH, 106 Vancouver Pl, Sequim, WA 98382.*

Theoretical Void

You will be interested to know that your invitation to subscribe to *QEX* which was published in *QST* for August appealed to my curiosity, and I have today sent a check for the first 12 issues to Newington. A particular void that seems to exist in amateur radio publications is the absence of new theoritical work of the kind that appears in engineering and scientific journals, as opposed to descriptions of applications. Of course, hams are not usually concerned with doing new theoretical work, but they must know of it in order to be inspired to use it. I therefore suggest that one feature which would be of value in *QEX* would be regular reviews of information published elsewhere but of interest to hams. - *Michael S. Bilow, N1BEE, 40 Plantations, Cranston, RI 02920.*

Kepro Electroless Tin Plating Kit

Professionally done printed circuit boards have a nice bright silver appearance. This "silver" is actually a tin plating which has been electrochemically bonded to the copper surface with expensive plating machinery. Now, the amateur can make professional looking boards by using the Kepro kit. It consists of one quart of plating fluid, a glass tray, a thermometer and a pair of tongs. The kit will plat a ten-millionths of an inch thick tin coating on up to 25 square feet of pc board.

The tin plating material is very toxic, so caution must be exercised. First, a pc board is etched in the normal manner and dried after washing. Before plating, the board must be carefully scrubbed with steel wool to remove all etch resist. Any remaining resist will result in poor plating of that area of copper. After cleaning, the board is immersed in the plating solution at room temperature for about three minutes, then washed. The result is a professional looking pc board.

The plating serves a more valuable purpose than making esthetically nice looking boards too. The tin gives the builder a good base to solder to and also prevents oxidation of the copper clad surface which can result in resistive traces and the inability to resolder connections after a time.

The kit is reasonably priced (around $20) and may be obtained from your local distributor or from Kepro Circuit Systems, Inc., 630 Axminster Drive, Fenton, MO 63026. - *Mark Forbes, KC9C, 1000 Shendoah Dr, Lafayette, IN 47905.*

QEX: The ARRL Experimenters' Exchange is published by the

American Radio Relay League
225 Main Street
Newington, Connecticut 06111
telephone 203-666-1541

The purposes of QEX are to:

1) provide a medium for the exchange of ideas and information between Amateur Radio experimenters,

2) document advanced technical work in the Amateur Radio field, and

3) support efforts to advance the state of the Amateur Radio art.

QEX subscriptions are available to ARRL members at the special rate of $6 for 12 issues. For nonmembers, the subscription rate is $12 for 12 issues. The foregoing rates apply only to subscribers with mailing addresses in the U.S. and possessions; Canadian and Mexican subscribers must add $1.74, and will be serviced by First Class mail. Overseas subscribers should add $6.78 for air mail delivery or $2.34 for surface mail. Because of the uncertainty of postal rates, prices are subject to change without notice.

Applications for subscriptions to QEX should be sent to the American Radio Relay League, Newington, CT 06111. Members are asked to include their membership control number, or a mailing label from their QST wrapper.

QEX is edited in, and mailed from, McLean, Virginia. Authors are invited to submit articles to Editor, QEX, 1524 Springvale Ave., McLean, VA 22101. Both theoretical and practical technical articles are welcomed. Manuscripts should be typewritten and double spaced. Please use the standard ARRL abbvreviations found on page 65 of the December 1980 issue of QST. Authors should supply their own artwork using black ink on white paper. When essential to the article, photographs may be included. Photos should be glossy, black-and-white prints of good definition and contrast.

Any opinions expressed in QEX are those of the authors, not necessarily those of the editor or the League. While we attempt to ensure that all articles are technically valid, authors are expected to defend their own material.

QEX: The ARRL
Experimenters' Exchange
1524 Springvale Avenue
McLean, VA USA 22101

Nonprofit Organization
U.S. Postage
PAID
McLean, Virginia 22101
Permit No. 235

Scott Roleson, KC7CJ

14938 Amso St., Poway, CA 92064; **kc7cj@arrl.net**

Re-Purposing an Obsolete Instrument Enclosure

Recovered obsolete test equipment becomes a rugged and attractive new project enclosure.

While searching for an enclosure for a new project, I was not impressed by the folded sheet-metal boxes typically available. I wanted something better that wouldn't cost much more than those typical boxes but would be rugged and relatively easy to modify. Searching the Internet, I stumbled on an advertisement for an HP-436A Power Meter "non-working, parts only" for US$20 from an industrial liquidation firm just across town. I found they had two units available. Both had obviously seen a lot of use, but I happily handed over the $20 for the one that appeared least abused. It was about the right size for my project, if I could strip out the innards and if the instrument's "bones" were recoverable.

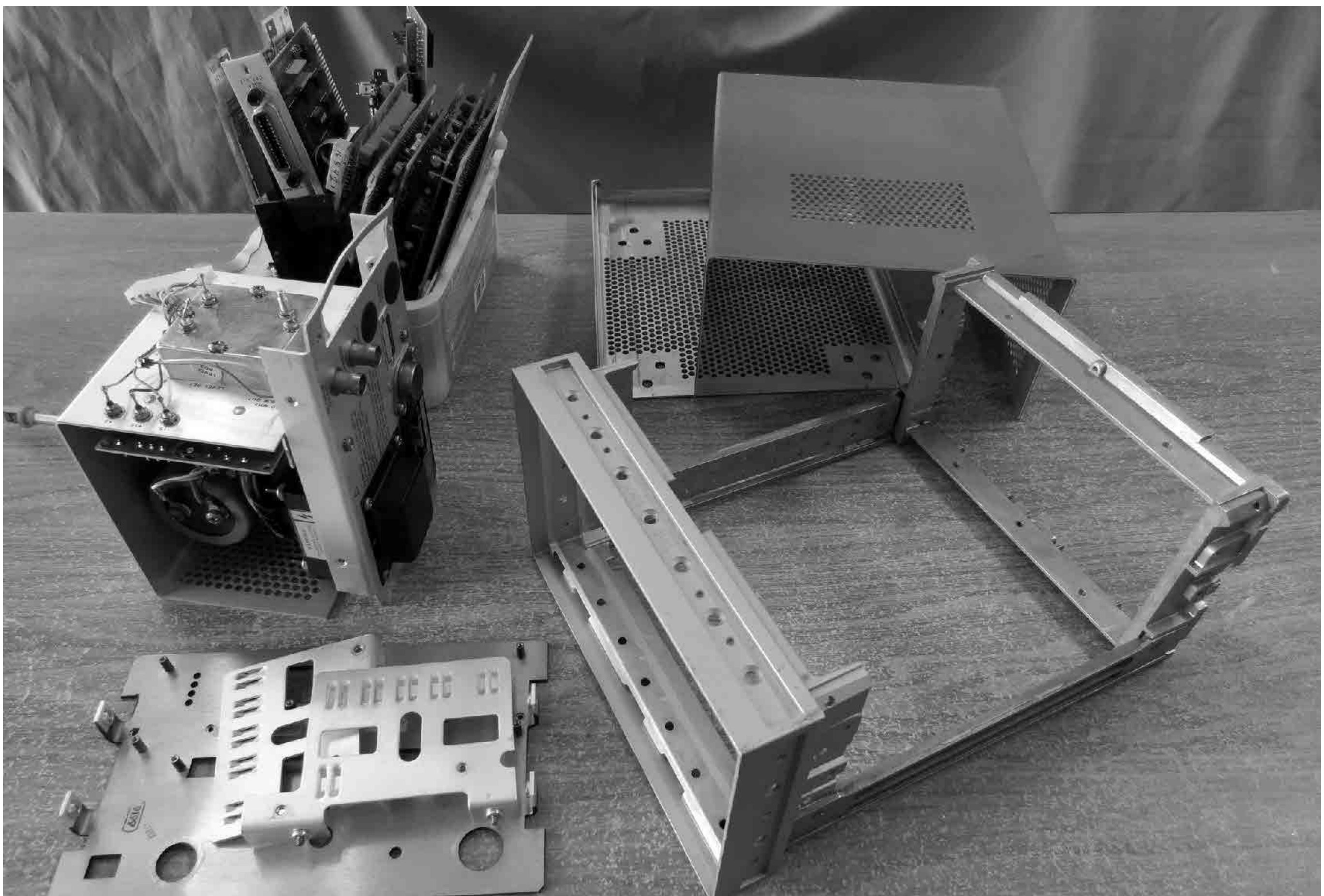

Figure 1 — Disassembled HP-436A power meter.

Background

The HP-436A Power Meter dates from the mid-1970s, and its industrial design was based on the rugged Hewlett-Packard System II instrument enclosure.[1] This cabinet design was used with many HP laboratory instruments and was compatible with standard 19-in equipment racks. The cabinets could easily nest together to form rack-mountable systems, or could be used individually on a lab bench. The HP-436A was a half-rack wide — about 8-5/8 in — and had a standard 4-EIA height — just under 6 in with feet attached — and a depth just under 11 in. Its cast-aluminum internal front and back frames, and the two horizontal side frames, were designed to form a very rigid frame held together by 8 flat-head #8-32 machine screws in threaded holes. With the top and bottom covers installed, the enclosure also provided some degree of RF shielding.

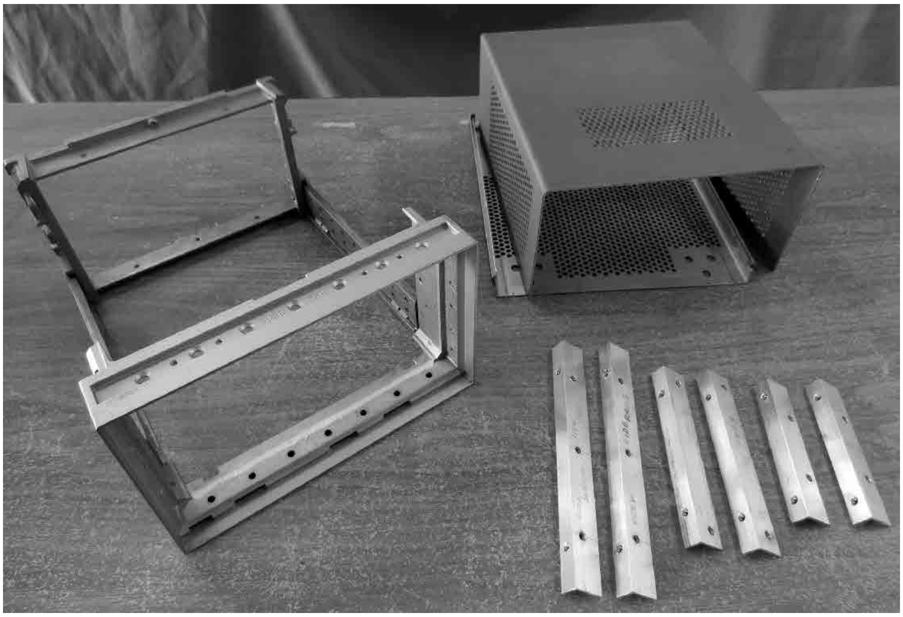

Figure 2 — Recovered instrument frame and new brackets.

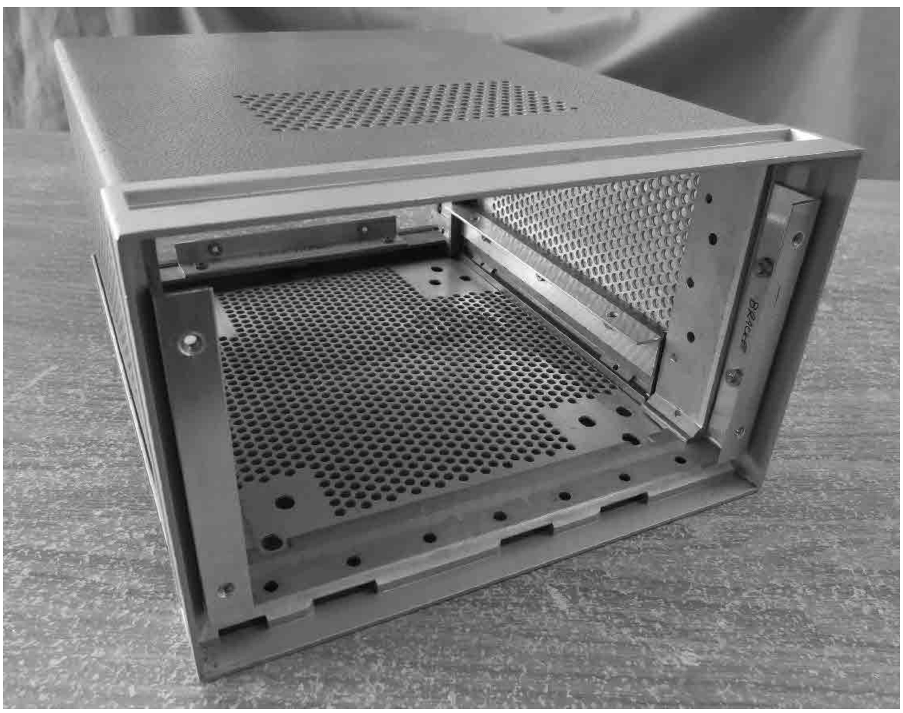

Figure 3 — Instrument frame with new brackets installed.

Disassembly

Just to make sure it really was non-working, I plugged it in, and saw that some, but not all, of the display digits lit up. I saw no smoke, but I didn't leave it turned on very long just in case. As advertised, it was "non-working." Having satisfied my lingering guilt that I might destroy a repairable instrument, I began a careful disassembly. I took my time because they don't build stuff like this anymore.

Several pleasant hours later I had recovered the cast-aluminum front and rear panel frames, two cast-aluminum horizontal frame parts, the outer enclosure shell (top and bottom painted sheet aluminum covers), and some useful screws. I set the rest aside for recycling, including the original front panel and rear panel with integral power supply (Figure 1). While potentially useful, I didn't need this power supply for my intended project, and the holes in the front and rear panels were not where I wanted them. I also set aside a pair of printed circuit card support frames that were not suitable for my new project.

Clearly the result of superb industrial design, I was pleased to find this instrument case in reasonably good physical condition. There was clear evidence of heavy use and possibly some abuse. The slightly indented front panel in the area of a type-N connector suggested that the instrument had once been dropped on its face. I was planning to make a new front panel anyway so this minor damage didn't matter. Liquid stain marks on the inside surface of the shell, along with some dried, brown sludge on the horizontal frame parts, implied that perhaps a small quantity of heavily-sugared coffee or brown soft drink had been spilled into the instrument long ago. A dish-soap warm water scrub of the disassembled structural components removed these remnants of a hard prior life.

Reassembly

I then got busy cutting new flat sheet aluminum front and rear panels, and an internal electronics deck to hold the new project.[2] The original design for the front and rear panels used sheet metal with bent integral brackets screwed directly into the frame. It's a great design if you are building lots of these, but this was more than I wanted to tackle for my one-off job. Figure 2 shows six L brackets, each several inches long, that I cut from 1/2 by 3/4-in extruded aluminum angle stock bought at a local home supply store. This angle stock came in 48-in long

Figure 4 — Finished enclosure showing sheet aluminum panels installed.

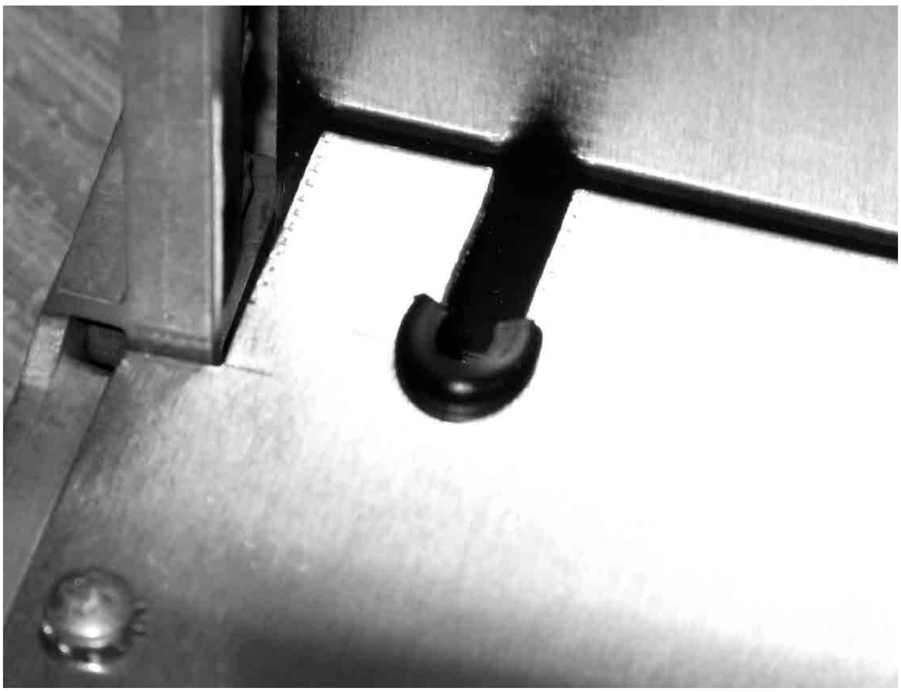

Figure 5 — Access slots in electronics deck facilitate wire/cable routing.

pieces, which easily allowed for the six brackets and some mistakes!

To simplify assembly, I mounted #6-32 swage or self-clinching nuts in the angle bracket mounting holes to avoid having to deal with nuts and washers.[3] Swage nuts also allow quick removal of both the front and rear panels. Mounting these nuts was tricky — not having an arbor press, I managed to press them into the mounting holes with a small and a large vice. I clamped the small vice to a support so the jaws closed vertically and used it to make an initial set. Then I used the large vice with horizontally closing jaws to make the final set. This seemed to work reasonably well.

Figure 3 shows the new brackets ready to hold the front and rear panels to the front and rear frames and the internal deck to the side rails. I mounted the electronics deck brackets on the side rails such that the brackets were even with the upper edge of the side rails. This arrangement provided more than an inch of clearance below the deck and about 3 inches above. The deck turned out to have just over 65 square inches of usable surface area. Figure 4 shows the completed frame with the front and rear panels and the electronics deck installed.

I thought about routing wires or cables between the upper and lower parts of this deck using simple holes and grommets. Instead, I punched 1/4-in diameter holes about an inch from each deck corner then used a metal nibbler to cut a connecting slot from the edges facing the nearby front and rear panels (Figure 5). A vinyl grommet cut in half provided abrasion relief. This way I don't need to remove the electronics deck just to route some wires, but can access these slots by removing a panel.

Table 1 shows that the finished material cost was just under $70. Figure 6 shows the final product, a rugged and attractive enclosure ready for my next project.

Scott Roleson, KC7CJ, was licensed in 1964. He has a BSEE from Arizona State University, and MSEE from the University of Arizona, is a licensed professional engineer in California, and is a Life Senior Member of the IEEE. From 1993 to 1995 he was a Distinguished Lecturer of the IEEE EMC Society, and was the Distinguished Lecturer program chair

Table 1
Re-purposed instrument materials list.

Item	*Qty*	*Suggested source*	*Cost, US$*
HP-436A, non-working	1	See Note 4	20
Aluminum, grade 5052, 12 by 24 in sheet, 0.063 in thick	1	**amazon.com**	27
Aluminum angle stock, 0.75 x 0.5 inches, 0.063 in thick, 48 in long	1	**www.homedepot.com**	6
Clinch nuts, #6-32-2	30	**www.fastenal.com**	15
Total			**$68**

1995-1997. Scott retired after a 32-year career in electrical engineering where he worked on spectrum analyzer design, EMC and telecom regulatory engineering. Scott now gets to pick his own projects and maximize the fun return on investment.

Figure 6 — Finished re-purposed enclosure is both rugged and attractive.

Notes

[1]E. Allen Inhelder, "A New Instrument Enclosure with Greater Convenience, Better Accessibility, and Higher Attenuation of RF Interference," *Hewlett-Packard Journal*, Vol. 27, No. 1, Sept. 1975, pp. 19-24. [Online: **www.hparchive.com/hp_journals.htm**]

[2]Sheet aluminum is available from several online vendors. I bought a 12 by 24 in sheet of 1/16 in grade-5052 aluminum from **amazon.com**. This was more than sufficient for the front and rear panels and the internal deck.

[3]Swage or "self-clinching" nuts are designed to permanently anchor in sheet metal and provide load-bearing threads. They do away with the need for separate, loose nuts and washers. See **www.pemnet.com/fastening_products/pdf/Handbook.pdf** and **https://www.fastenal.com/content/product_specifications/SCN.Z.pdf**.

[4]Possible sources of surplus equipment include hamfests, swap meets, and ham estate sales, as well as, Sphere Research Corporation, **www.sphere.bc.ca** +1-250-769-1834, and Test Equipment Depot, **www.testequipmentdepot.com**.

Flavio Egano, IK3XTV

Via N. Sauro 20, Thiene (V) 36016, Italy; **ik3xtv@gmail.com**

A Study of Long Path Echoes

Long term observations by IK3XTV suggest that long path echoes might propagate with low attenuation by ionospheric ducts.

Introduction

I've listened to many transmissions — both in telephony and telegraphy — that are characterized by a pronounced echo effect. Intrigued by this phenomenon, I enlisted the help of Annibale Malagoli, IK2GRA, and Loris Bonora, IK3PCZ, to make further measurements and to research the echo phenomenon on their transmissions. My papers (available online in Italian)[1, 2] report some experimental reception of echoes on the 15 m and 10 m HF bands, that I believe are due to multiple reception via short and long path. Under the right conditions, the signal can be received via both the short path and the long path. The resulting multipath generates a significant echo effect. The time it takes a radio wave to make a complete revolution of the Earth's circumference is 40,021 / 299.792458=133 ms. The literature on the radio propagation reports long-path propagation delay of as much as 138 ms, since they take into account a further 1400 km length of the route due to reflections between the Earth and the ionosphere (ionospheric jumps). In most cases we measured a consistent delay of 140 ms.

My belief is that this type of propagation is not via the classic ionospheric reflections, but by a the mechanism of ionospheric low-attenuation ducting.

The Long Path Signal

Figure 1 shows a very short extract from a recording of a CW signal transmitted by Upcev Anton, YU5D, and received by Annibale Malagoli, IK2GRA. The first dash is the CW signal received via the short path distance of about 650 km. The second dash, slightly overlapping the first, is the echo of the first dash, that it is probably received from the long path with a very low attenuation of about 3 dB more than the short path signal. I have analyzed the audio track in great detail and speculate that it is possible that the signal of YU5D has made a further circuit round the Earth within an ionospheric duct. I can also detect another signal echo, that might be called Long Path+1 (LP + 1), starting at about 270 ms from the main short path signal. This LP +1 signal shows an additional 3 dB attenuation and it is evident above the background noise.

The Equipment

The station configuration for reception is a Kenwood TS930S transceiver with a Hy-Gain AV-640 vertical multiband antenna. The receiver AGC setting is zero. The MP3 software program was *QARTest* by IK3QAR recorded by a PC with a sound card. The receiving frequencies were in the 28 and 21 MHz bands.

Audio recordings were analyzed with *Audacity*, a free open-source cross-platform software for recording and editing sounds. The transmissions were on a frequency in the 28 MHz band on December 22, 2013 at 11:00 UTC. The solar indices at the time were SFU 144 and Kp 1.

Ionospheric Ducts

I am convinced that the HF propagation in the ionosphere does not always occur according to the classical model of ionospheric/ground reflections, but in some cases there is the phenomenon of ionospheric ducting. The high plasma density of the duct is capable of trapping radio signals. The radio waves may follow a spiraling motion within these ducts with very low attenuation. Moreover, propagation often occurs towards trans-equatorial paths, considering that the lines of force of Earth's magnetic field are oriented from north to south. It also appears possible that the signal can make more than one revolution within the duct. The formation and the efficiency of the ducts seems to be much greater when the geomagnetic field is quiet.

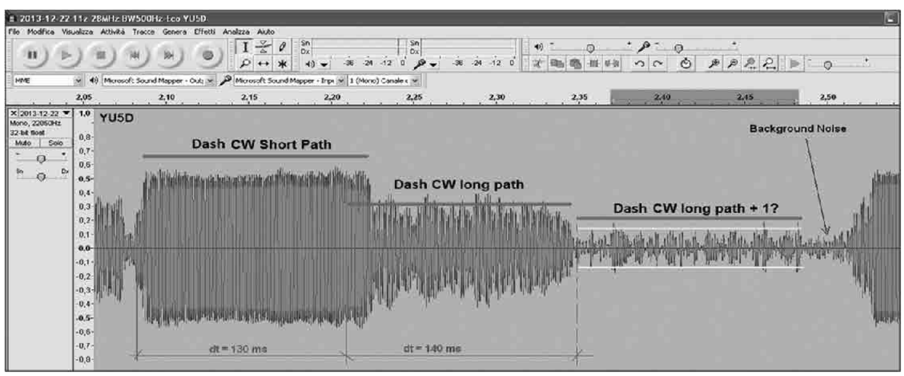

Figure 1 — Reception of YU5D by IK2GRA. This sample recording of a 28 MHz band CW dash signal was received via short path, and the first echo is received via long path with a delay of 130 ms.

The ducts form for certain frequencies, from long wave to short wave, the height of the ducts is variable and the delays are related to the frequency and height of the duct. I generally observed the event when the operating frequency was near the F2 critical frequency.

The existence of these geo-magnetically aligned structures is consistent with studies[3] conducted using the Murchison Widefield Array and published by Shyeh Tjing [Cleo] Loi, an Australian astrophysicist at the University of Sydney School of Physics. Loi is credited with the first imaging of Earth magnetic field aligned density ducts inside the Earth's magnetosphere that extend into the plasmasphere.

Attenuation

Signal attenuation is an important issue. All observations and recordings of echoes from long path show very low attenuation. In the case of Figure 1, YU5D short path is 650 km, while the long path is 39,400 km, a ratio of 60:1. According to inverse square law propagation, the attenuation difference should be 20log60 = 35 dB. Instead it is 3 dB. Clearly the propagation can not be free space propagation, but rather a duct mode propagation, similar to a microwave waveguide.

Conclusion and Acknowledgements

It is not clear what processes can produce echo ducting conditions in the ionosphere. I think that further studies are needed to understand the impact that this discovery can have on HF radio propagation. Recordings of the echoes were made during a high phase of the solar cycle. I would like to analyze the impact in the low phase of the solar cycle to understand the role of the solar cycle in the mechanism.

Special thanks to Cleo Loi for providing me with material and some additional information. Thanks to Adolfo Brochetelli, IK1DQW, for his cooperation. His experience as Officer (Radio Telegraphist) in the Italian Navy has been a great help to me. Thanks to Annibale Malagoli, IK2GRA, and Loris Bonora, IK3PCZ for several audio recordings and reports.

Flavio Egano, IK3XTV, has been an Amateur Radio operator since 1993 with a Class A license. He is an ARRL member and a member of ARI, the Italian Amateur Radio Association. Flavio has spent many years studying radio propagation. He successfully completed and passed, "Sensing Planet Earth – from Core to Outer Space," a course offered by Chalmers University of Technology, an online learning initiative through EDX. Flavio is an electronics engineering technician in Italy, and works as a technical salesman for a multinational company. He lives with his wife and their daughter in Thiene, Vicenza Province, Italy.

Notes

[1]**www.qsl.net/ik3xtv/ARCHIVIO/studio%20sugli%20echi%20long%20path.pdf**

[2]**www.qsl.net/ik3xtv/ARCHIVIO/studio%20sugli%20echi%20long%20path-%20sintesi.pdf**

[3]Shyeh Tjing Loi, et al. [40 co-authors], "Real-time imaging of density ducts between the plasmasphere and ionosphere", *Geophysical Research Letters*, Vol. 42, Issue 10, pp. 3708-3714, 25 May 2015.

Tom C. McDermott, N5EG

3950 Southview Ter., Medford, OR 97504-9367; **n5eg@tapr.org**

Measuring the Ionosphere at Vertical Incidence using Hermes, Alex and Munin Open HPSDR and Gnuradio

A version of this article appeared in the Proceedings of the 34th ARRL/TAPR Digital Communications Conference, Chicago, Illinois, October 9-11, 2015.

This paper describes a monostatic method for measuring the virtual height and the vertical velocity of the F-layer of the ionosphere. The equipment uses the Open HPSDR Hermes transceiver module, Munin broadband power amplifier (PA), and Alex RF filter module. The antennas consist of a 40 m dipole and antenna tuner for transmit and an active receive loop antenna. The software real-time processing is done using Gnuradio on a Linux PC, followed by post-processing by a Python program.

Ionosphere

Figure 1 shows typical critical frequency for the E- and F-layers versus local time of day. While the MUF depends on the angle of incidence to the ionosphere, the critical frequency is defined at vertical incidence. Measuring the E-layer requires using the 160 m band. Measuring the F2-layer critical frequency can be done on the 80 m band much of the day, and sometimes on the 40 m band. When measuring the F-layer, the higher the frequency used the less the F-layer echo attenuation caused by transiting the E-layer twice.

The ionosphere reflects vertically incident signals below the critical frequency. The time-of-flight of the transmitted plus return signal indicates the height of the ionospheric layer. Additionally, the ionosphere layer may have a vertical velocity — either upwards or downwards — that induces Doppler shift onto the reflected signal. Figure 2 shows the basic setup. Transmit and receive antennas are located within about 100 ft of each other, and configured as a monostatic radar.

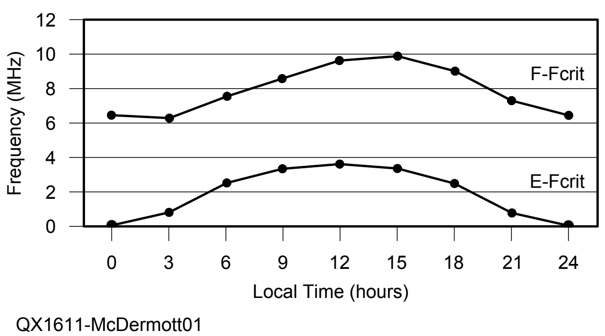

Figure 1 — Typical critical frequencies for E- and F- layers, summertime, 40 degrees N, local solar time, Sunspot Number = 86.

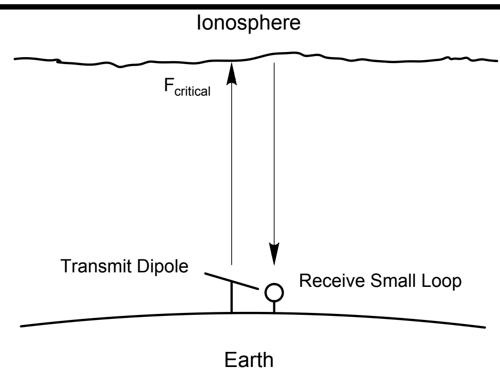

Figure 2 — Basic setup: co-located transmitter and receiver and antennas.

Chirp Measurement

Practical measurements pose some difficult requirements because the echo is delayed less than 1 ms for the E-layer, or about 1.6 ms for the F-layer. The monostatic approach also means that the transmit signal will be much stronger than the received signal, thus the receiver dynamic range must be large.

We transmit a linear FM chirp signal and correlate the received signal against the signal used to drive the transmitter — a matched filter approach. The number of correlation taps is large in order to provide enough dynamic range and time resolution to see echoes 100 dB below the transmit signal. This approach requires full-duplex equipment. If the transmitter and receiver are co-located the transmit signal tends to overload the receiver. The present experiment uses co-located transmitter/receiver (Tx/Rx) on the same circuit board, and Tx/Rx antennas separated by about 20 m. A similar experimental approach using 60 m antenna separation was previously demonstrated by the Institute of Solar-Terrestrial Physics.[1] The low phase-noise and good ADC dynamic range performance of the Hermes receiver helps minimize receive noise that would otherwise obscure the desired receive echo.[2] Chirp modulation is discussed in some recent Amateur Radio literature.[3]

A linear FM-chirp signal is a constant-amplitude signal that sweeps in frequency at a constant rate. For example, an up-chirp could sweep from $-f_d$ kHz below the channel center frequency to $+f_d$ kHz above the channel center frequency, then 'snap back to $-f_d$ kHz and start again. It's possible to turn off the transmit signal for a period of time during the retrace. The turn-on and turn-off parts of the signal are amplitude ramped with a raised-cosine waveform to prevent spectral transients. A down chirp starts above the channel center and sweeps down at a constant sweep rate to below the channel center frequency.

The received signal is correlated against a stored version of the transmit signal. The DSP correlation filter is acting as a matched filter of the chirp signal. When using a chirp to measure the ionosphere we are searching for a weak replica of the chirp delayed by the propagation delay, equipment delay, and frequency shift due to the Doppler shift induced by the vertical movement of the ionosphere. Doppler shift of the received echo appears to alter the time delay — and thus the virtual height measurement — of the received signal. The effect of Doppler is equal and opposite for an up-chirp signal compared to a down-chirp signal. By transmitting both kinds of chirps, and analyzing them independently, we can compensate for the Doppler-induced height range error and additionally, measure the amount of Doppler shift induced thus allowing computation of the vertical velocity of the ionosphere. Figure 3 shows reception of an up-chirped signal with no Doppler shift. Figure 4 shows reception of an up-chirped signal with (+) Doppler shift, and Figure 5 shows reception of a Down-chirped signal with (+) Doppler shift.

The up-chirp and down-chirp exhibit opposite range errors. This allows us to resolve the correct range and the Doppler shift. The amount of range error caused by Doppler shift is dependent on the chirp rate.

The range to the ionosphere is proportional to half of the round-trip time.

$$Range[height] = c\frac{t_{echo}}{2}. \quad (1)$$

Where c m/s is the speed of light and t s is the time of the echo. The range error caused by Doppler shift is:

$$Range\ Error = c\frac{d}{s} \quad (2)$$

where d is the Doppler shift, Hz, and s is the chirp sweep rate, Hz/s.

A chirp rate of 15 kHz/s implies an error of 19.9 km/Hz of Doppler shift. The vertical velocity of the ionosphere is measured by the induced Doppler shift, which we infer from the range error.

$$Doppler\ shift = s\frac{Range\ Error}{c}. \quad (3)$$

The vertical movement of the layer induces a doubled Doppler shift. The chirp signal hits a moving ionosphere layer, and is Doppler shifted as received by the ionospheric layer. Then the signal is re-emitted by the ionosphere and received back at the ground, inducing another Doppler shift. Doppler shift is related to the layer velocity and the frequency of the radio wave, adding the factor of two for reflection from a moving ionosphere.

$$\Delta f = 2f_0\frac{\Delta v}{c}. \quad (4)$$

Compute the velocity of the ionosphere as,

$$\Delta v = \frac{\Delta f\, c}{2f_0}. \quad (5)$$

Relate the velocity to range error,

$$\Delta v = \frac{s \bullet Range\ Error}{2f_0}. \quad (6)$$

Range error is found by measuring the difference between the ranges determined by the up -and-down-chirp time measurements. Since each chirp introduces an equal and opposite error, the actual range error is the difference divided by two.

$$\Delta v = \frac{s \bullet (UpRange - DownRange)}{2f_0}. \quad (7)$$

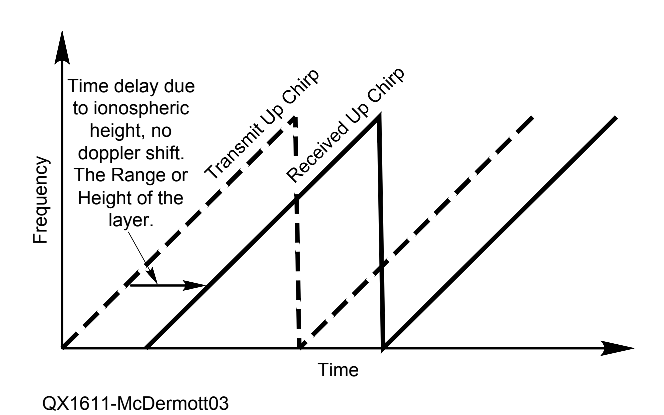

Figure 3 — Up-chirp reception with no Doppler shift.

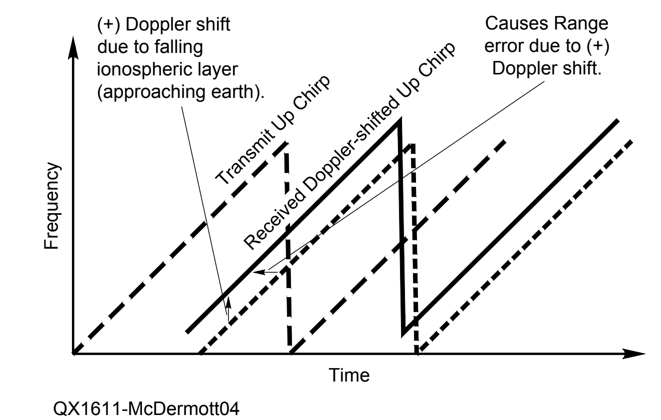

Figure 4 — Up-chirp reception with positive Doppler shift due to falling ionospheric layer.

A slower chirp rate yields higher sensitivity to Doppler shift allowing more resolution of the ionosphere Doppler shift and thus the ionosphere vertical velocity.

Signal Processing

The basic receive algorithm consists of cross-correlating the received signal against a stored replica copy of the transmit signal. This is known as a matched filter. It provides several benefits; (1) the actual transmit signal strongly correlates with its own replica providing a convenient way to compensate for fixed equipment delays, (2) a weak echo is easily seen above the background noise even in the presence of a strong transmit signal.

The delay of the echo signal is the difference in time between the received transmit peak and the received echo peak. This removes the requirement of knowing the absolute delay through the radio, Ethernet switch, and DSP processing. Such errors or unknowns are subtracted out.

The DSP algorithm that correlates the received signal with the replica is factored through several steps in order to improve the computational efficiency. We define the two signals, the transmit replica copy *f*(*t*), and the received signal and *g*(*t*). The convolution of *f*(*t*) with *g*(*t*) is,

$$f(t) \oplus g(t) = \int_{-\infty}^{+\infty} f(\tau) g(t-\tau) d\tau \,. \quad (8)$$

Convolution is implemented in DSP using an FIR filter kernel, a ready-made DSP block exists within Gnuradio that directly implements an FIR filter.

$$[f \otimes g](t) = \int_{-\infty}^{+\infty} f(-\tau) g(t-\tau) d\tau \,. \quad (9)$$

We need only time-reverse the stored replica copy of the transmit chirp signal

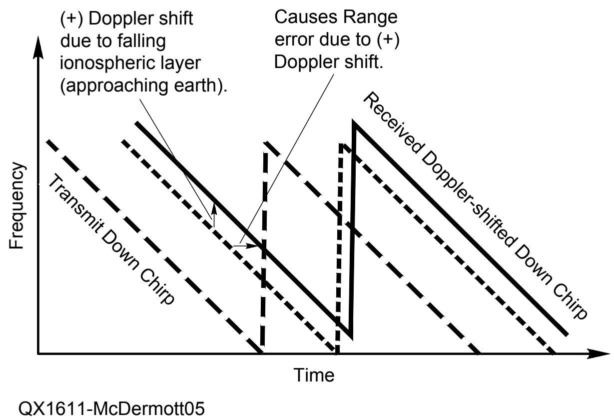

Figure 5 — Down-chirp reception with positive Doppler shift due to falling ionospheric layer.

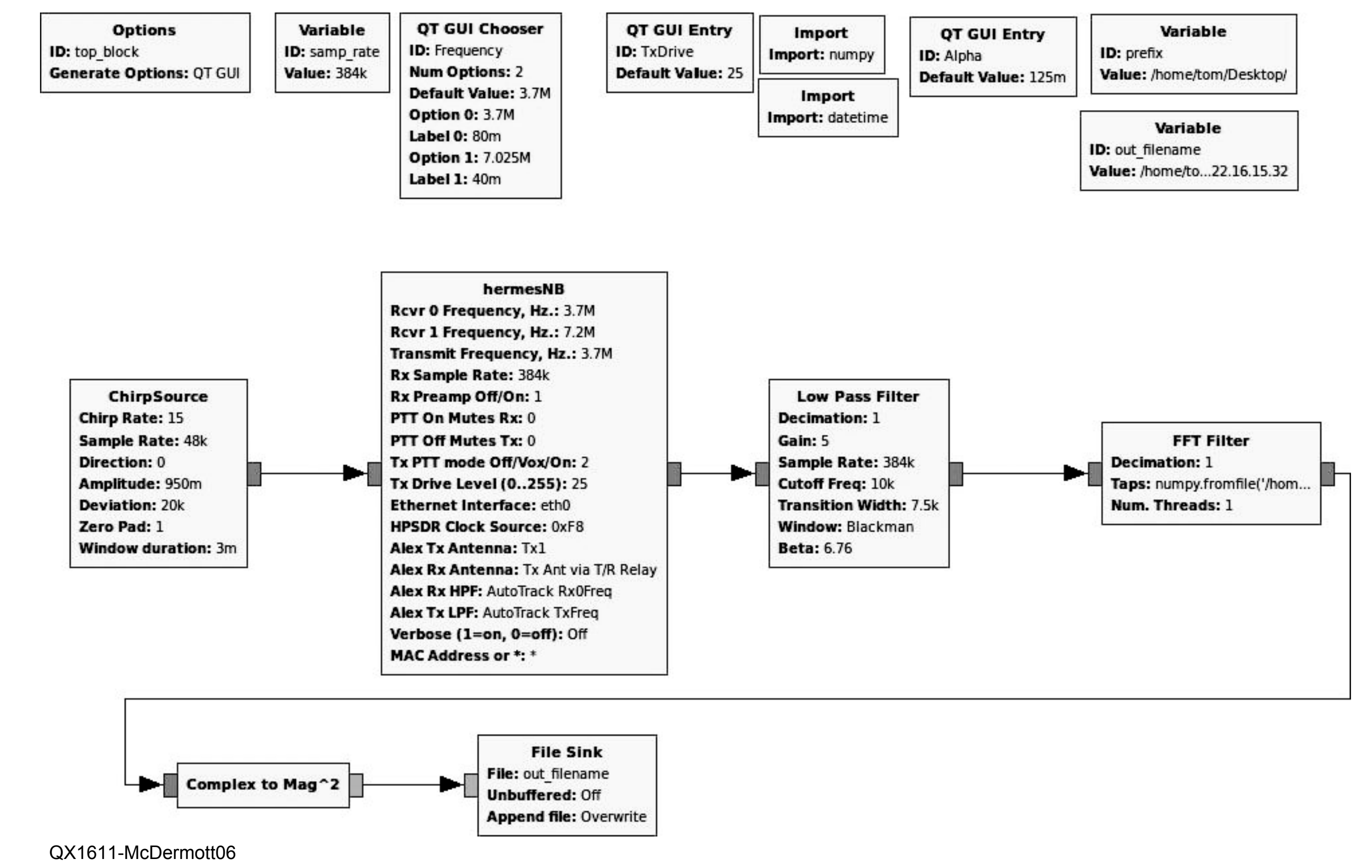

Figure 6 — Block diagram of the Gnuradio chirp transmit and receive data processing flow graph.

before introducing it as the taps of the FIR filter. We can use the existing Gnuradio FIR filter and read in the taps from a file containing the stored time-reversed chirp signal.

Unfortunately an FIR filter requires on the order of N^2 operations, abbreviated $O(N^2)$. This means that if we try to implement a correlation of 1 million taps (10^6), the correlation operation requires on the order of one trillion cycles, which is infeasible. Both the signal and the taps are complex numbers (I and Q), requiring at least four floating-point multiplies and two additions per tap.

Fortunately there is a more efficient way to implement the FIR filter in the frequency domain using the Fast Fourier Transform (FFT). This FFT filter is also a built in block in Gnuradio. The correlation can be implemented by taking the FFT of $f(-t)$ and the FFT of $g(t)$ and then pair-wise multiplying each element of f and g. Finally, take the inverse FFT of the result to get back to the time domain. The FFT operation is extremely efficient. The FFT filter requires far fewer computations, $O(N \log_2 N)$ operations. For a 1-million element correlation, this is on the order of 18 million operations (2 FFT and 1 IFFT) compared to one trillion operations using the direct FIR filter. For convolution,

$$f(t) \oplus g(t) = IFFT \left[FFT\left(f(t)\right) \bullet FFT\left(g(t)\right) \right] \tag{10}$$

Similarly to an FIR filter used for correlation, the FFT filter can be used for correlation by time-reversing the waveform used for the filter taps.

$$f(-t) \otimes g(t) = IFFT \left[FFT\left(f(-t)\right) \bullet FFT\left(g(t)\right) \right]. \tag{11}$$

Properly constructed linear chirp signals have several interesting symmetry properties. An up-chirp is the frequency conjugate of the down-chirp. An up-chirp is also the time reverse of a down-chirp. This means we don't need to bother time-reversing the stored chirp signal. To correlate a receive echo, we load the FFT filter taps (or FIR filter taps) with the opposite type of stored transmit chirp.

$$f(t) \otimes g(t) = IFFT \left[FFT\left(opposite\ chirp(t)\right) \bullet FFT\left(g(t)\right) \right]. \tag{12}$$

This series of steps, leading to Eq (12), reduces the computational effort required to correlate the received signal against the stored transmit signal by a large amount. At 384 ksps, a Core i7-3770 3.4 GHz processor can easily keep up with the one million point correlation in real time in Gnuradio. In fact, several can run in parallel to directly compare various algorithm tradeoffs.

Figure 6 is a block diagram of the DSP steps implemented in the flow graph. The FFT taps utilize a stored version of the chirp waveform created at 384 ksps, so no decimation is performed in the receive chain of the active flow graph. Very few steps are required. The time domain output of the correlation filter is stored as a file on disk (File Sink) for later post processing in Python (receive integration).

Receive Lowpass Shaping Filter (Windowing in the Time domain)

In Figure 6 the signal received from Hermes is first low pass filtered in frequency before being applied to the correlation function. This low pass filter has a gentle shape defined with a Blackman-Harris window. The shaping in the frequency domain results in the time-domain samples in the correlation filter being windowed because a linear chirp is being received. The frequencies at the extreme positive and negative ends of the chirp are the most attenuated. Without this windowing, spectral leakage would obscure the echoes. Figure 7 shows the correlator output side lobes with and without receive low pass filtering. The time delay of the Blackman-Harris filtered and the unfiltered signals have been approximately normalized with a delay element to roughly time-align the two to ease visual comparison in Figure 7.

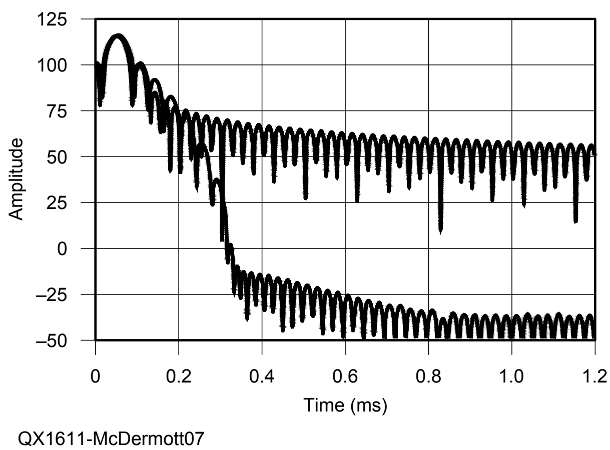

Figure 7 — Rectangular filter with no low pass filter has high residual correlation side lobes (top). A Blackman-Harris low pass filter reduces the side lobes out past about 0.3 ms (bottom).

Receive Integration

While the raw algorithm achieves about 110 – 120 dB of dynamic range, overloading of the receive antenna amplifier and other parts of the receiver degrades the dynamic range to about 90 dB. In order to bring the received signal up out of the noise, about 10 sweeps of the receive signal are recorded on disk. Then the signals are non-coherently averaged. This brings the F-layer echoes clearly up out of the noise level.

Figure 6 is the Gnuradio flow graph used to capture and real-time process the signal. A custom Gnuradio block generates a programmable chirp signal. Parameters are included to permit adjusting the frequency deviation, sweep rate, number of samples per sweep, and providing a raised-cosine start and stop shape. The Chirp block feeds the Hermes transmitter port. The HermesNB module was written to provide access to many features of Hermes and Alex, and has been previously described.[4]

The Hermes FPGA code also filters the transmit signal, it limits the maximum frequency response of the transmitter to ±20 kHz of the transmit center frequency. Echoes are non-coherently integrated. If coherently integrated, the echoes would average towards zero. Non-coherently, we just integrate the magnitude of each echo neglecting phase. A 3 dB improvement in SNR should be possible through echo phase de-rotation and coherent integration.

Block Diagram

Figure 8 is a block diagram of the test setup. The Alex module is used as the transmit band pass filter, however it is not used in the receiver path due to insufficient isolation between the transmitter and the separate receive connector on the Alex module. Input to the Hermes receiver had to completely bypass the Alex module. Gnuradio sends a FM chirp signal of constant amplitude to the transmit section of Hermes, and then to the Munin broadband PA, where it is amplified to about 20 W. The amplifier output is filtered by the Alex RF filters, and

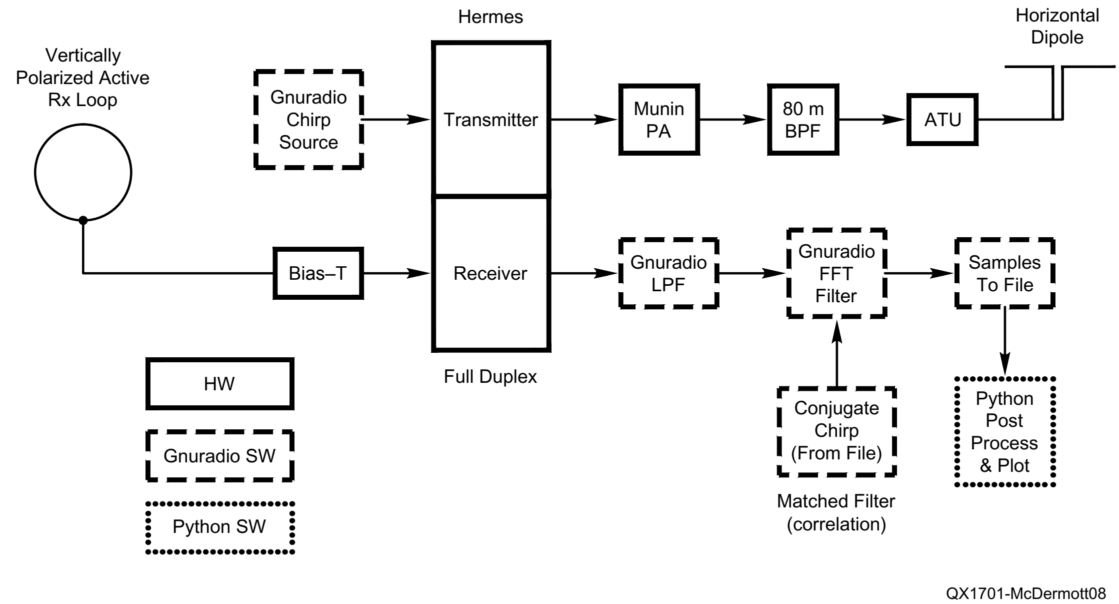

Figure 8 — Block diagram of test setup. Boxes indicate functions implemented in hardware, Gnuradio software, and Python software.

sent to an antenna tuner and ladder line, and to a 40 m dipole. For F-layer echoes, the transmit signal is about 3.6 MHz.

Because of high SWR on the ladder line, about 6 W of transmit power is actually radiated by the antenna. On receive a homebrew active loop antenna one meter in diameter feeds a differential amplifier and balanced-to-differential transformer through a common mode choke. The antenna is remotely powered over the RG-6 feed line. After reception, the Hermes signal is filtered in Gnuradio through a base band low pass shaping filter to window the samples in time before sending them to the FFT correlator.

Figure 9 shows some of the components of the experimental setup. The RF Alex band pass filters and the Core i7 Linux computer running Gnuradio are not shown.

Figure 10 is a photograph of the active receive loop antenna. Only one of the two loops are used in this experiment. The loop antenna is polarized parallel to the loop wire, vertically polarized at the horizon, helping to reduce coupling to the horizontally polarized transmit antenna. The antenna was constructed with future experiments in mind, where it should be possible to discriminate between the Ordinary-ray (O) and eXtraordinary-ray (X) waves reflected by the ionosphere.

Results

So far, measurements have been made on the F-layer at several times of day at 3.6 MHz channel center frequency. Before dawn in fall/winter this is above the critical frequency, and no vertical reflections were received. In the evening local time the critical frequency is usually higher than 3.6 MHz, and vertical reflections were received.

Figure 11 is a graph of the up-chirp (dashed line) and down-chirp (solid line) signals. Notice that the up- and down-chirps exhibit range differences due to the Doppler shift of the moving ionospheric F-layer. This Figure represents ten sweeps that have been non-coherently integrated. The vertical axis is the magnitude of the correlation while the horizontal axis is time. The transmit peak has been adjusted to zero time by the post-processing Python integration program. Primary reflections are seen at about 1.7 ms after the transmit peak. There is a spurious peak at 4 ms, as well as at multiples of 4 ms for both sweeps, the cause has not yet been determined.

Figure 9 — Test setup, showing dc power supply, Munin amplifier, active loop bias-T, Hermes board. Not shown: Alex RF band pass filter, computer (outside the photo).

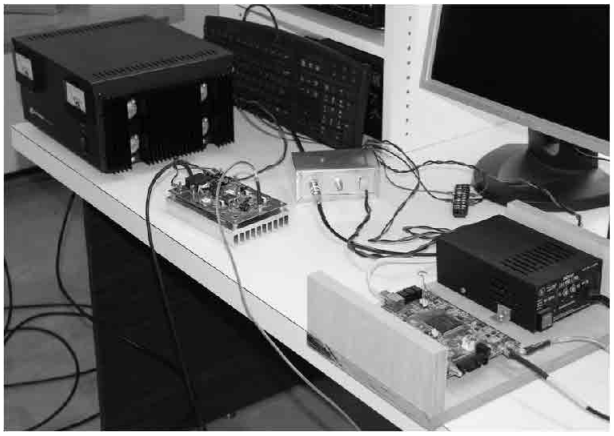

Figure 10 — Homebrew dual active loop receive antenna. Only one of the two loops is used in this experiment.

Small peaks in the up- and down-chirps can be seen at 3.4 ms. These are double-transit reflections. The signals traveled up to the ionosphere, down to ground, reflected by the ground back up to the ionosphere, and reflected back downward a second time. The Doppler range error is doubled as well.

Doppler induced range errors indicate that the F-layer is ascending at the time of this measurement. The average of the two time measurements is the F-layer height, while the difference between the two is proportional to 4 times the Doppler shift. The moving ionosphere reflects the signal, thus doubling the Doppler shift, and the up- and down-chirps have opposite range errors induced. Thus the measured range difference quadruples the Doppler shift.

Calculations from Figure 11 show the F-layer height at 254 km, and the layer upward velocity of +15.4 m/s. The Doppler shift is about -0.38 Hz. Both range and Doppler resolution are limited by the filters and the correlation width. The half-lobe width is about ±17 µs implying a range bin size of roughly 5 km.

Further Work

Figure 12 shows F-layer reflections that include reception of both the Ordinary (O) wave and the Extraordinary (X) wave. With a single receiver and linearly polarized receive antenna it is not possible to know which is O and which is X. The current single linearly polarized receive antenna sums the Right Hand Circular (*RHC*) and Left Hand Circular (*LHC*) components into one received signal. The dual-receive crossed linear loops, shown in Figure 10, plus two phase-coherent receivers could be used to capture two signals, one per loop antenna. Then the Gnuradio DSP software would be able to synthesize the *RHC* and *LHC* signals from the two linearly polarized received signal components.

Circularly polarized signals identify which reflection is O and which is X. Since the transmit antenna is linearly polarized, it emits a *RHC* plus a *LHC* signal simultaneously. These two signals remain coupled as one linearly polarized signal until encountering the ionosphere undergoing magnetic bias from Earth's magnetic field. This causes them to decouple into independent *LHC* and *RHC* components, which are the O and X waves. The effective ionospheric refractive index is different for the *RHC* and *LHC* components, which then propagate with different characteristics in the ionosphere and are received as two different reflections.

We can construct the *RHC* and *LHC* components from the two received signals. Designating these two received complex valued signals as RX_a and RX_b then,

$$RCH = RX_a + e^{j\pi/2} RX_b \qquad (13)$$

$$LCH = RX_a + e^{-j\pi/2} RX_b \,. \qquad (14)$$

LHC and *RHC* can be generated at baseband using standard Gnuradio complex multiply blocks.

E-layer reflections have not been received at this time due to lack of appropriate transmit antenna.

Acknowledgements

Thanks to Andrew Martin, VK3OE, John Petrich, W7FU, and Phil Harman, VK6PH for helpful reviews and comments.

Tom McDermott, N5EG, has been licensed 46 years. He is a long time member of TAPR, and an ARRL Life Member. He has published previously in QEX and the TAPR/ARRL proceedings. Tom has a BSEE degree from the University of California, Berkeley. His professional experience is mostly in transmission and fiber optic telecommunication systems. He is a member of IEEE, the IEEE Standards Association, and is a voting member of the IEEE 802.3 Ethernet Standards working group. Tom has 13 patents. He enjoys an occasional SSB contest, building homebrew electronic and radio equipment, and writing software as needed. Tom edits a local radio club newsletter.

Notes

[1]A.V. Podlesny, V.I. Kurkin, A.V. Medvedev, K.G. Ratovsky, "Vertical ionosphere sounding using continuous signals with linear frequency modulation," Institute of Solar Terrestrial Physics, Irkutsk, Russia, Conference General Assembly and Scientific Symposium 2011, Istanbul, IEEE 2011. INSPEC Accession Number: 12354018.

[2]Phil Harman, VK6APH/VK6PH, "Software defined radio: The Hermes state of the art single board SDR transceiver," *RadCom* 86(05):28-29.

[3]Phil Harman, VK6APH/VK6PH, "Chirp Modulation: A sophisticated radar-like technique for propagation study that makes 100 W act like 100 megawatts", *RadComm* 2012(3):32-38.

[4]Tom McDermott, N5EG, "Gnuradio Companion module for openHPSDR Hermes / Metis SDR Radio", *Proceedings of the 32nd ARRL and TAPR Digital Communications Conference* (2013), pp. 36-42.

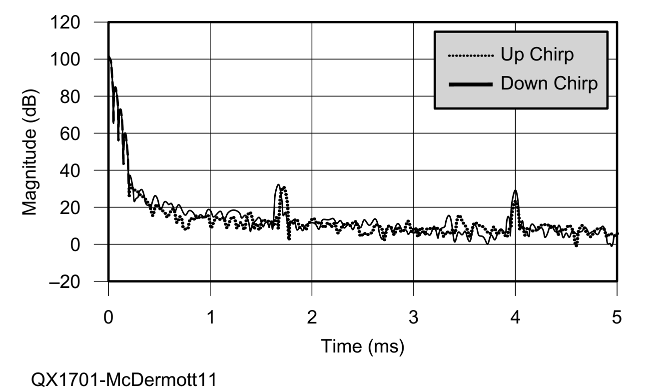

Figure 11 — F-layer reflection at 3.6 MHz in the evening local time shows the correlation integral output after post-processing and integrating about 10 sweeps with Python software. Vertical axis is decibels, horizontal axis is delay time. The signals near 1.7 ms are the F-layer reflections. Signals near 3.4 ms are double-transit reflections. The signals at 4.0 ms are system artifacts.

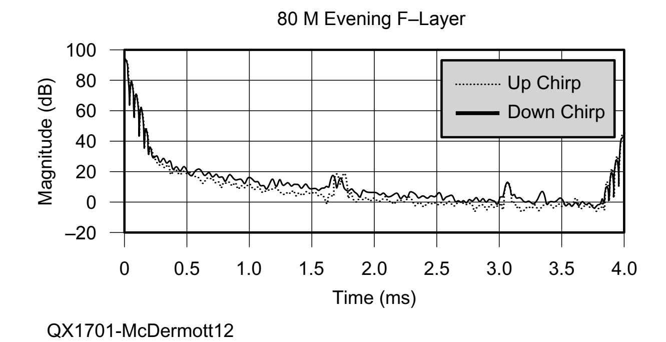

Figure 12 — F-layer reflection at 3.6 MHz showing Ordinary (O-wave) and Extraordinary (X-wave) reflection components from the F-layer near 1.7 ms. The signals at 3.06 and 4 ms are spurious artifacts.

Robert J. Zavrel, W7SX

P.O. Box 303, Corvallis, OR 97339; **w7sx@arrl.net**

A Different Approach to Yagi-Uda Antenna Design

This center-fed version of the Yagi-Uda antenna for 40 through 10 meters achieves better gain by using a new parasitic element design.

The Yagi-Uda antenna array is an exceptionally effective antenna over a narrow band of frequencies where matching, and optimum forward gain, and front-to-back ratios can be achieved. The attraction of using this exceptional antenna has led to intense development for extending designs for multi-band operation. This development began soon after the invention came to light in the 1930s and continues in earnest today. The usual goal is to provide automatic matching — usually for 50 Ω feed-lines — while providing some level of optimized trade-offs for forward gain and front-to-back ratio over a number of bands.

Various popular techniques have emerged for providing multi-band coverage: traps, inter-laced elements, log-periodic configurations, linear loading, and motor-driven length adjustment of the elements. With the advent of the WARC bands, design complexity grew dramatically. This complexity led to the motor driven length as a near-optimum solution for providing continuous coverage over a wide frequency range, even 7 – 30 MHz. However, the complexity of the motor driven configuration results in a relatively high cost.

There is yet another disadvantage to all the above solutions. Higher frequencies cannot take advantage of the potential aperture — and thus gain — made available by the large physical dimensions. For example, at 28 MHz, the typical tri-band Yagi-Uda antenna utilizes little more than one half of the potential gain made available by all the metal put up in the air. The main incentive for this compromise in performance is for automatic matching. An alternative is to simply "bite the bullet" and use open wire feed-line and a tuner. This provides exceptional flexibility in antenna design, providing more gain on each band by utilizing the total length of the elements on all bands, and lowering feeder loss by using open-wire line.

Yet another approach

An optimized 2-element Yagi-Uda antenna will yield about 5 dBd — 5 dB more than a half wave dipole — or about 7.15 dBi. Therefore, the goal will be to achieve 5 dBd over the five amateur bands (14 – 30 MHz) and also provide bi-directional patterns on 10.1 and 7 MHz. This will result in a seven-band rotatable array. Also, we want the boom length and number of elements to be minimum. This design uses a 7-ft boom (about 2.5 m) with 3 elements. Maximum gain from a center-fed linear antenna is achieved with a total length of 1.25 wavelengths, the length of an extended double Zepp. Therefore we begin with approximately this length for the highest operating frequency (the 28 MHz band). The three elements consist of the driven element, a reflector for 20/15/10 m, and a reflector for 12/17 m. Only two traps are used in the array, one each at the *centers* of the parasitic elements. The driven element is a simple 40-ft center-fed dipole with open wire line. Calling these two "traps" is a bit misleading, on one band each is indeed a trap, but on other bands they provide critical reactance values to affect optimized parasitic responses. The advantages of this design are,

(1) No traps or loading along any antenna element.

(2) Only two traps needed, one each at the reflector element centers.

(3) A very short 7-ft boom.

(4) Simple, single feed point.

(5) All bands take full advantage of the complete physical length of the elements (more gain, especially at the higher frequencies).

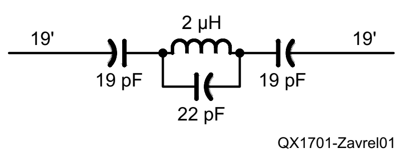

Figure 1 — Reflector for the 12 and 17 m bands.

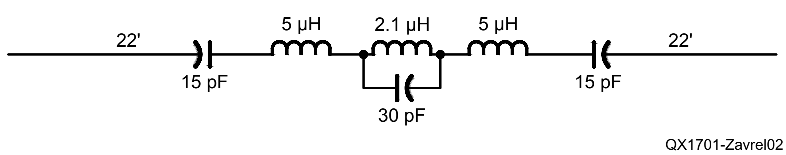

Figure 2 — Reflector for the 20, 15 and 10 m bands.

(6) Tune a perfect match anywhere between 7 and 30 MHz.

The main disadvantage is the requirement for a tuner, however, with the development of auto-tune circuits this problem is or soon could be mitigated.

The new trap design (dual-band)

First I will explain the simpler two-band trap for 12/17 meters shown in Figure 1. We can optimize a reflector by actually configuring two co-linear reflectors on the same element. The optimum reflector element length for the 12 m band is about 19 ft. So we simply build an element twice this length or 38 ft. However, it is necessary to break this element in two, which would be simple if we only needed a reflector at 12 m. Instead we place a resonant parallel *LC* circuit at the center and affect the break. We now have two collinear reflectors on 12 m. On 17 m, this element now looks too long for a reflector, so we simply add two capacitors on either side of the 12 m trap. This "tunes" the longer element for optimum length at 18.1 MHz, and we now have a very effective 12/17 m reflector element. Figure 1 shows the component values. However, the current remains distributed over a longer-than-required physical length, thus increasing the antenna gain.

Tri-band trap

We can extend the idea of the dual-band trap into a tri-band trap, as in Figure 2. In this case we start with the two-element collinear at 15 m, and as above, breaking the 44 ft length in two at 15 m using another parallel *LC* tank, thus providing two collinear reflectors. At 14 MHz, this creates a center-loaded 44 ft reflector, too long for a traditional 20 m parasitic array. At 10 m, the element is more than one wavelength. We can take full advantage of this extra length at both bands by using a proper series *LC* circuit on both sides of the 15 m trap, which tunes the element simultaneously for both 10 and 20 m.

I won't duplicate the hand calculations I performed, but computer modeling tools such as *MATLAB* could be used to set up the necessary simultaneous equations and/or a matrix to optimize the *L* and *C* values. I did not optimize, but I suspect these values are close enough. The front-to-back performance, in particular, may benefit more by such elaborate optimization efforts.

EZNEC model and results

Figure 3 shows the 3-element dipole/Yagi antenna. The gain plots are taken in free space, and *dBref* is set to 2.15 dBi, the gain of a dipole. The gain of an optimized two

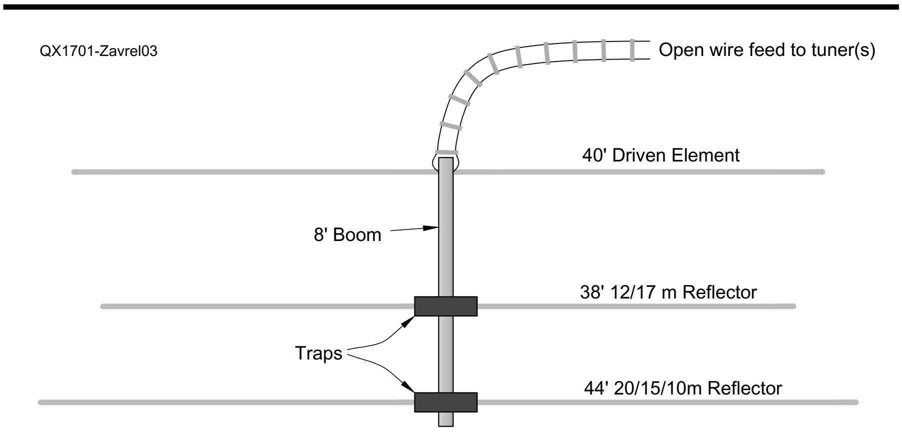

Figure 3 — Antenna dimensions for the 3-element 7-band dipole/Yagi antenna. The distance between the driven element and the 20/15/10 m reflector is 7 ft.

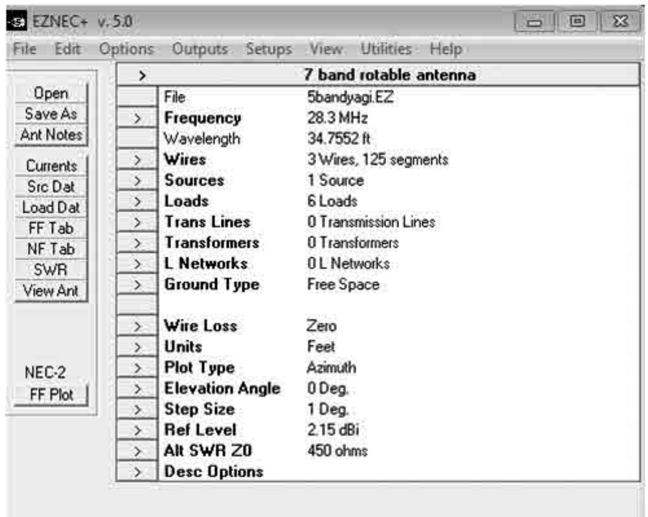

Figure 4 — *EZNEC* model overview.

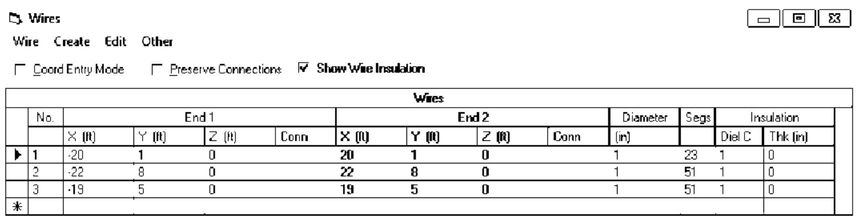

Wires

No.	End 1				End 2				Diameter	Segs	Insulation	
	X (ft)	Y (ft)	Z (ft)	Conn	X (ft)	Y (ft)	Z (ft)	Conn	(in)		Diel C	Thk (in)
1	-20	1	0		20	1	0		1	23	1	0
2	-22	8	0		22	8	0		1	51	1	0
3	-19	5	0		19	5	0		1	51	1	0

QX1701-Zavrel05

Figure 5 — *EZNEC* model antenna wire details.

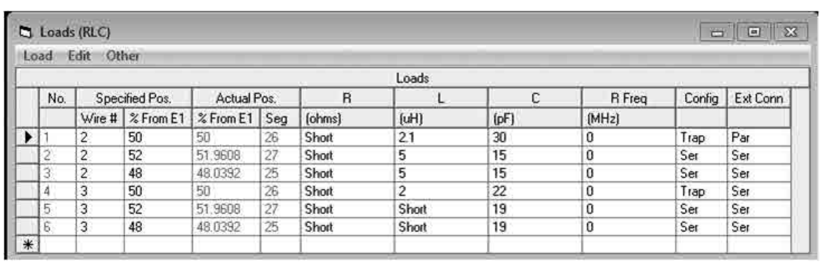

Loads

No.	Specified Pos.		Actual Pos.		R	L	C	R Freq	Config	Ext Conn
	Wire #	% From E1	% From E1	Seg	(ohms)	(uH)	(pF)	(MHz)		
1	2	50	50	26	Short	2.1	30	0	Trap	Par
2	2	52	51.9608	27	Short	5	15	0	Ser	Ser
3	2	48	48.0392	25	Short	5	15	0	Ser	Ser
4	3	50	50	26	Short	2	22	0	Trap	Ser
5	3	52	51.9608	27	Short	Short	19	0	Ser	Ser
6	3	48	48.0392	25	Short	Short	19	0	Ser	Ser

Figure 6 — *EZNEC* model *L* and *C* loads.

element Yagi-Uda is about 5 dBd, while that of an optimized three element Yagi-Uda is about 7 dBd. These plots compare favorably in that the higher frequencies see about the equivalent of a three-element response, but on an 8-ft boom. Figure 4 shows the *EZNEC* model overview, Figure 5 shows the antenna wire details, and Figure 6 shows the *L* and *C* loads. Finally, Figure 7 shows the modeled current amplitudes on the wires at 28.3 MHz.

Figures 8 – 14 show the azimuth free space antenna patterns for the seven bands 10 m through 40 m. Table 1 shows a summary of the performance, including free space gain, equivalent number of Yagi elements, feed-point impedance, and VSWR on the 450 Ω line.

Conclusions

The VSWR values are included in Table 1 since very high values may become problematic. All frequencies show reasonable VSWR values for 450 Ω ladder

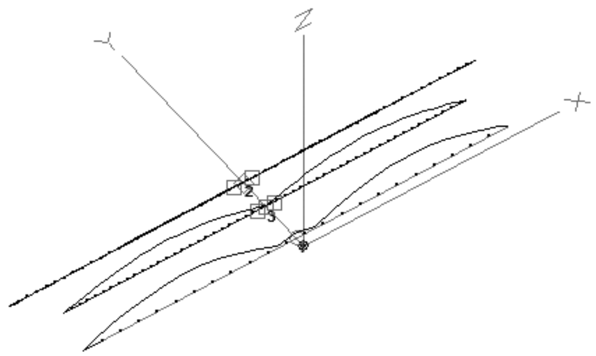

QX1701-Zavrel07

Figure 7 — Modeled current amplitudes on the wires at 28.3 MHz.

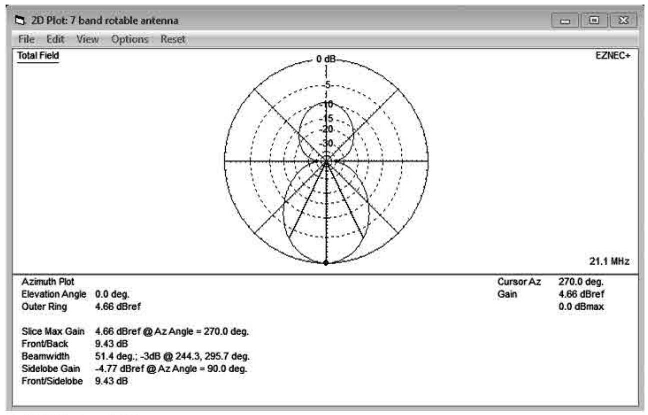

QX1701-Zavrel10

Figure 10 — Free space azimuth antenna pattern at 21.1 MHz.

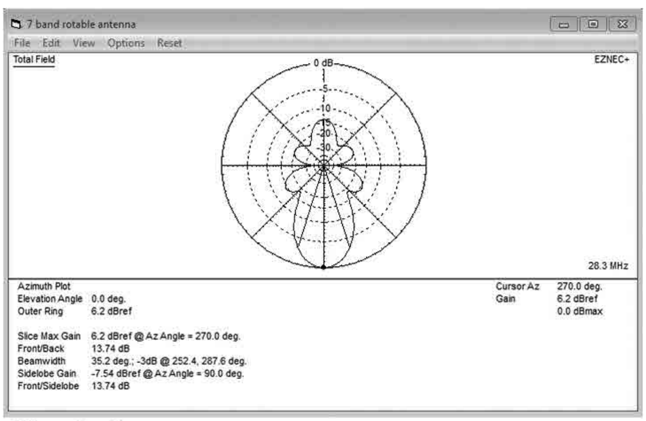

QX1701-Zavrel08

Figure 8 — Free space azimuth antenna pattern at 28.3 MHz.

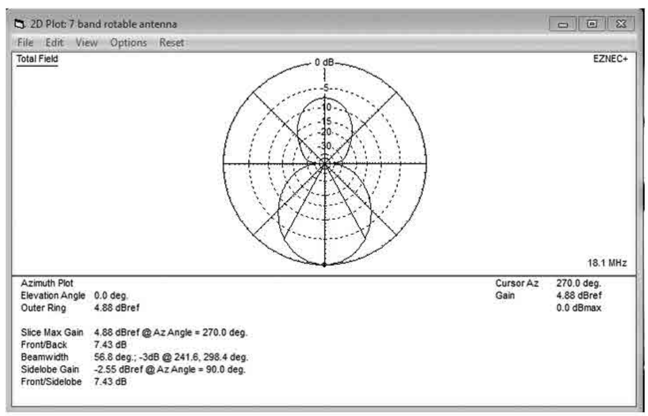

QX1701-Zavrel11

Figure 11 — Free space azimuth antenna pattern at 18.1 MHz.

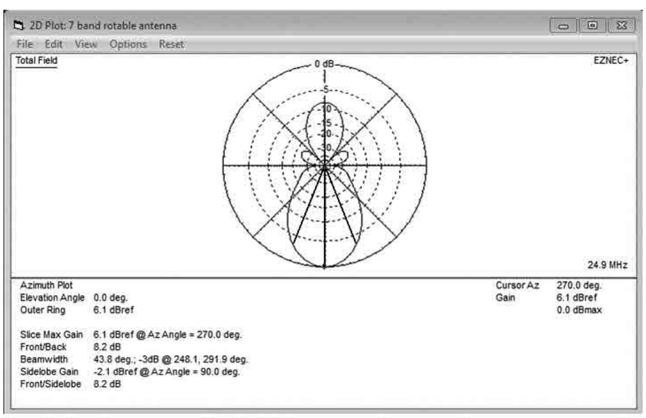

QX1701-Zavrel09

Figure 9 — Free space azimuth antenna pattern at 24.9 MHz.

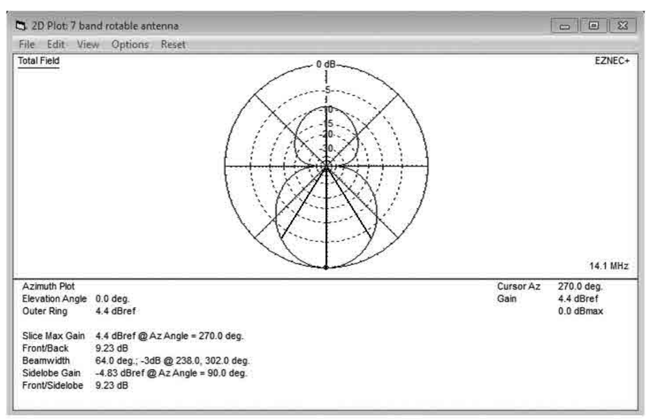

QX1701-Zavrel12

Figure 12 — Free space azimuth antenna pattern at 14.1 MHz.

Table 1
Overall performance summary.

Frequency	*Free space gain, dBd*	*Equivalent Yagi elements*	*Feed point impedance*	*VSWR on 450 Ω line*
7.1	–0.18	1	17 – *j* 472	54
10.1	+0.26	1	46 – *j* 153	10.7
14.1	+4.4	2	46 + *j* 239	12.7
18.1	+4.88	2	77 + *j* 700	20.1
21.1	+4.66	2	1978+ *j* 1525	7.0
24.9	+6.1	3	786 – *j* 2343	17.8
28.3	+6.2	3	174 – *j* 704	9.1

line with the possible exception of the high value at 40 m. However, losses generally decrease with lower frequencies, an obvious advantage at 7 MHz. In any event an open wire line will exhibit very high voltages at maximum points, and *must* be protected from accidental contact with people, animals and flammable objects. The antenna is, in effect, a rotatable dipole for 7 and 10.1 MHz, a 2-element Yagi for 14, 18.1, and 21 MHz, and a 3-element Yagi for 24.9 and 28 MHz. The result is a multi-band antenna with excellent gain for its physical size. I hope this paper will stimulate interest in more complex trap/loading designs for antennas. Contrary to widely held beliefs, there is no reason a parasitic or driven element must be limited to electrical lengths near a half wavelength. How much elevated aluminum and wire is wasted for the convenience of automatic matching?

Bob Zavrel, W7SX, is an ARRL Life Member, Technical Advisor and Amateur Extra class licensee. He has been licensed since 1966. His primary interest in Amateur Radio is low-band DXing and designing and building antennas, tuners, and amplifiers. Bob holds 5BDXCC, 5BWAZ (200), has 349 mixed, and 342 CW entities confirmed. He is on the DXCC Honor Roll and the CW DXCC Honor Roll, all using only tree-supported wire antennas. Bob also earned 9 Band DXCC on 160 through 10 meters. Previous call signs include WN9RAT, WA9RAT, WA9RAT/HR2 and SV1/W7SX.

Bob has a BS in Physics from the University of Oregon and has worked in RF engineering for over 30 years. He has five patents, and has published over 50 papers in professional and Amateur Radio publications, including the first block diagram of an SDR receiver in 1987. He was involved with the first generation of RF integrated circuits for cellular phones, and worked extensively with DDS, WLAN and passive mixer development. Bob is currently a RF Research and Development Engineer for Trimble Navigation with a primary focus on antenna design.

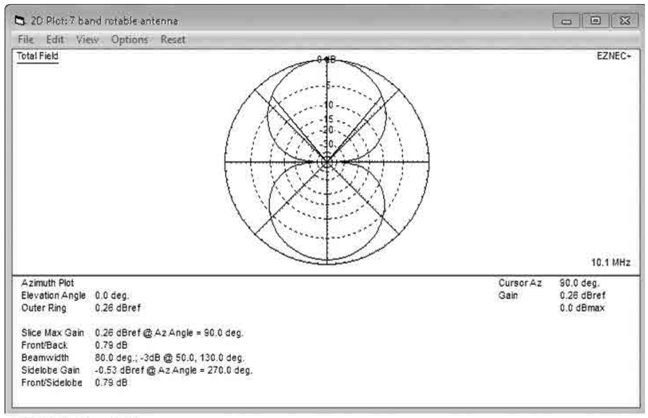

QX1701-Zavrel13

Figure 13 — Free space azimuth antenna pattern at 10.1 MHz.

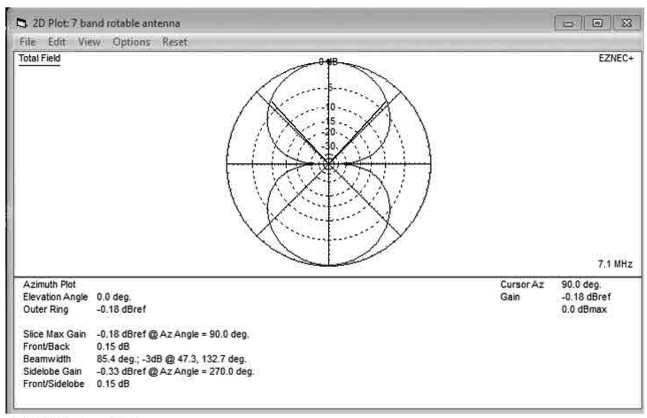

QX1701-Zavrel14

Figure 14 — Free space azimuth antenna pattern at 7.1 MHz.

Bill Kaune, W7IEQ

160 Cedarville Dr., Port Townsent, WA 98368; **w7ieq@arrl.net**

Pi Networks with Loss

Inductor losses can substantially alter the behavior of a pi network and place strong constraints on the overall circuit quality factor.

In a recent *QEX* paper[1] I examined the relation between the quality factor Q and bandwidth of pi networks. Several definitions of Q that appeared in the *ARRL Handbook for Radio Communications*[2] were not good predictors of the bandwidth of pi networks, but a revision of one did predict bandwidth, especially for values of Q greater than about 5. That paper assumed that any loss in the pi networks under consideration could be neglected.

After the publication of the paper, I received an e-mail communication suggesting that I look at the loss in the inductor used in pi networks. I decided to extend my analysis to include inductive loss. Several months later, I finished this analysis, which turned out to be considerably more difficult than I expected. The results were interesting, and in some cases striking. Inductive loss can substantially alter the behavior of a pi network and place quite strong constraints on the overall circuit quality factor.

There seems to be general agreement that losses in the inductors in pi networks are more significant than those in the capacitors. I discovered a paper online[3] which found that the Q's for typical air variable capacitor are typically 500 or more. Q's for practical inductors are considerably less. Consequently, I limited my analysis to inductor loss.

The following sections of the paper develop equations for the values of the various components of a pi network and the Q and internal loss in this network. I also measured the actual loss of the rotary variable inductor in my antenna tuner and used these data to demonstrate how a pi network could be designed taking into account loss within the network itself.

Analysis of a Pi Network Including Inductive Loss

Figure 1 shows a pi network. Loss in the inductor is represented by the inductor's "equivalent series resistance," labeled R_2. R_2 will be referred to as the loss resistance in the remainder of this paper. Initially, the loss resistance will be assumed constant, regardless of the value of the inductance. This is a substantial limitation because, in reality, R_2 will always vary as the inductance of L_2 varies. At the end of this paper I will describe how data relating R_2 to L_2 can be used to overcome this limitation.

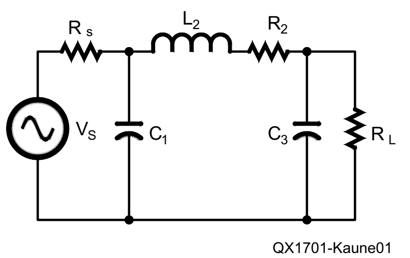

Figure 1 — Schematic of pi network showing R_2, the loss resistance of the inductor.

Pi networks are used frequently in power amplifiers — especially those using electron tubes — to match a load resistance — often an antenna — to a much larger source resistance. Load matching is accomplished when the impedance looking into the input of the pi network equals the source impedance. Here, this condition means that that the resistance looking into the input must be equal to the source resistance, R_S, and the reactance looking into the input must be 0. To achieve these two requirements, we have three quantities that we can adjust, C_1, L_2, and C_3. Thus, to uniquely specify the capacitances and the inductance, we need a third parameter to be specified. In my earlier paper the reactance of C_1 was used as this parameter. However, I found after some experimentation that, when inductive loss is included, simpler results were obtained by dividing the pi network into two cascaded

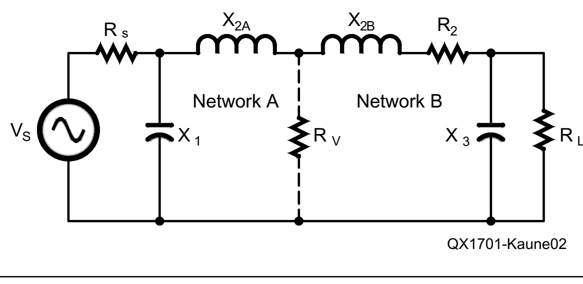

Figure 2 — Pi network divided into two cascaded sub-networks, *A* and *B*. The load for network *A* is a virtual resistance R_V, which is also the source for Network *B*. Network *A* is adjusted to match R_V to R_S, and Network *B* is adjusted to match R_L to R_V.

L-type networks with a virtual resistance, R_V, as the matched load of the first and the source of the second. R_V then becomes the third parameter needed to uniquely specify the components that are labeled by their reactances in Figure 2.

In Figure 2, the two sub-networks are *A* and *B* and the inductor L_2 (with reactance X_2) has been divided into two parts, L_{2A} (X_{2A}) and L_{2B} (X_{2B}). For a given value of R_V, unique values of X_1 and X_{2A} can always be found that match R_V to the source resistance R_S, provided that R_V satisfies certain criteria that will be derived shortly. And, X_{2B} and X_3 can also always be adjusted to obtain a match between R_L and R_V as long as R_V satisfies additional constraints.

Consider then Network *A* shown in Figure 3. This network can be simplified by replacing the series combination of X_{2A} and R_V with their parallel equivalents, X'_{2A} and R'_V, respectively. The parallel-equivalent quantities are related to the series value by the following well-known equations:

$$R'_V = \frac{R_V^2 + X_{2A}^2}{R_V} \tag{1}$$

and

$$X'_{2A} = \frac{R_V^2 + X_{2A}^2}{X_{2A}}. \tag{2}$$

This reconfigured network is shown in Figure 4. It has become a simple parallel *RLC* network. In order for the load, R'_V, to be matched to the source, the following equations must be satisfied:

$$R_S = R'_V \tag{3}$$

and

$$X_1 + X'_{2A} = 0. \tag{4}$$

Now use Eq. (1) to eliminate R'_V in Eq. (3) and Eq. (2) to eliminate X'_{2A} in Eq. (4), and solve the resulting two equations for X_{2A} and X_1. The results are

$$X_1 = -R_S\sqrt{\frac{R_V}{R_S - R_V}}, \tag{5}$$

$$X_{2A} = \sqrt{R_V\left(R_S - R_v\right)}. \tag{6}$$

Both X_1 and X_{2A} must be real numbers, which requires that

$$R_V < R_S. \tag{7}$$

Turn to Network *B* in Figure 2. With R_V matched to R_S in Network *A*, its Thevenin equivalent is an ideal voltage source, V_A, in series with a resistance R_V. Thus, Network *B* can be diagrammed in Figure 5. Next convert the parallel pair of X_3 and R_L to an equivalent series pair, X'_3 and R'_L, where

$$R'_L = R_L\frac{X_3^2}{R_L^2 + X_3^2}, \tag{8}$$

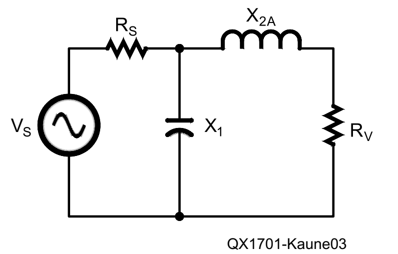

Figure 3 — Schematic of Network *A*.

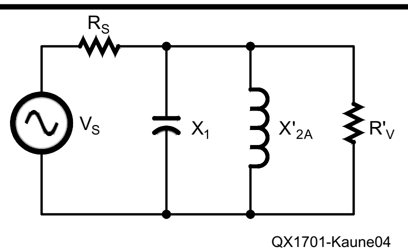

Figure 4 — Network *A* with the series combination of X_{2A} and R_V shown in Figure 3 replaced with their parallel equivalents X'_{2A} and R'_V.

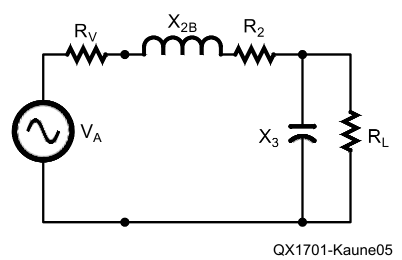

Figure 5 — Schematic of Network *B* with Network *A* replaced with its Thevenin equivalent of an ideal voltage source V_A in series with a resistance R_V.

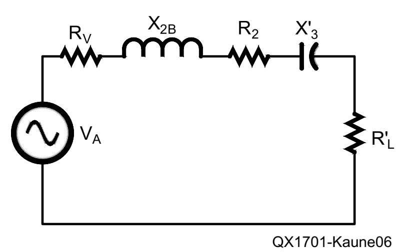

Figure 6 — Network *B* with the parallel combination of X_3 and R_L shown in Figure 5 replaced with its series equivalent X'_3 and R'_L.

and

$$X'_3 = X_3\frac{R_L^2}{R_L^2 + X_3^2}. \tag{9}$$

The resulting simple series *RLC* network is shown in Figure 6. The load is R_2 and R'_L in series. To match this load to the source resistance R_V the following two equations must be satisfied:

$$R_V = R_2 + R'_L, \tag{10}$$

and

$$X_{2B} + X'_3 = 0. \tag{11}$$

Use Eq. (8) to eliminate R'_L in Eq. (10), and Eq. (9) to eliminate X'_3 in Eq. (11). Then solve the resulting two equations for X_{2B} and X_3. The results are:

$$X_{2B} = \sqrt{\left(R_V - R_2\right)\left(R_L + R_2 - R_V\right)} \tag{12}$$

$$X_3 = -R_L\sqrt{\frac{R_V - R_2}{R_L + R_2 - R_V}}. \tag{13}$$

X_{2B} and X_3 must both be real numbers, which requires that

$$R_2 \le R_V < R_L + R_2. \tag{14}$$

The results so far are below:

$$\left.\begin{aligned} X_1 &= -R_S\sqrt{\frac{R_V}{R_S - R_V}} \\ X_2 &= \sqrt{R_V\left(R_S - R_v\right)} \\ &\quad + \sqrt{\left(R_V - R_2\right)\left(R_L + R_2 - R_V\right)} \\ X_3 &= -R_L\sqrt{\frac{R_V - R_2}{R_L + R_2 - R_V}} \\ R_2 &\le R_V < \mathrm{Min}\left(R_S, R_L + R_2\right) \end{aligned}\right\} \tag{15}$$

Quality Factor and Loss

The quality factor Q of a network is defined by the following equation.

$$Q = 2\pi f\,\frac{\text{Energy stored in network}}{\text{Power dissipated in network}}, \tag{16}$$

where f is frequency. There are several definitions of Q in use, depending on which contributors to loss are included in the denominator. Since in this paper we are concerned with the behavior of the network (i.e. its bandwidth and harmonic attenuation) when it is used to match a load to a source, we will include all sources of power loss including the source and load resistances.

To calculate the Q of a pi network, first calculate the quality factors, Q_A and Q_B, of Networks A and B, respectively. Network A (Figure 3) was transformed into a simple parallel RLC network (Figure 4). The quality factor of this network is the net resistance in the network divided by the inductive (or capacitive) reactance. As shown in Figure 4, the resistors R_S and R'_V are in parallel because the resistance of the ideal voltage source V_S is 0. But, Eq. (3) states that the two resistances are equal, so the net resistance is $R_S/2$. Consequently,

$$Q_A = \frac{R_S}{2|X_1|} = \frac{1}{2}\sqrt{\frac{R_S - R_V}{R_V}}\,, \tag{17}$$

where Eq. (5) has been used to eliminate $|X_1|$.

Network B (Figure 5) was transformed into a simple series RLC network (Figure 6). The quality factor for this network is the reactance of the inductor (or capacitor) divided by the net resistance, $R_V + R_2 + R'_L$, in the circuit. But Eq. (10) states that $R_V = R_2 + R'_L$, so

$$Q_B = \frac{X_{2B}}{2R_V} = \frac{\sqrt{(R_V - R_2)(R_L + R_2 - R_V)}}{2R_V}\,, \tag{18}$$

where Eq. (12) has been used to eliminate X_{2B}.

What is the composite Q of the cascaded network consisting of Networks A and B given Q_A and Q_B, the Q's of the component sub networks? I treated this problem [Note 1] for the case where the two networks were lossless; the overall Q was obtained by simply adding the individual Q values of the constituent networks. In Appendix A, the case where the network has loss is analyzed, with the same result that the Q for the overall network is still obtained by adding the Q values for the constituent parts. (This is true only if the network loss occurs only in Network B. This is why I placed the loss resistor, R_2, in Network B. R_2 could have been placed in Network A, or it could have been divided in any way between the two networks with equivalent results.) Consequently, the system Q for the entire pi network is

$$Q = \frac{1}{2}\left[\sqrt{\frac{R_S - R_V}{R_V}} + \sqrt{\left(\frac{R_V - R_2}{R_V}\right)\left(\frac{R_L + R_2 - R_V}{R_V}\right)}\right] \tag{19}$$

We now calculate the loss in the pi network. The loss, of course, occurs in the inductor loss resistance, R_2. Since this resistance was placed entirely in Network B, there is no loss in Network A. Referring to Figure 6, we see that the current through the load, R'_L, is the same as the current through R_2. Consequently, the powers, P_L and P_2, dissipated in the load and inductor resistance, respectively, are proportional to R'_L and R_2. The efficiency, ε, of the pi network to deliver power to its load is

$$\varepsilon = \frac{P_L}{P_2 + P_L} = \frac{R'_L}{R_2 + R'_L}\,. \tag{20}$$

According to Eq. (10), $R'_L = R_V - R_2$. Using this to eliminate R'_L in Eq. (20), we arrive at the remarkably simple result

$$\varepsilon = 1 - R_2/R_V\,. \tag{21}$$

It is conventional to express loss in decibels. Denote this quantity L_{dB}. Then,

$$L_{dB} = -10\log_{10}\left(1 - R_2/R_V\right). \tag{22}$$

All of the quantities in Eqs. (15), (19), and (22) are functions of the parameter R_V. In a later section we address the question of how to select values of R_V to achieve either a desired Q or loss for a pi network.

Relationship between *Q*, Bandwidth, and Harmonic Attenuation

Previously (Note 1), I found that the following definition provided an accurate prediction of lossless network bandwidth and harmonic attenuation:

$$Q = \frac{1}{2}\left(\frac{R_S}{|X_1|} + \frac{R_L}{|X_3|}\right). \tag{23}$$

For a pi network with loss, Q is given by Eq. (19) which appears different than Eq. (23). It can be recast into a form more like Eq. (23) using the expressions for X_1 and X_3 in Eqs. (15) to eliminate the square roots that appear in Eq. (19).

$$Q = \frac{1}{2}\left[\frac{R_S}{|X_1|} + \frac{R_L}{|X_3|}\left(\frac{R_V - R_2}{R_V}\right)\right]. \tag{24}$$

In the no-loss case (i.e., $R_2 = 0$), Eq. (24) reduces to Eq. (23).

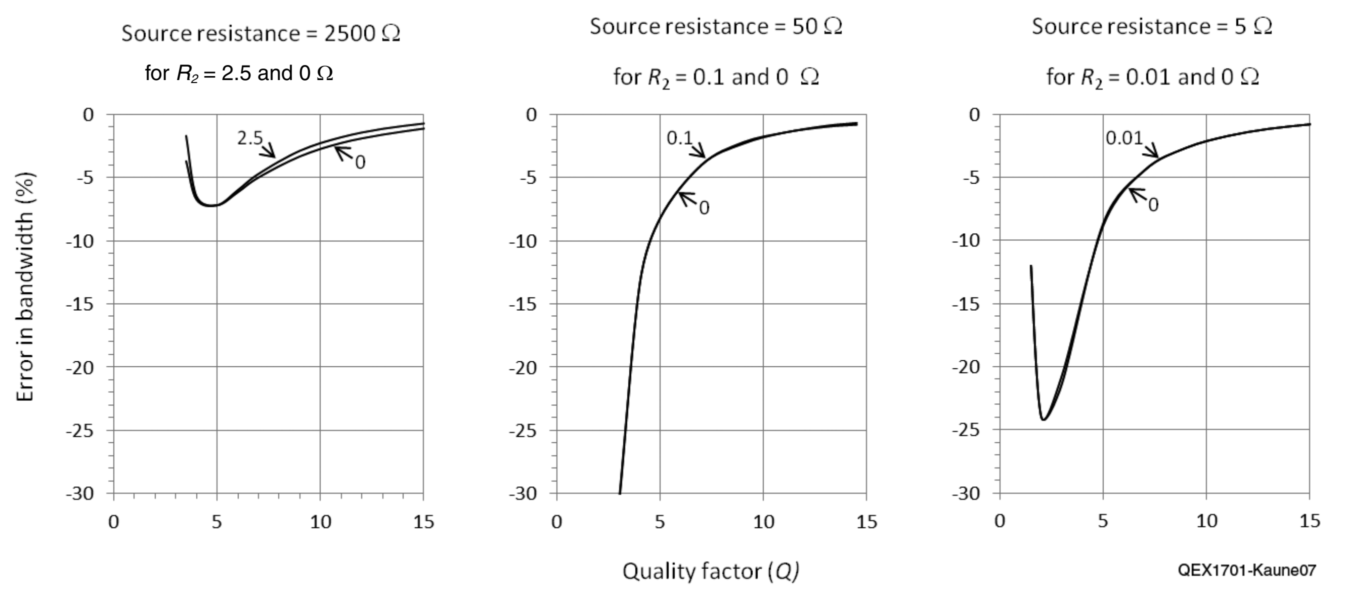

Figure 7 — Error when using calculated quality factor Q of a pi network to estimate its bandwidth, for source resistances of 2500 Ω (left), 50 Ω (center), and 5 Ω (right). The load resistance was 50 Ω in all cases. Curves are for loss resistances of the inductors of 0 Ω and for non-zero values selected to be about in the middle of the range of real inductors.

Is Eq. (24) a good predictor of bandwidth and harmonic distortion? I wrote a computer program (in Visual Basic 2010) that calculated the frequency response of a specified pi network and from this determined bandwidth and harmonic attenuation. Figures 7 and 8 summarize these results.

Figure 7 shows the error resulting from the use of Q, given by Eq. (19), to estimate the bandwidth of a pi network. Graphs are given for a load resistance of 50 Ω and source resistances of 2500, 50, and 5 Ω. In each graph, I selected two values of the loss resistance, one was 0 Ω and the other a value that I thought might be in the middle of the range of loss resistances of actual inductors. For source resistances of 50 and 5 Ω, the curves were not distinguishable. The figure shows that bandwidths estimated using Eq. (19) are always smaller than the actual values. But, for Q values above 5, errors are less than 10% in magnitude.

Pi networks are used not only to match a load to a source but also to attenuate harmonics of the design frequency (i.e., the frequency where the source and load are matched). Figure 8 shows the attenuations of the second, third, and fourth harmonics. As in Figure 7, graphs are given for source resistances of 2500, 50, and 5 Ω. The data in each graph are for the same two loss resistances used in Figure 7; the two curves were indistinguishable. For Q values above 5, attenuation of the second, third, and fourth harmonics were greater than 27 dB.

Specifying Q to Determine R_V

Equation (20) relates the network Q to the virtual resistance, R_V. Values of R_V are limited by the last of Eqs. (17). It is convenient to work with the ratio R_V/R_2 rather than R_V. The limits on this ratio are

$$1 \le \frac{R_V}{R_2} < \mathrm{Min}\left(\frac{R_S}{R_2}, 1 + \frac{R_L}{R_2}\right). \qquad (25)$$

Figure 9 shows, for source resistances of 2500, 50, and 5 Ω and a load resistance of

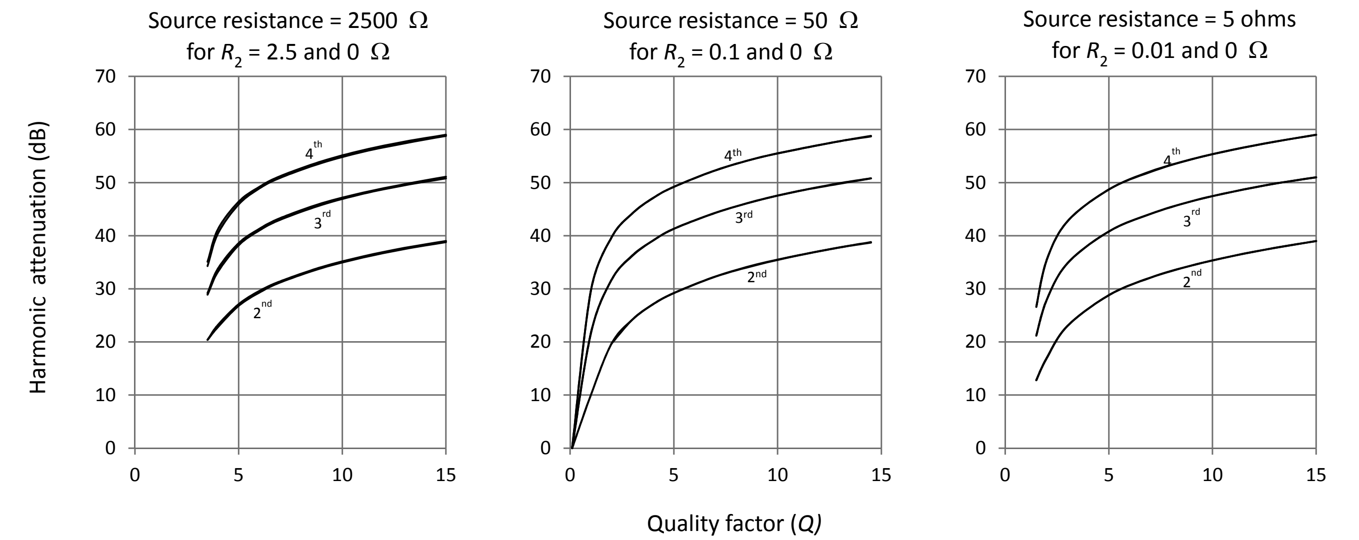

Figure 8 — Harmonic attenuation as a function of quality factor Q of a pi network, for source resistances of 2500 Ω (left), 50 Ω (center), and 5 Ω (right). The load resistance was 50 Ω in all cases. Curves are for loss resistances of the inductors of 0 Ω and for non-zero values selected to be about in the middle of the range of real inductors.

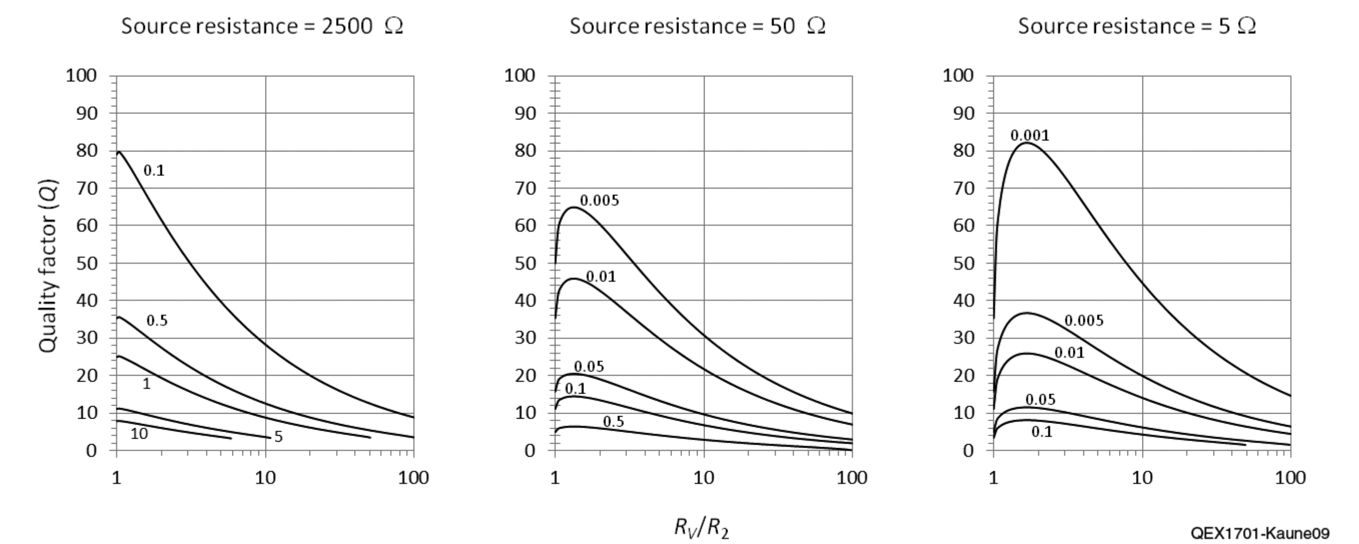

Figure 9 — Quality factor Q as a function of ratio R_V/R_2 for source resistances of 2500 Ω (left), 50 Ω (center), and 5 Ω (right). The load resistance in all cases was 50 Ω. Each curve in a graph is labeled with its respective value of R_2.

50 Ω, the relation between the quality factor of a pi network and R_V/R_2. Curves are shown for various values of the loss resistance, R_2. These data indicate that, at least for the smaller values of R_2, values of Q in excess of 10 can easily be reached. However, these values are obtained as the ratio R_V/R_2 tends towards 1, and loss also increases as R_V/R_2 tends towards 1 as shown by Eq. (23).

The data in Figure 9 can be used to estimate a value for R_V to obtain a specified value of Q. However, it would seem more convenient to have an analytic method for accomplishing this by solving Eq. (19) for R_V as a function of Q. It turns out that inverting Eq. (19) is fairly complicated. Appendix B explains how this solution can be obtained. I do not think it is particularly useful because it seems a better choice is to start with an acceptable level of loss and see what range of Q's can be achieved. The next section addresses this issue.

Specifying Loss to Determine R_V

The relationship between loss, in dB, and R_V is given by Eq. (22). This equation is easily inverted to express R_V as a function of loss.

$$R_V = \frac{R_2}{1-10^{-L_{dB}/10}}. \tag{26}$$

Once loss is specified, R_V and Q are uniquely determined by Eqs. (26) and (19), respectively. Figure 10 shows this relationship for a source impedance of 2500 Ω, 50 Ω, and 5 Ω. The load impedance is 50 Ω in all cases. Each graph contains a family of curves for selected values of the loss resistance R_2 placed on the right edge of each graph.

The graphs in Figure 10 show that there are potentially severe limits on the Q of a pi network if the loss is to be held to a manageable level. For example, suppose we wish to design a pi network whose loss is 1 dB. This means that 20.6% of the power input to the pi network will not appear in the output but is absorbed by R_2, the loss resistance of the inductor. If the transmitter output power is 100 W, this loss might result in warming of the inductor but would probably be acceptable. If the transmitter power is 1 kW, the power dissipation in the inductor would be 206 W, probably

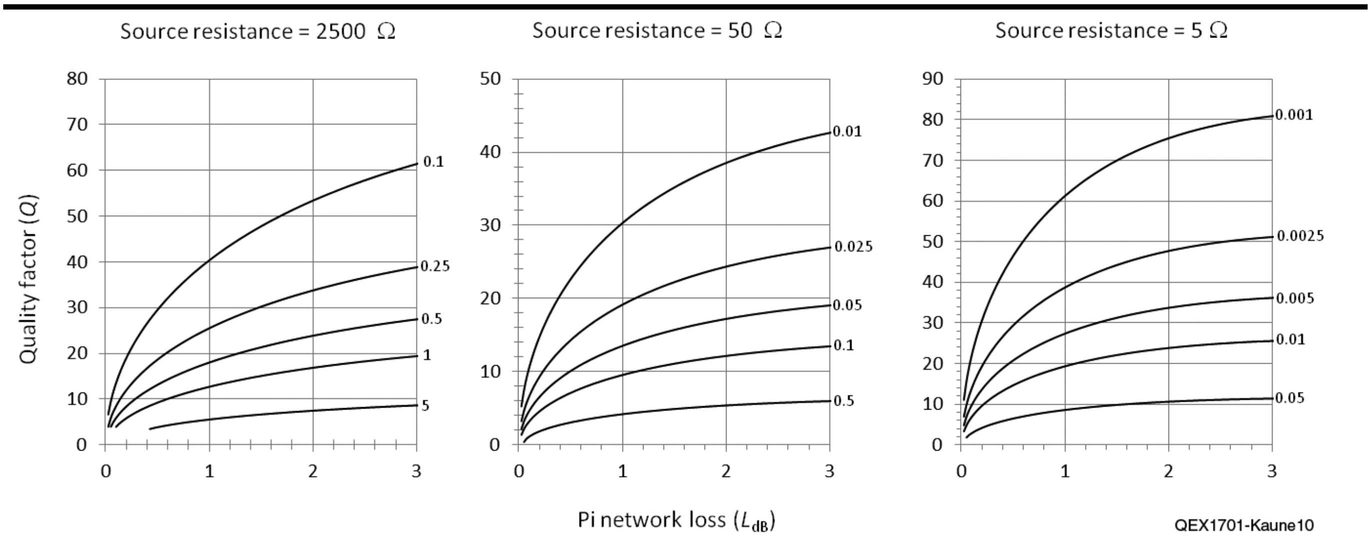

Figure 10 — Quality factor Q as a function of loss in a pi network. Data are shown for source resistances of 2500 Ω (left), 50 Ω (center), and 5 Ω (right). In all cases the load resistance was 50 Ω. Each curve in each graph is labeled with its respective value of R_2.

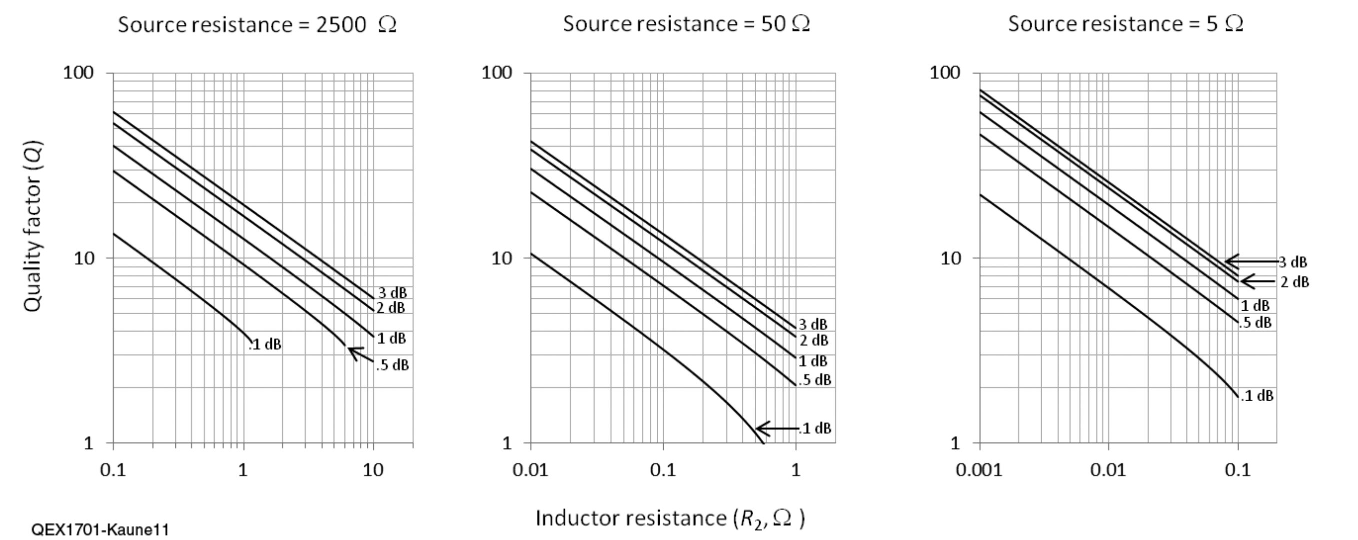

Figure 11 — Quality factor Q as a function of the inductor loss resistance R_2. Data are shown for source resistances of 2500 Ω (left), 50 Ω (center), and 5 Ω (right). In all cases the load resistance was 50 Ω. Each curve in each graph is labeled with its respective value of loss in the pi network.

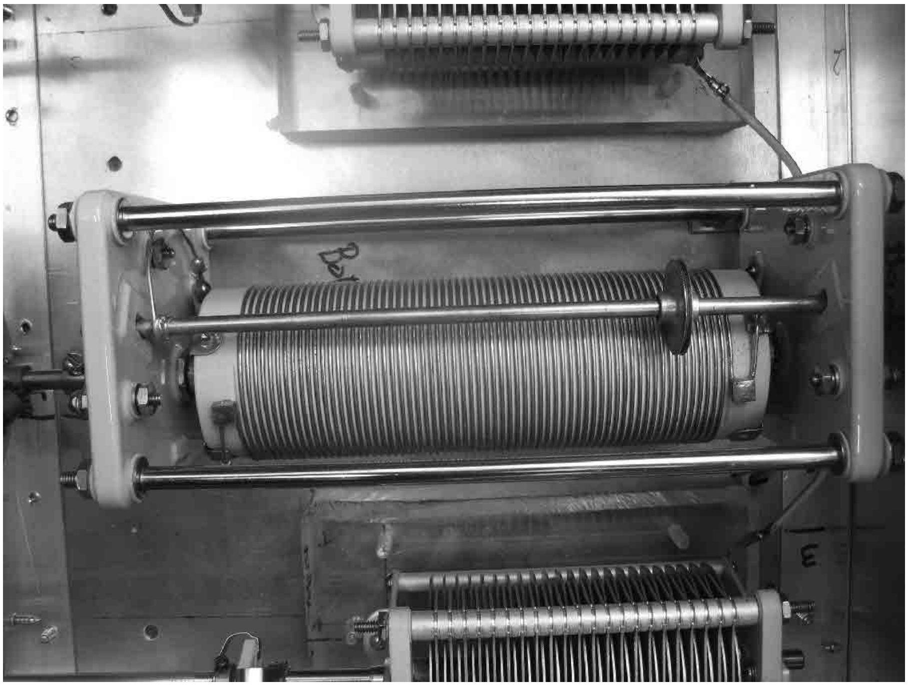

Figure 12 — Variable rotary inductor used in T-network tuner.

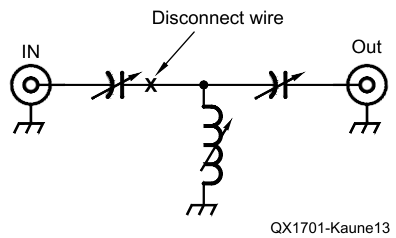

Figure 13 — Schematic diagram of a T network tuner. The wire between the input capacitor and the shunt inductor was disconnected to create a series circuit with the output capacitor and inductor.

unacceptable. But to limit losses to 1 dB and achieve a Q of 10 to 15, a figure that is a typical design goal for transmitters, the data in Figure 10 show that the loss resistance R_2 must be less than about 1 Ω if the source resistance is 2500 Ω, less than about 50 mΩ if the source resistance is 50 Ω, and less than about 20 mΩ for a source resistance of 5 Ω. To achieve losses even less than 1 dB, the loss resistance of the inductor must be substantially less than the values listed in the preceding sentence.

Figure 11 shows the same data in an alternate way that seems quite useful to me. In the three graphs in the figure, Q is plotted

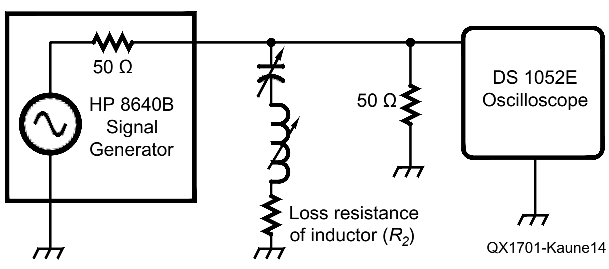

Figure 14 — Experimental setup to measured loss resistance R_2 of inductor shown in Figure 12. The series capacitor and inductor were adjusted to resonance so that their reactances would cancel leaving only R_2 in the circuit.

as a function of the inductor loss resistance, R_2. Families of curves are shown for losses of 0.1, 0.5, 1, 2, and 3 dB. As an example, suppose the source resistance is 2500 Ω and our goal is a pi network with a loss of 0.5 dB (11% of input power dissipated in the inductor) and a Q of 10. The left-hand graph in Figure 11 shows that this can only be accomplished if R_2 is less than about 0.84 Ω.

The work described so far is theoretical. As I progressed, I decided that I needed to obtain some loss data on a real inductor. Therefore, I set out to measure the loss resistance of an actual rotary variable inductor that one might use in a pi network. The next section describes this measurement and the results.

Loss Resistance of a Rotary Variable Inductor

I have a T-network antenna tuner that I built using a rotary variable inductor and two air variable capacitors. Figure 12 shows a photograph of the inductor and part of one of its variable capacitors. Figure 13 is the circuit diagram of a basic T-network tuner. I disconnected the wire between the input capacitor and the shunt inductor; see Figure 13. This change left the output capacitor and the inductor in series with the output connector. I then connected a HP 8640B signal generator to the output connector through a BNC-T. The other side of the T was connected to a Rigol DS1052D digital oscilloscope. Figure 14 shows the complete layout, including the 50 Ω output impedance of the HP signal generator, the 50 Ω input impedance of the oscilloscope (accomplished by placing a 50 Ω terminator at the input of the scope), and the loss resistance R_2 of the inductor. I assume that the loss resistance of the variable capacitor is negligible compared to that of the inductor.

The basic idea is to tune the series capacitor to minimize the voltage measured by the oscilloscope, at which point the reactances of the capacitor and the inductor will cancel each other leaving just R_2, the loss resistance of the inductor. In practice, this is a little more difficult than it might at first sound. First of all, the dip in voltage as resonance is passed through is quite sharp, making it difficult to find the true minimum by adjusting the variable capacitor. I solved this by first adjusting the variable capacitor to as close to the minimum as possible, then using the vernier frequency adjustment on the signal generator to find the true minimum; typically this final adjustment involved a frequency change of no more than about 100 Hz. The second problem stems from the fact that the signal from the signal generator is not a pure sinusoid but contains both fundamental and small harmonic components. The series capacitor-inductor can only be adjusted to null out one frequency, so the harmonic components pass through without attenuation. This problem was solved by using the ability of the Rigol oscilloscope (using its Fourier transform function) to separate a signal into its frequency components and measure the amplitude only of the fundamental.

A measurement occurred in three steps. (1) The inductor was set to a particular value of interest. (2) The series capacitor-inductor were removed from the circuit and the voltage V_1 of the fundamental of the signal noted. (3) The series capacitor-inductor was returned to the circuit and the capacitor and signal generator frequency were adjusted to minimize the fundamental voltage V_2, which was then noted. Referring once again to Figure 14, it is easy to show that

$$V_1 = \frac{V_S}{2} \qquad (27)$$

$$V_2 = \frac{R_2}{Z_0 + 2R_2} V_S$$

where Z_0 = 50 Ω. Use the first of these equations to eliminate V_S in the second and then solve the result for the loss resistance R_2 of the inductor. The final equation is

$$R_2 = \frac{Z_0}{2\left(V_1/V_2 - 1\right)}. \qquad (28)$$

I took data at 3.75 MHz and 14.2 MHz. The results are in Tables 1 and 2 and show

Table 1.
Measured loss resistances R_2 at a frequency of 3.75 MHz for the inductor shown in Figure 13.

L, μH	*R2*, Ω	*Inductor Q*
24.8	7.49	78
22.1	6.32	82
19.5	4.83	95
16.9	3.88	103
14.4	3.17	107
12.0	2.52	112
9.6	2.01	113
7.4	1.60	109
5.3	1.26	99
4.5	1.15	93
3.8	1.04	86

Table 2.
Measured loss resistances R_2 at 14.2 MHz for the inductor shown in Figure 13.

L, μH	*R2*, Ω	*Inductor Q*
2.5	5.80	38
2.2	4.13	47
1.9	2.96	57
1.6	2.22	65
1.4	1.70	72
1.1	1.36	74
0.92	1.12	74
0.74	0.93	71
0.57	0.79	64
0.43	0.69	56
0.33	0.62	47
0.29	0.61	42
0.26	0.58	39

Table 3.
Example design of a pi network to match a source impedance of 2500 Ω to a load of 50 Ω at a frequency of 3.75 MHz and with a network loss of 0.5 dB. Each row in the table is a successive iteration, obtained from the row before it by using the value for L_2 and the data in Table 1 to calculate an improved estimate of the loss resistance R_2.

Loss, dB	R_2, Ω	C_1, pF	L_2, μH	C_3, pF	*Q*
0.5	1.00	279	7.21	1917	9.2
0.5	1.57	222	8.97	1442	7.3
0.5	1.89	203	9.80	1267	6.6
0.5	2.05	195	10.18	1193	6.4
0.5	2.13	191	10.37	1159	6.2
0.5	2.17	189	10.46	1142	6.2
0.5	2.19	188	10.50	1134	6.1
0.5	2.20	188	10.52	1130	6.1

Table 4.
Example design of a pi network to match a source impedance of 2500 Ω to a load of 50 Ω at a frequency of 3.75 MHz and with a network loss of 1 dB. Each row in the table is a successive iteration, obtained from the row before it by using the value for L_2 and the data in Table 1 to calculate an improved estimate of the loss resistance R_2.

Loss, dB	R_2, Ω	C_1, pF	L_2, μH	C_3, pF	*Q*
1.0	1.00	385	5.24	2934	12.7
1.0	1.25	344	5.85	2596	11.3
1.0	1.35	331	6.08	2488	10.9
1.0	1.39	326	6.17	2448	10.8
1.0	1.40	325	6.19	2438	10.7

inductance, the measured loss resistance, and the resulting Q of the inductor ($2\pi fL/R_2$).

I do not know enough about inductors to be able to say whether the data in Tables 1 and 2 are typical of rotary variable inductors. The inductor Q values range from about 78 to 113 at 3.75 MHz and from about 38 to 74 at 14.2 MHz, which are similar to values I have read in various ham-radio-oriented publications.

Designing Pi Networks

All of the analysis presented so far has assumed that the loss resistance R_2 is constant. But, the data in Tables 1 and 2 demonstrate that R_2 varies as the inductance of L_2 varies. This complicates the design process and requires an iterative technique.

Suppose we wish to design a pi network, using my variable rotary inductor, for operation at 3.75 MHz with a loss of 0.5 dB and a Q of about 10. As a first step, the left graph in Figure 10 indicates that the loss resistance must be 1 Ω (or less) to limit loss to 0.5 dB. Thus as a starting point, assume $R_2 = 1\ \Omega$. Then use Eq. (26) to calculate R_V, Eqs. (15) to calculate C_1, L_2, and C_3, and Eq. (19) to calculate Q. Results are listed in the first row of Table 3. The calculated inductance is 7.21 µH. Referring to Table 1, we see this inductance is associated with a loss resistance around 1.57 Ω, estimated using linear extrapolation. Now repeat the calculations listed above using $R_2 = 1.57\ \Omega$. The second row in the table gives the results. Note that the inductance has increased to a value of 8.97 µH which, according to Table 1, is associated with a loss resistance of 1.89 Ω. The remaining rows in Table 3 give additional iterations, continuing until there is little change from one to the next iteration. The final result shows that with a loss of 0.5 dB, $Q = 6.1$. This Q is significantly less than our design goal of 10. I find it surprising, and striking, that a loss resistance as small as 2.2 Ω limits so strongly the overall Q of the pi network.

I believe it is generally the case when using a pi network to match the output of a power amplifier to an antenna that one would like to have a Q near 10. To accomplish this, we are evidently going to have to accept a higher loss. Table 4 contains data similar to that in Table 3 but for a loss of 1 dB. After five iterations, we find $Q = 10.7$. These two examples demonstrate that there is tradeoff between Q and loss. Higher values of Q are associated with larger losses. This is easy to understand. Higher values of Q are a result of a larger storage of energy in the reactive elements of a pi network, and larger stored energy means a larger current circulating between the inductor and the two capacitors. But, this larger current must pass through the loss resistance of the inductor, which leads to larger loss.

Conclusions

Inductor loss plays a substantial role in the design of pi networks. The use of my rotary inductor in a pi network would place substantial constraints on loss and Q: A Q of 10 at 3.75 MHz would require the acceptance of a loss of 1 dB. Lowering loss to 0.5 dB would limit Q to about 6. In designing a pi network, one would want to use a high quality (high Q) inductor. The inductor in Figure 12 is not of sufficient high quality and would not be a good choice for a pi network design.

I developed a computer program that I use to analyze pi networks with inductive loss. This program allows a user to enter source and load resistances, the frequency at which the pi network will be used, the loss resistance R_2, and any one of the following parameters: virtual resistance R_V; Q defined by Eq. (19); Q defined by bandwidth, reactance of C_1, or the network loss in dB. The program calculates the values of C_1, L_2, and C_3, the attenuation of the second through 10th harmonics, and a graph of the frequency response of the network. I would be happy to share this program with interested parties.

APPENDIX A: *Q* of a Cascaded Network

According to Eq. (16), the Q of any network is

$$Q = 2\pi f \frac{W}{D_S + D + D_L}, \qquad \text{(A-1)}$$

where W is the energy stored in the reactive elements, D_S is the power dissipated in the source resistance, D is the power dissipated internally within the network, and D_L is the power dissipated in the load resistance. We assume that the network is used to match a load resistance to a source resistance. This means that the resistance looking into the input of the network will equal the source resistance, which means that the power dissipated in the source resistance will be the same as the power dissipated internally within the network and in the load. That is, $D_S = D + D_L$. Consequently, Eq. (A-1) can be rewritten as

$$Q = 2\pi f \frac{W}{2D_S}. \qquad \text{(A-2)}$$

Now suppose the network can be broken into two cascaded networks, A and B, so that the first network A matches the source resistance R_S to a virtual resistance R_V and the second network B matches R_V to the final load resistance, R_L. Let D_A and D_B be the powers dissipated internally by networks

A and B, respectively, and D_V the power dissipated by the virtual load resistance R_V. Then the quality factors, Q_A and Q_B, for the two networks are

$$Q_A = 2\pi f \frac{W_A}{D_S + D_A + D_V} \quad \text{(A-3)}$$

and

$$Q_B = 2\pi f \frac{W_B}{D_V + D_B + D_L} \quad \text{(A-4)}$$

The source resistance is matched by network A to the virtual load so $D_S = D_A + D_V$. Similarly, the virtual resistance is matched by network B to the load resistance so $D_V = D_B + D_L$. Using these two results, Eqs. (A-3) and (A-4) can be rewritten

$$Q_A = 2\pi f \frac{W_A}{2D_S} \quad \text{(A-5)}$$

and

$$Q_B = 2\pi f \frac{W_B}{2D_V} \quad \text{(A-6)}$$

The energy, W, stored in the entire network is the sum of the energies stored in networks A and B, that is, $W = W_A + W_B$. Using this result in Eq. (A-2), we get

$$Q = 2\pi f \frac{W_A}{2D_S} + 2\pi f \frac{W_B}{2D_S} \quad \text{(A-7)}$$

Now insert Eqs. (A-5) and (A-6) into (A-7). The result is

$$Q = Q_A + \frac{D_V}{D_S} Q_B \,. \quad \text{(A-8)}$$

The ratio D_V/D_S is just the efficiency, ε_A, of network A to deliver power to its load. The final result is, then,

$$Q = Q_A + \varepsilon_A Q_B \quad \text{(A-9)}$$

In the pi network case treated in this paper, the loss occurred only in network B so ε_A=1

APPENDIX B: Calculate R_V from Q

The calculation of R_V from a specification of Q starts with Eq. (19) which expresses Q as a function of R_V. This equation is

$$Q = \frac{1}{2}\left[\sqrt{\frac{R_S - R_V}{R_V}} + \sqrt{\left(\frac{R_V - R_2}{R_V}\right)\left(\frac{R_L + R_2 - R_V}{R_V}\right)}\right]. \quad \text{(B-1)}$$

Inverting this equation involves considerable algebra. It must be squared twice to eliminate the square roots. The result is a polynomial equation in R_V:

$$AR_V^4 + BR_V^3 + CR_V^2 + DR_V + E = 0 \quad \text{(B-2)}$$

where

$$\left.\begin{aligned}
A &= 16Q^2\left(Q^2 + 1\right) \\
B &= -8Q^2\left(R_S + 2R_2 + R_L\right) \\
C &= \left(R_L + 2R_2 - R_S\right)^2 + 8Q^2 R_2\left(R_L + R_2\right) \\
D &= -2R_2\left(R_L + R_2\right)\left(R_L + 2R_2 - R_S\right) \\
E &= R_2^2\left(R_L + R_2\right)^2
\end{aligned}\right\} \quad \text{(B-3)}$$

There are four roots to equations like (B-2). To calculate these roots, I used a method on a website.[4] Some (or all) of the roots may be complex numbers that we can reject immediately. If there are two or four real roots, some may not satisfy Eq. (B-1) and can be rejected. Others may not satisfy the inequality listed last in Eqs. (15). If there are two remaining roots, select the larger of the two because it will involve less loss in the network.

Consider this example: R_S = 2500 Ω, R_L = 50 Ω, R_2 = 2 Ω, and Q = 10. Use Eqs. (B-3) to calculate the coefficients A through E, and calculate the roots of Eq. (B-2) using the method mentioned above. The four solutions for R_V are 7.74 Ω, 4.98 Ω, (-0.0411 + j 0.00683) Ω, and (-0.0411 – j 0.00683) Ω. The latter two are complex and can be discarded. When placed in Eq. (B-1), the second solution yields a value for Q of 12.4, not the target value of 10. The first solution, 7.74 Ω, yields Q of 10 and is the desired value.

Bill Kaune, W7IEQ, is a retired physicist (BS, PhD). He is married and has two grown daughters and four grandchildren. Bill spent most of his career collaborating with biologists and epidemiologists researching the biological effects of power-frequency electric and magnetic fields. Along with Amateur Radio, Bill spends his time hiking, backpacking, and doing some volunteer work. Bill was first licensed in 1956 as a novice and then a general, but became inactive while in college. He was licensed again in 1998 and upgraded to the Amateur Extra class in 2000. Bill is a member of the Jefferson County Amateur Radio Club and the ARRL.

Notes

[1] Bill Kaune, W7IEQ, "Quality Factor, Bandwidth and Harmonic Attenuation of Pi Networks", *QEX*, Sep 2015, p. 2.

[2] *The ARRL Handbook Book, 2016 Edition.* ARRL item no. 0413, available from your ARRL dealer, or from the ARRL Store, Telephone toll-free in the US 888-277-5289, or 860-594-0355, fax 860-594-0303; **www.arrl.org/shop/**; **pubsales@arrl.org**, ARRL, Newington, CT.

[3] Alan Payne, "Measuring the Loss in Variable Air Capacitors", **g3rbj.co.uk**, 2013.

[4] **jwilson.coe.uga.edu/EMAT6680Fa09/Davenport/Solving%20Quartic%20Equations.pdf**

Letters to the Editor

How to Tune an L-network Matchbox, Charles R. MacCluer, W8MQW (Nov/Dec 2016)

Dear Editor,

It looks like the latter part of W8MQW's article is missing. — *Bob Wilson, WA9D.*

[Others also noticed that we inadvertently omitted page 3, reproduced here. A full copy is at **www.arrl.org/this-month-in-qex**, and **www.arrl.org/QEXfiles** — Ed.]

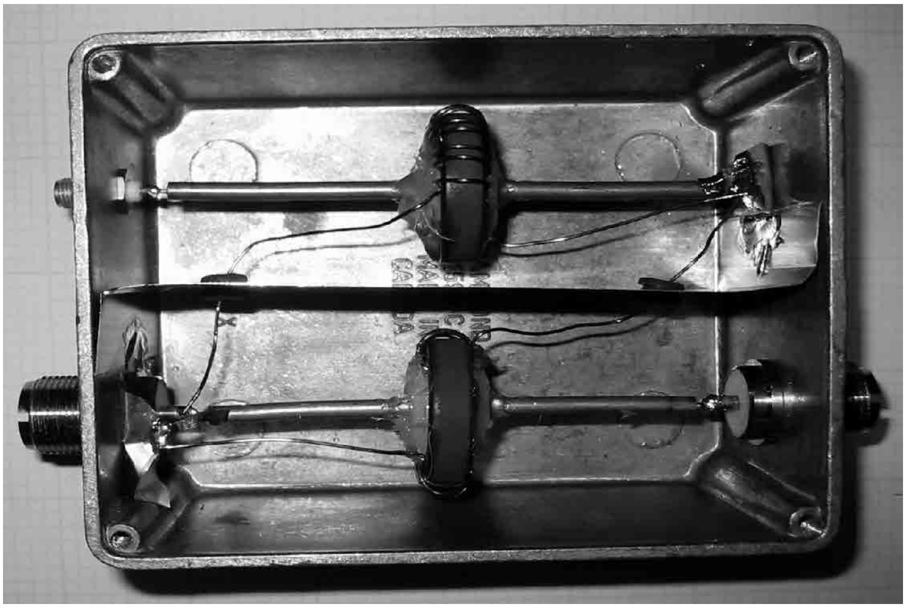

Figure 5 — Tandem coupler design by Larry Phipps, N8LP.

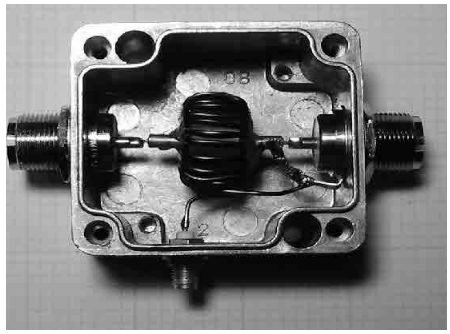

Figure 6 — The current sampler used to sample the difference between forward and reflected voltage.

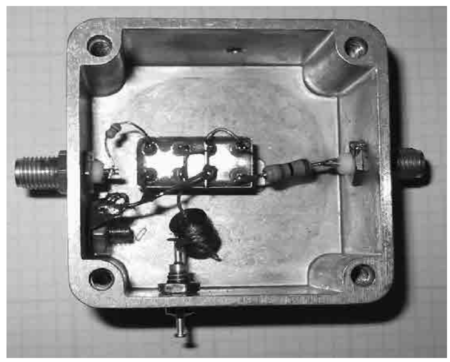

Figure 7 — A phase detector employing a MiniCircuits SBL-1.

But even with the minor interaction of the *L* and *C* controls, convergence to match is much quicker because of the added information available from the phase voltage. If phase voltage is negative, decrease *C*; if phase voltage is positive, increase *C*. Thus the 50 Ω real part is matched immediately. Then proceed in the usual way to a one-to-one match by adjusting *L*.

Some Final Thoughts

To save space, the current sampler of Figures 2 and 6 could possibly be incorporated into the tandem coupler of Figure 5 by adding its toroid as a second toroid on the through line. I did not try this.

Both meter *A* and *B* can be any 100 μA or smaller ammeters. The meter *A* must be a center-zero meter since the phase detector reports both positive and negative voltages. Select by trial and error the current limiting resistors, marked '*', for your particular meters. As a starting point try 1 kΩ.

The fortuitous levels of the sampled voltages require no active devices. This permitted all signals to be piped about with my favorite coax, RG402 semi-rigid coax with SMA connectors, lending a microwave look to the construction.

This algorithm is valid for any *L* network matchbox, whether it is a balanced network preceded by a balun or an unbalanced network followed by a balun.

It would be easy to add an outboard current sampler and phase detector plus meter to existing manual L-network tuners to achieve expedited two-step tuning.

Displaying V_r (horizontal input) against $V_f - V_r$ (vertical input) as an oscilloscope Lissajous diagram is an exceptionally efficient aid in finding a match — one adjusts *C* to rotate the ellipse vertical, then *L* to shrink the ellipse to a vertical line.

An outboard current sampler/phase detector/meter might also speed *T*-match tuning.

The above matchbox construction details were merely sketched. Instead the thrust of this note is to reveal that *tuning an* L network *need not be a tedious iterative process*. It can in theory be done in two steps by carefully observing two simple-to-measure voltages.

Acknowledgements

This project grew from a challenge from Gary Adamowicz, WA1OXT, who is developing a competing approach. I thank Mike Blake, K9JRI, and Chuck Hawley, KE9UW, for their many helpful comments and suggestions.

Chuck MacCluer, W8MQW, was first licensed in 1952 with the novice call sign WN8MQW, and progressed to Amateur Extra license. He has been very active in EME on 432 and 1296 MHz, and recently is active on SSB, CW, and digital modes on 160, 80, and 40 meters. Chuck received a PhD in Mathematics in 1966 from the University of Michigan and is now Professor Emeritus of Mathematics at Michigan State University. Chuck is a Life member of ARRL, IEEE, SIAM, and ASHRAE.

Notes

[1] The intermediate quotient of [EQ 3] is the core computation that underlies the Smith Chart. ARRL item no. 0413, available from your ARRL dealer, or from the ARRL Store, Telephone toll-free in the US 888-277-5289, or 860-594-0355, fax 860-594-0303; **www.arrl.org/shop/**; **pubsales@arrl.org**.

[2] L. Phipps, N8LP, "The LP-100 Wattmeter", *QEX*, Jan/Feb 2006.

2016 *QEX* Index

Features

About the Cover

Bits

Empirical Outlook (Wolfgang)

Hands-On-SDR (Cowling)

Letters to the Editor

Perspectives/In this Issue (Siwiak)

SDR Simplified (Mack)

Up Coming Conferences

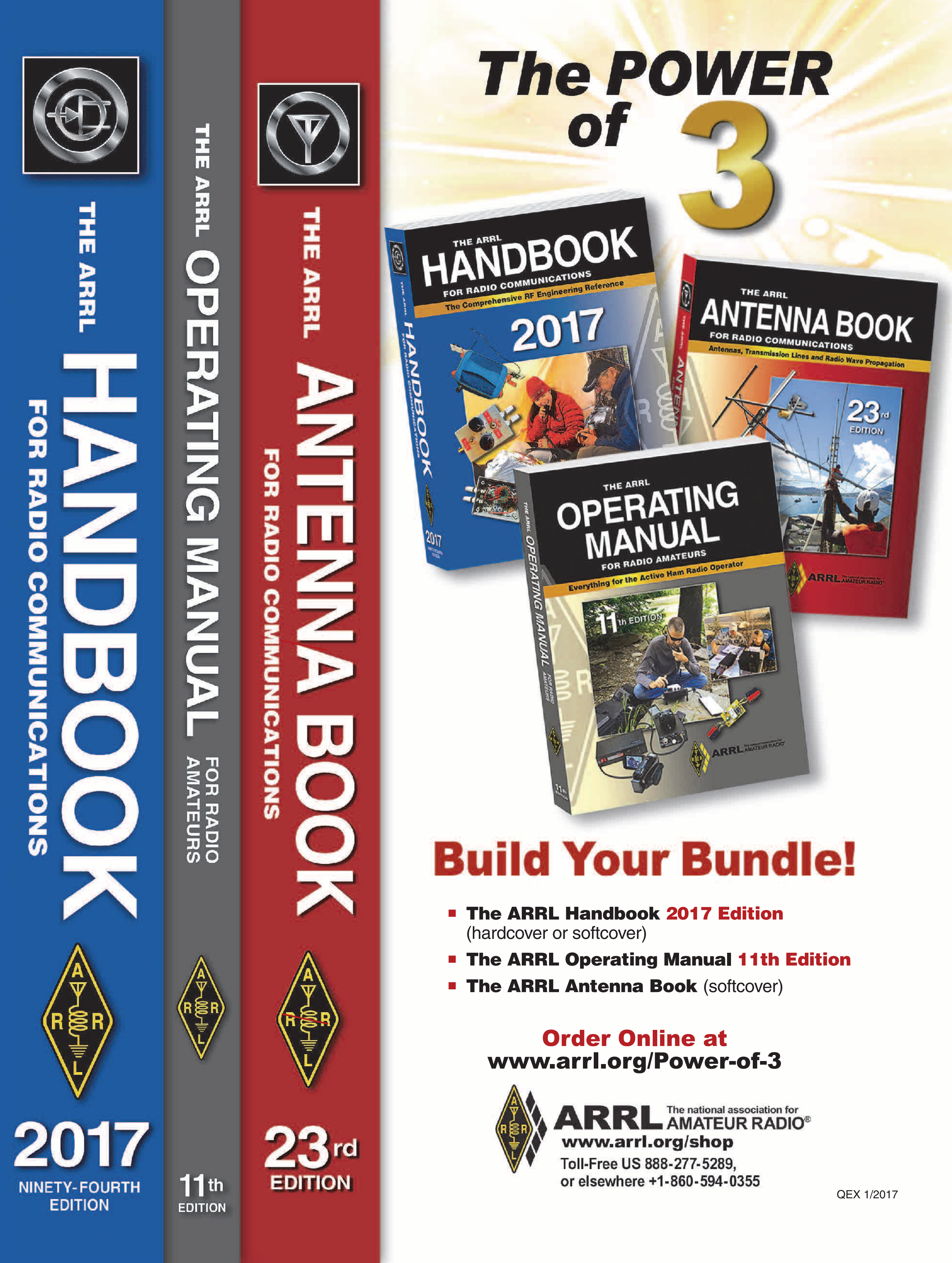
THE ARRL
HANDBOOK
FOR RADIO COMMUNICATIONS
2017
NINETY-FOURTH EDITION
THE ARRL
OPERATING MANUAL
FOR RADIO AMATEURS
11th EDITION
THE ARRL
ANTENNA BOOK
FOR RADIO COMMUNICATIONS
23rd EDITION
The POWER of 3
THE ARRL
HANDBOOK
FOR RADIO COMMUNICATIONS
The Comprehensive RF Engineering Reference
2017
THE ARRL
ANTENNA BOOK
FOR RADIO COMMUNICATIONS
Antennas, Transmission Lines and Radio Wave Propagation
23rd EDITION
THE ARRL
OPERATING MANUAL
FOR RADIO AMATEURS
Everything for the Active Ham Radio Operator
11th EDITION
Build Your Bundle!
▪ The ARRL Handbook 2017 Edition (hardcover or softcover)
▪ The ARRL Operating Manual 11th Edition
▪ The ARRL Antenna Book (softcover)
Order Online at
www.arrl.org/Power-of-3
ARRL The national association for AMATEUR RADIO®
www.arrl.org/shop
Toll-Free US 888-277-5289,
or elsewhere +1-860-594-0355
QEX 1/2017